

Supporting Information

Wide-Range Color-Tunable Polycyclo-heteraborin Multi-resonance Emitters Containing B-N Covalent Bonds

Guoyun Meng,^{‡a} Hengyi Dai,^{‡a} Jianping Zhou,^a Tianyu Huang,^a Xuan Zeng,^a Qi Wang,^a Xiang Wang,^a Yuewei Zhang,^a Tianjiao Fan,^a Dezhi Yang,^c Dongge Ma,^c Dongdong Zhang,^{*a} and Lian Duan^{*a,b}

^a Dr. G. Meng, H. Dai, J. Zhou, T. Huang, Dr. X. Zeng, Q. Wang, Dr. X. Wang, Dr. Y. Zhang, T. Fan, Dr. D. Zhang, Prof. L. Duan

Key Lab of Organic Optoelectronics and Molecular Engineering of Ministry of Education, Department of Chemistry

Tsinghua University

Beijing, 100084, P. R. China

E-mail: ddzhang@mail.tsinghua.edu.cn; duanl@mail.tsinghua.edu.cn

^b Prof. L. Duan

Laboratory of Flexible Electronics Technology, Tsinghua University, Beijing, 100084, P. R. China

^c Prof. D. Ma, Dr. D. Yang

Institute of Polymer Optoelectronic Materials and Devices State Key Laboratory of Luminescent Materials and Devices, South China University of Technology, Guangzhou, 510640, P. R. China

[‡] These authors contributed equally to this work.

Table of Contents

1. Experimental section	1
1.1 General information	1
1.2 Computational methods	1
1.3 Measurement of absorption and emission characteristics	1
1.4 Electrochemical measurements	1
1.5 Determination of the emitting dipole orientation	1
1.6 Device fabrication and measurement of EL characteristics	1
1.7 Synthesis	3
2. Supplementary figures and tables	8
3. References	50

1. Experimental Section

1.1 General Information. All reagents used for reaction, purification and measurements were purchased from Shanghai Bide Medical Technology Co. Ltd. All other reagents used for device fabrication were purchased from Jilin Optical and Electronic Materials Co. Ltd. These materials were received and used without further purification. The other reagents and solvents were used as received from commercial sources without further purification. 400, 600, 700 MHz ^1H -NMR and 150 MHz ^{13}C -NMR spectra were measured by a JEOL JNM-ECS600 spectrometer at room temperature in deuterated dichloromethane and chloroform respectively with tetramethyl silane as the internal standard. MALDI-TOF-MS data was performed on a Shimadzu AXIMA Performance MALDI-TOF instrument in positive detection modes.

1.2 Computational methods. The calculations were performed with the Gaussian 09 package, using the density functional theory (DFT) and time-dependent density functional theory (TD-DFT) method with the B3LYP hybrid functional.^[1-3] The structures were optimized using TD-DFT (S_1 and T_1 state) methods with a 6-31G(d,p) basis set. Franck-Condon analyses of the emission spectra were performed according to the literature^[4] using the Gaussian 16 package. Natural transition orbital analyses^[5] were also performed to examine the nature of the excited states. Electron-hole analysis was carried out using the Multiwfn software.^[6] The RMSDs of the optimized structures at S_0 and S_1 states were analyzed by VMD software.^[7] The Huang-Rhys (HR) factors and reorganization energies were calculated using the MOMAP software.^[8]

1.3 Measurement of absorption and emission characteristics. 1×10^{-5} M solutions were prepared by stepwise dilution for solution measurements. Thin films for photophysical characterization were prepared by thermal evaporation on quartz substrates at $1\text{-}2 \text{ \AA sec}^{-1}$ in a vacuum chamber with a base pressure of $< 10^{-5}$ torr. UV-vis absorption and PL spectra were measured using UV-2600 (Shimadzu) and FluoroMax-4P (Horiba) instruments at 77 and 298 K. The PLQYs were obtained with an absolute photoluminescence quantum yield: measurement system Hamamatsu C9920-03G in an integrating sphere. The solution sample was bubbled with nitrogen for 10 minutes before measurement while the films were measured in air. The transient spectra were collected on an Edinburgh Fluorescence Spectroscopy FLS1000.

1.4 Electrochemical measurements. Cyclic voltammetry was performed on a CHI

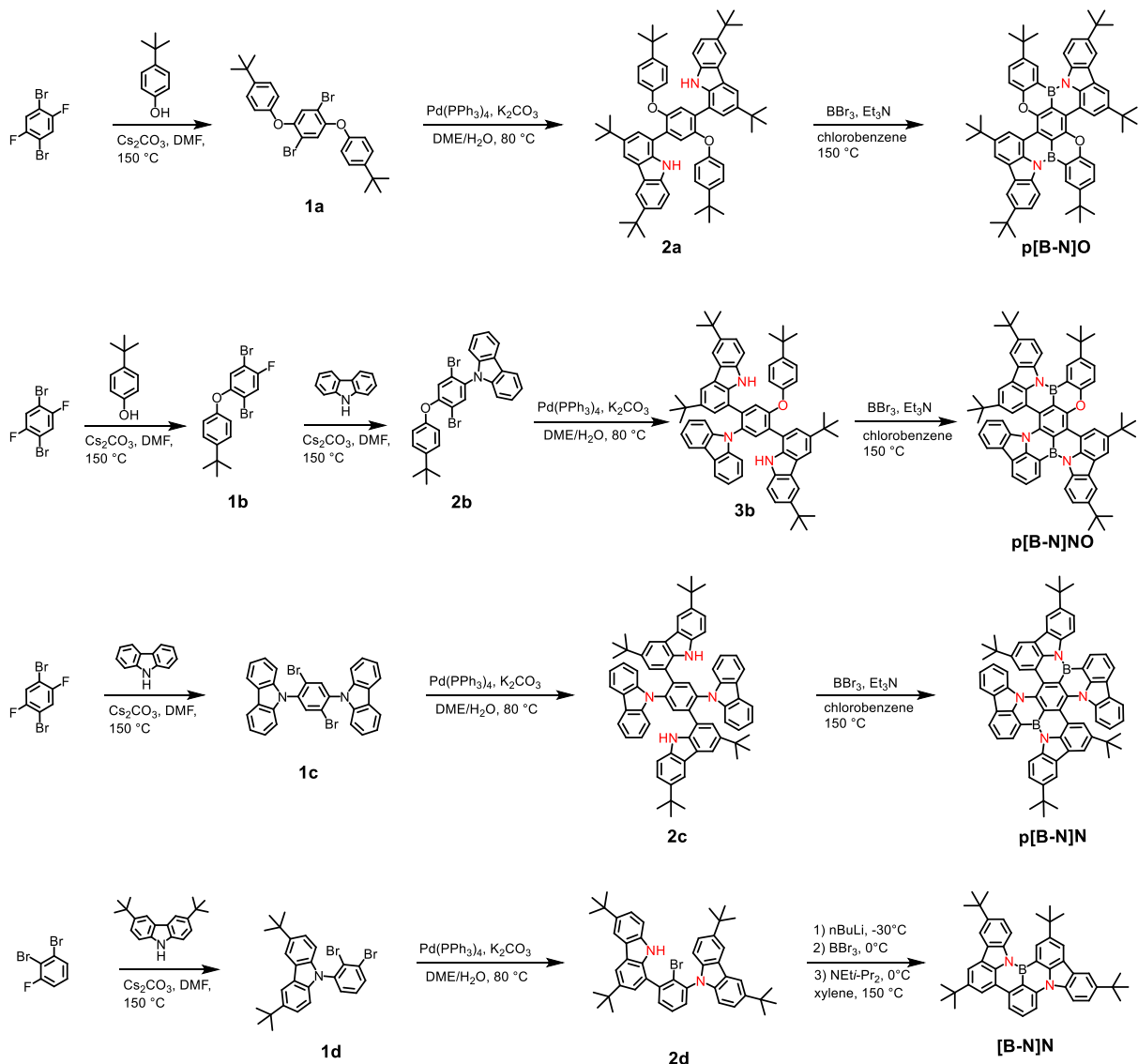
660 instrument, using a platinum (Pt) electrode as the working electrode, a Pt wire as the auxiliary electrode and an Ag/Ag⁺ electrode as the reference electrode. The oxidation/reduction potentials were measured in dry dichloromethane/DMF solutions with 0.1 M of TBAPF₆ (tetrabutylammonium hexafluorophosphate) as a supporting electrolyte at a scan rate of 100 mV s⁻¹.

$$E_{\text{HOMO}} = -(E_{[\text{onset,ox} \text{ vs. } \text{Fc}^+/\text{Fc}]} + 4.8) \text{ (eV)} \quad E_{\text{LUMO}} = -(E_{[\text{onset,red} \text{ vs. } \text{Fc}^+/\text{Fc}]} + 4.8) \text{ (eV)}$$

1.5 Determination of the emitting dipole orientation. To determine emitting dipole orientation of an emitting film, angle-resolved and polarization-resolved PL measurements were performed by a setup RSQX-01 made by Changchun Ruoshui Technology Development Co. Ltd. The dipole orientation of doped films was determined by angle-resolved and polarization-resolved PL on a half quartz cylinder prism. A continuous-wave He:Cd laser (325 nm) with a fixed angle of 45° to the substrate was used as excitation source. *p*-Polarized emitted light was detected at the respective peak wavelength of the PL spectrum of each film. The emitting dipole orientation was then determined by least-square fitting of the measured angle-dependent polarized emission intensity with calculated results.

1.6 Device fabrication and measurement of EL characteristics. All compounds were subjected to temperature-gradient sublimation under a high vacuum before use. OLEDs were fabricated on the ITO-coated glass substrates with multiple organic layers sandwiched between the transparent bottom indium-tin-oxide (ITO) anode and the top metal cathode. Before device fabrication, the ITO glass substrates were pre-cleaned carefully. All material layers were deposited by vacuum evaporation in a vacuum chamber with a base pressure of 10⁻⁶ torr. The deposition system permits the fabrication of the complete device structure in a single vacuum pump-down without breaking vacuum. The deposition rate of organic layers was kept at 0.1~0.2 nm s⁻¹. The doping was conducted by co-evaporation from separate evaporation sources with different evaporation rates. The current density, voltage, luminance, external quantum efficiency, electroluminescent spectra and other characteristics were measured with a Keithley 2400 source meter and an absolute EQE measurement system in an integrating sphere at the same time. The EQE measurement system is Hamamatsu C9920-12, which is equipped with Hamamatsu PMA-12 Photonic multichannel analyzer C10027-02 whose longest detection wavelength is 1100 nm.

1.7 Synthesis



Scheme S1. The synthetic routes of **p[B-N]O**, **p[B-N]NO**, **p[B-N]N** and **[B-N]N**.

*Synthesis of 4,4'-(2,5-dibromo-1,4-phenylene)bis(oxy))bis(tert-butylbenzene) (**1a**):* 4-(tert-butyl)phenol (6.35 g, 42.3 mmol), 1,4-dibromo-2,5-difluorobenzene (5.0 g, 18.4 mmol) and CsCO₃ (24.0 g, 73.6 mmol) were dissolved in dry DMF (150 mL) at room temperature. The mixture was stirred at 150 °C for 18 h. After cooling to room temperature, the reaction mixture was poured into water. After filtration, the crude product was purified by recrystallization from methanol to afford **1a** as white solid, 8.8 g, yield: 90%. ¹H NMR (700 MHz, Chloroform-d) δ (ppm): 7.41 – 7.38 (m, 4H), 7.23 (s, 2H), 6.96 – 6.93 (m, 4H), 1.36 (s, 19H).

Synthesis of 1,4-dibromo-2-(4-(tert-butyl)phenoxy)-5-fluorobenzene (1b): Compound **1b** was synthesized according to the same procedure described above for the synthesis of **1a** by using only half of the (tert-butyl)phenol (3.04 g, 20.2 mmol) instead. **1b** was obtained as white solid after recrystallization from methanol, 7.1 g, yield: 87%. ¹H NMR (700 MHz, Chloroform-d) δ (ppm): 7.44 (d, J=7.6, 1H), 7.40 – 7.38 (m, 2H), 7.14 (d, J=6.2, 1H), 6.93 – 6.90 (m, 2H), 1.35 (s, 10H).

Synthesis of 9-(2,5-dibromo-4-(4-(tert-butyl)phenoxy)phenyl)-9H-carbazole (2b): Compound **2b** was synthesized according to the same procedure described above for the synthesis of **1a** by using 9H-carbazole (2.29 g, 13.7 mmol) instead (tert-butyl)phenol and using **1b** (5.5 g, 13.7 mmol) instead 1,4-dibromo-2,5-difluorobenzene. **2b** was obtained as white solid, 6.8 g, yield: 91%. ¹H NMR (700 MHz, Chloroform-d) δ (ppm): 8.17 (d, J=7.7, 2H), 7.78 (s, 1H), 7.52 – 7.49 (m, 2H), 7.48 – 7.44 (m, 2H), 7.36 – 7.32 (m, 2H), 7.31 (s, 1H), 7.16 – 7.10 (m, 4H), 1.40 (s, 9H).

Synthesis of 9,9'-(2,5-dibromo-1,4-phenylene)bis(9H-carbazole) (1c): Compound **1c** was synthesized according to the same procedure described above for the synthesis of **1a** by using 9H-carbazole (7.07 g, 42.3 mmol) instead (tert-butyl)phenol. **1c** was obtained as white solid, 10.8 g, yield: 90%. ¹H NMR (700 MHz, Chloroform-d) δ (ppm): 8.21 (d, J=7.7, 4H), 8.03 (s, 2H), 7.54 – 7.50 (m, 4H), 7.41 – 7.37 (m, 4H), 7.28 (t, J=4.0, 6H).

Synthesis of 1,1'-(2,5-bis(4-(tert-butyl)phenoxy)-1,4-phenylene)bis(3,6-di-tert-butyl-9H-carbazole) (2a): In a 100 mL Schlenk flask, 3,6-di-tert-butyl-1-(4,4,5,5-tetramethyl-1,3,2-dioxaborolan-2-yl)-9H-carbazole (1.5 g, 3.7 mmol) and **1a** (0.82 g, 1.5 mmol) were charged under nitrogen. After adding 20 mL dimethoxyethane and 5 mL K₂CO₃ (2.1 g, 15.2 mmol) aqueous solution, the mixture was degassed for 30 min. Pd(PPh₃)₄ (0.18 g, 0.16 mmol) was added, then the mixture was heated to 80 °C and stirred for 4 hours. The reactant was poured into brine and extracted by CH₂Cl₂ for three times. The organic phase was dried over MgSO₄ and the solvent was evaporated in vacuo. The crude product was purified by flash chromatography on silica gel with petroleum ether / CH₂Cl₂ (5:1, v/v) to give **2a** as white solid, 1.12 g, yield: 78%. ¹H NMR (700 MHz, DMSO-d₆) δ (ppm): 10.70 (s, 2H), 8.14 (s, 2H), 8.11 (s, 2H), 7.44 (s, 4H), 7.33 (s, 2H), 7.29 (s, 2H), 7.22 (d, J=8.7, 4H), 6.98 (d, J=8.7, 4H), 1.40 (s,

22H), 1.30 (s, 18H), 1.14 (s, 18H). ^{13}C NMR (176 MHz, DMSO-d₆) δ (ppm): 155.63, 150.02, 145.43, 141.40, 141.01, 139.04, 138.67, 136.73, 131.63, 126.68, 124.32, 123.71, 123.67, 123.48, 123.14, 122.83, 116.55, 116.51, 116.44, 111.17, 110.71, 84.12, 34.89, 34.75, 34.31, 32.40, 32.24, 31.61, 25.22. MALDI-TOF: Calculated: 928.5907, Found: 928.5769.

*Synthesis of 1,1'-(2-(4-(tert-butyl)phenoxy)-5-(9H-carbazol-9-yl)-1,4-phenylene)bis(3,6-di-tert-butyl-9H-carbazole) (**3b**):* Compound **3b** was synthesized according to the same procedure described above for the synthesis of **2a**. **2b** (0.93 g, 1.7 mmol), 3,6-di-tert-butyl-1-(4,4,5,5-tetramethyl-1,3,2-dioxaborolan-2-yl)-9H-carbazole (1.65 g, 4.1 mmol), Pd(PPh₃)₄ (0.20 g, 0.17 mmol) and K₂CO₃ (2.34 g, 16.9 mmol), and obtained **3b** as white solid, 1.4 g, yield: 86%. ^1H NMR (600 MHz, DMSO-d₆) δ (ppm): 10.92 (s, 1H), 10.84 (s, 1H), 8.16 – 8.13 (m, 2H), 7.98 (d, J = 25.1 Hz, 3H), 7.84 (s, 1H), 7.70 (d, J = 1.6 Hz, 1H), 7.44 (d, J = 6.4 Hz, 4H), 7.39 (s, 2H), 7.29 – 7.21 (m, 5H), 7.18 – 6.85 (m, 3H), 6.50 (d, J = 1.7 Hz, 1H), 1.37 (s, 9H), 1.34 (s, 9H), 1.33 (s, 9H), 1.10 (s, 9H), 0.67 (s, 9H). ^{13}C NMR (151 MHz, DMSO-d₆) δ (ppm): 155.00, 154.14, 146.56, 141.48, 141.31, 140.70, 139.20, 138.93, 137.17, 136.32, 133.39, 130.99, 130.11, 126.91, 124.59, 123.75, 123.71, 123.55, 123.00, 122.96, 122.88, 122.21, 120.59, 120.50, 120.00, 119.81, 119.43, 116.67, 116.62, 116.35, 111.29, 111.18, 110.32, 34.96, 34.93, 34.90, 34.08, 32.48, 32.42, 31.64, 31.50. MALDI-TOF: Calculated: 945.5597, Found: 945.5621.

*Synthesis of 9,9'-(2,5-bis(3,6-di-tert-butyl-9H-carbazol-1-yl)-1,4-phenylene)bis(9H-carbazole) (**2c**):* Compound **2c** was synthesized according to the same procedure described above for the synthesis of **2a**. **1c** (0.85 g, 1.5 mmol), 3,6-di-tert-butyl-1-(4,4,5,5-tetramethyl-1,3,2-dioxaborolan-2-yl)-9H-carbazole (1.46 g, 3.6 mmol), Pd(PPh₃)₄ (0.17 g, 0.15 mmol) and K₂CO₃ (2.07 g, 54.2 mmol), and obtained **2c** as white solid, 1.2 g, yield: 86%. ^1H NMR (600 MHz, Chloroform-d) δ (ppm): 8.33 (s, 2H), 7.99 (d, J = 7.7 Hz, 4H), 7.93 – 7.83 (m, 4H), 7.76 (d, J = 1.7 Hz, 2H), 7.45 – 7.31 (m, 6H), 7.23 (d, J = 8.0 Hz, 2H), 7.16 (t, J = 7.2 Hz, 4H), 7.07 – 6.98 (m, 4H), 1.39 (s, 18H), 0.98 (s, 18H). ^{13}C NMR (151 MHz, Chloroform-d) δ (ppm): 142.47, 142.38, 138.35, 137.85, 135.66, 135.39, 132.65, 125.98, 124.01, 123.77, 123.62, 123.54, 123.22, 120.37, 119.24, 116.34, 116.17, 110.06, 109.76, 34.27, 31.45. MALDI-TOF: Calculated: 962.5287, Found: 962.5792.

*Synthesis of 3,6-di-tert-butyl-9-(2,3-dibromophenyl)-9H-carbazole (**1d**):* Compound **1d**

was synthesized according to the same procedure described above for the synthesis of **1a** by using 3,6-di-tert-butyl-9H-carbazole instead (tert-butyl)phenol (0.85 g, 3.0 mmol). **1d** was obtained as white solid, 1.4 g, yield: 90%. ¹H NMR (700 MHz, Chloroform-d) δ (ppm): 8.17 (d, J = 1.6 Hz, 2H), 7.83 (dd, J = 7.8, 1.8 Hz, 1H), 7.47 (dd, J = 8.5, 1.8 Hz, 2H), 7.43 – 7.37 (m, 2H), 6.99 (d, J = 8.5 Hz, 2H), 1.49 (s, 18H).

*Synthesis of 1-(2-bromo-3-(3,6-di-tert-butyl-9H-carbazol-9-yl)phenyl)-3,6-di-tert-butyl-9H-carbazole (**2d**):* Compound **2d** was synthesized according to the same procedure described above for the synthesis of **2a**, **1d** (1.0 g, 1.95 mmol), 3,6-di-tert-butyl-1-(4,4,5,5-tetramethyl-1,3,2-dioxaborolan-2-yl)-9H-carbazole (0.95 g, 2.34 mmol), Pd(PPh₃)₄ (0.23 g, 0.2 mmol) and K₂CO₃ (1.35 g, 9.77 mmol), and obtained as **2d** white solid, 1.1 g, yield: 76%. ¹H NMR (700 MHz, DMSO-d₆) δ (ppm): 10.76 (s, 1H), 8.28 (d, J = 1.5 Hz, 2H), 8.21 (dd, J = 20.5, 1.4 Hz, 2H), 7.77 (t, J = 7.6 Hz, 1H), 7.72 (dd, J = 7.6, 1.6 Hz, 1H), 7.63 (dd, J = 7.7, 1.6 Hz, 1H), 7.49 (dd, J = 19.0, 8.3 Hz, 2H), 7.45 (dd, J = 8.6, 1.8 Hz, 1H), 7.41 – 7.38 (m, 2H), 7.04 (d, J = 8.3 Hz, 1H), 1.46 – 1.41 (m, 36H). ¹³C NMR (176 MHz, DMSO-d₆) δ (ppm): 142.95, 142.66, 141.43, 141.12, 139.60, 139.44, 139.07, 137.66, 132.56, 130.61, 129.57, 125.63, 124.30, 124.08, 123.96, 123.86, 123.69, 123.41, 123.10, 123.00, 122.94, 117.09, 117.01, 116.59, 111.09, 110.60, 109.73, 34.99, 34.96, 34.90, 32.43, 32.41, 32.37.

Synthesis of p[B-N]O: A mixture of **2a** (1.0 g, 1.1 mmol), triethylamine (0.4 mL, 4.16 mmol) in chlorobenzene (15 mL) was stirred at room temperature for 10 minutes. Then, BBr₃ (0.6 mL, 4.16 mmol) was dropwise added to the reaction mixture. The reaction mixture was heated up to 150 °C for 12 hours. After cooling to room temperature, toluene was added to the reaction mixture. Then, insoluble moieties were removed by filtration. After removed the solvent in vacuo, the solid materials were washed with hexane, collected by filtration. The obtained solid was sonicated with methanol, collected by filtration to give the title compound **p[B-N]O** as bright yellow solid, 0.91 g, yield: 90%. ¹H NMR (400 MHz, Methylene Chloride-d₂) δ (ppm): 9.69 (d, J=1.7, 2H), 8.64 (d, J=2.4, 2H), 8.29 (d, J=8.6, 2H), 8.22 (dd, J=10.5, 1.8, 4H), 7.77 (dd, J=8.7, 2.4, 2H), 7.70 (d, J=8.7, 2H), 7.54 (dd, J=8.6, 2.0, 2H), 1.66 (s, 18H), 1.53 (s, 18H), 1.42 (s, 19H). ¹³C NMR (101 MHz, Methylene Chloride-d₂) δ = 158.95, 151.26, 146.94, 145.76, 144.48, 140.85, 138.01, 131.03, 130.16, 129.45, 125.88, 124.78, 123.34,

121.41, 121.09, 117.39, 116.88, 116.61, 116.41, 35.52, 34.91, 34.73, 32.27, 31.67, 31.44. MALDI-TOF: Calculated: 944.5623, Found: 944.7152. Anal. Calcd (%) for C₆₆H₇₀B₂N₂O₂: C, 83.89; H, 7.47; B, 2.29; N, 2.96; O, 3.39 Found: C, 83.85; H, 7.41; B, 2.25; N, 2.99; O, 3.42.

Synthesis of p[B-N]NO: Compound **p[B-N]NO** was synthesized according to the same procedure described above for the synthesis of **p[B-N]O**, **3b** (0.88 g, 0.93 mmol), triethylamine (1.29 mL, 9.3 mmol) in chlorobenzene (15 mL), BBr₃ (0.35 mL, 3.7 mmol) and obtained as blight yellow solid, 0.65 g, yield: 72%. ¹H NMR (400 MHz, Methylene Chloride-d₂) δ (ppm): 9.75 (d, J=1.6, 1H), 8.98 (d, J=7.5, 1H), 8.76 (d, J=2.1, 1H), 8.63 (d, J=8.6, 1H), 8.46 (d, J=7.2, 1H), 8.30 (d, J=1.7, 1H), 8.29 – 8.24 (m, 2H), 8.20 – 8.16 (m, 2H), 7.99 (d, J=1.6, 1H), 7.82 (d, J=8.7, 1H), 7.77 – 7.69 (m, 2H), 7.63 (dd, J=8.7, 1.9, 1H), 7.51 (dd, J=8.6, 1.8, 1H), 7.20 (t, J=7.4, 1H), 7.07 (d, J=1.6, 1H), 6.85 (t, J=7.8, 1H), 6.64 (d, J=8.3, 1H), 1.66 (s, 9H), 1.54 (s, 9H), 1.52 (s, 9H), 1.36 (s, 9H), 0.85 (s, 9H). ¹³C NMR (151 MHz, Methylene Chloride-d₂) δ = 159.23, 152.50, 147.22, 147.08, 145.99, 145.02, 144.89, 144.59, 141.68, 141.39, 138.66, 137.81, 137.37, 132.40, 131.90, 131.21, 130.27, 129.70, 129.51, 126.00, 125.98, 125.84, 125.10, 124.59, 124.24, 123.82, 123.72, 123.56, 122.76, 122.34, 121.87, 121.46, 121.30, 121.22, 120.62, 120.35, 117.65, 117.06, 116.89, 116.80, 116.47, 116.22, 116.02, 115.81, 35.55, 34.94, 34.91, 34.78, 34.41, 32.24, 31.66, 31.40, 31.03. MALDI-TOF: Calculated: 961.5314, Found: 961.7857. Anal. Calcd (%) for C₆₈H₆₅B₂N₃O: C, 84.91; H, 6.81; B, 2.25; N, 4.37; O, 1.66; Found: C, 84.97; H, 6.83; B, 2.21; N, 4.36; O, 1.61.

Synthesis of p[B-N]N: Compound **p[B-N]N** was synthesized according to the same procedure described above for the synthesis of **p[B-N]O**, **2c** (1.0 g, 1.0 mmol), triethylamine (1.44 mL, 10.0 mmol) in chlorobenzene (15 mL), BBr₃ (0.39 mL, 4.0 mmol) and obtained as blight red solid, 0.93 g, yield: 92%. ¹H NMR (400 MHz, Methylene Chloride-d₂) δ (ppm): 9.06 (d, J=7.5, 2H), 8.65 (d, J=8.6, 2H), 8.48 (d, J=7.3, 2H), 8.23 – 8.14 (m, 4H), 8.00 (d, J=1.5, 2H), 7.72 (t, J=7.5, 2H), 7.66 (dd, J=8.6, 1.8, 2H), 7.19 (t, J=7.4, 2H), 7.00 (d, J=1.5, 2H), 6.81 (t, J=7.8, 2H), 6.63 (d, J=8.3, 2H), 1.52 (s, 18H), 0.84 (s, 18H). ¹³C NMR (101 MHz, Methylene Chloride-d₂) δ = 147.15, 144.70, 142.27, 138.35, 137.37, 132.66, 132.46, 129.84, 125.95, 125.90, 125.41, 124.46, 123.77, 122.46, 122.07, 121.67, 121.32, 120.59, 120.38, 117.15, 116.21, 116.04, 115.80, 34.94, 34.38, 31.66, 31.05. MALDI-TOF: Calculated: 978.5004, Found:

978.8860. Anal. Calcd (%) for C₇₀H₆₀B₂N₄: C, 85.89; H, 6.18; B, 2.21; N, 5.72; Found: C, 85.83; H, 6.12; B, 2.25; N, 5.77.

Synthesis of [B-N]N: A solution of butyllithium in hexane (1.6 M, 5.27 mL, 8.42 mmol) was added slowly to a solution of **2d** (3.0 g, 4.21 mmol) in xylene (50 mL) at -30 °C under a nitrogen atmosphere and maintained for 2 hours, boron tribromide (0.48 mL, 5.05 mmol) was added at -30 °C. After the reaction mixture was allowed to warm to room temperature and stirred for 1 h. *N,N*-diisopropylethylamine (1.39 mL, 8.42 mmol) was added at 0 °C, the reaction mixture was stirred at 150 °C for 24 h. Upon being cooled to room temperature, the precipitate was separated by filtration and recrystallized in methanol/dichloromethane to give the pale yellow solid, 1.13 g, yield: 42%. ¹H NMR (700 MHz, Methylene Chloride-d₂) δ (ppm): 8.97 (s, 1H), 8.62 (d, *J* = 8.5 Hz, 1H), 8.48 (s, 2H), 8.39 (s, 1H), 8.34 – 8.23 (m, 5H), 7.91 (t, *J* = 7.5 Hz, 1H), 7.70 (d, *J* = 9.5 Hz, 1H), 7.62 (d, *J* = 8.5 Hz, 1H), 1.64 (d, *J* = 7.0 Hz, 18H), 1.57 (d, *J* = 2.8 Hz, 18H). ¹³C NMR (176 MHz, Methylene Chloride-d₂) δ (ppm): 146.71, 145.84, 145.10, 143.99, 143.85, 143.22, 141.89, 138.70, 137.81, 137.56, 131.58, 129.59, 128.87, 126.78, 126.49, 125.07, 123.65, 123.59, 120.30, 118.33, 117.32, 117.11, 116.92, 115.42, 115.14, 113.98, 112.25, 35.23, 35.20, 34.83, 34.70, 31.95, 31.93, 31.62, 31.58. MALDI-TOF: Calculated: 640.3989, Found: 640.5559. Anal. Calcd (%) for C₄₆H₄₉BN₂: C, 86.23; H, 7.71; B, 1.69; N, 4.37; Found: C, 86.01; H, 7.82; B, 1.57; N, 4.53.

2. Supplementary figures and tables

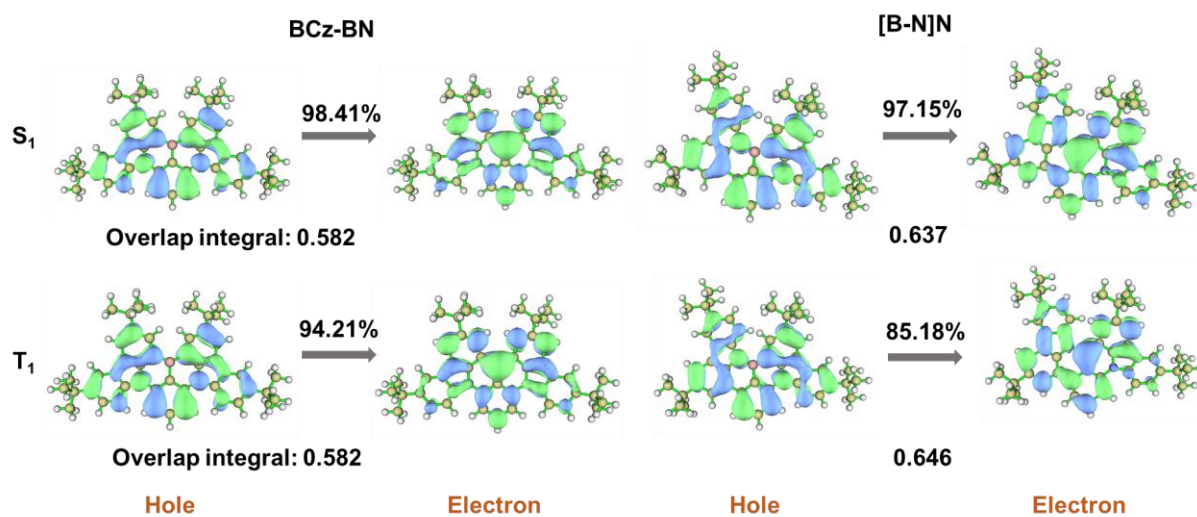


Figure S1. Natural Transition Orbitals (NTO) describing the excitation characters of the S_1 and T_1 states in BCzBN and [B-N]N. The weights of the hole-electron contributions to the excitations and the overlap integral of the two orbitals are included.

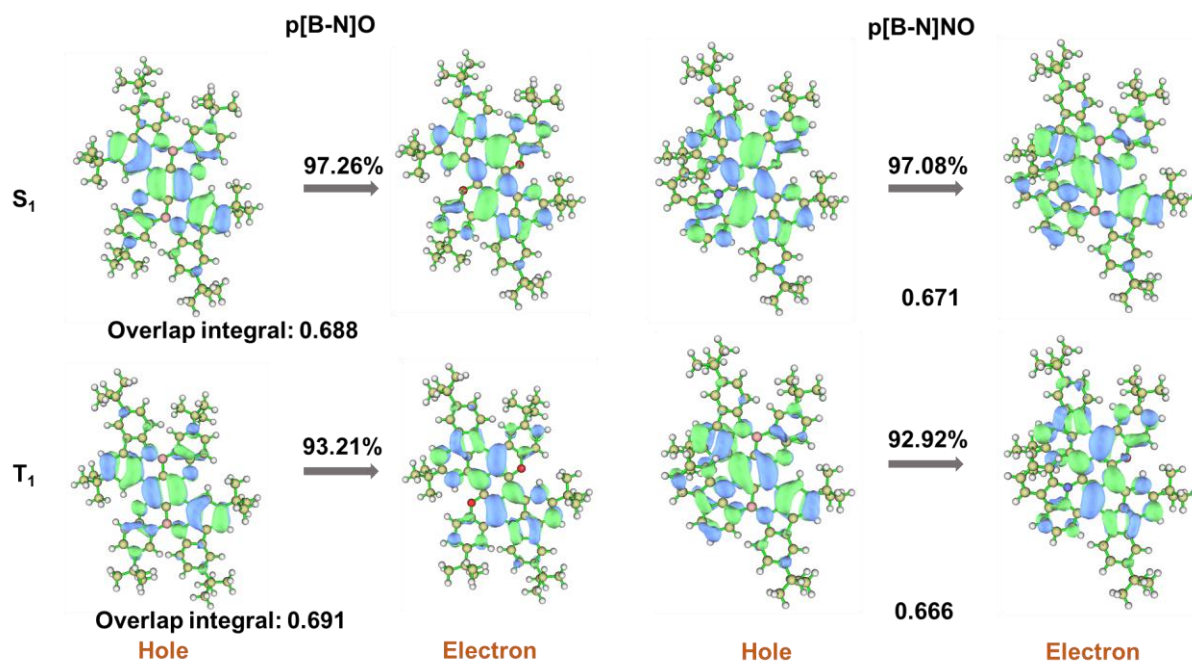


Figure S2. Natural Transition Orbitals (NTO) describing the excitation characters of the S_1 and T_1 states in $p[B\text{-}N]\text{O}$ and $p[B\text{-}N]\text{NO}$. The weights of the hole-electron contributions to the excitations and the overlap integral of the two orbitals are included.

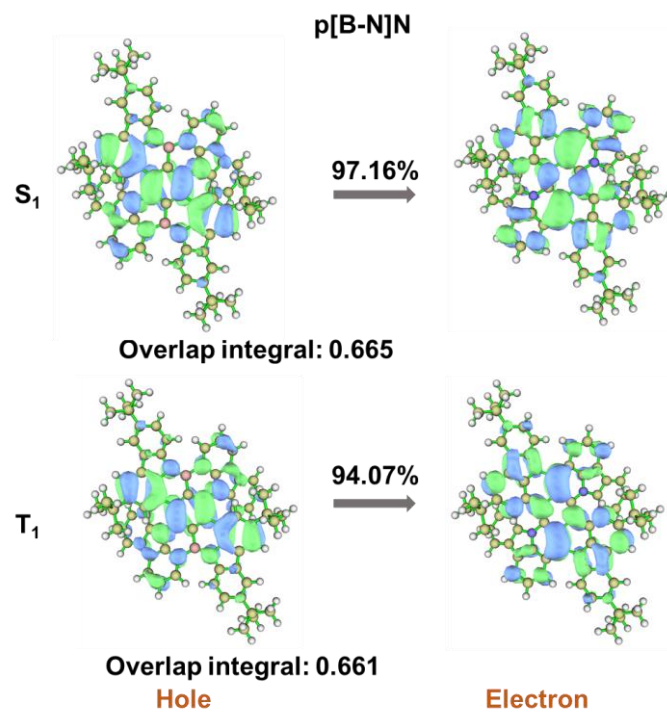


Figure S3. Natural Transition Orbitals (NTO) describing the excitation characters of the S_1 and T_1 states in $\mathbf{p[B-N]N}$. The weights of the hole-electron contributions to the excitations and the overlap integral of the two orbitals are included.

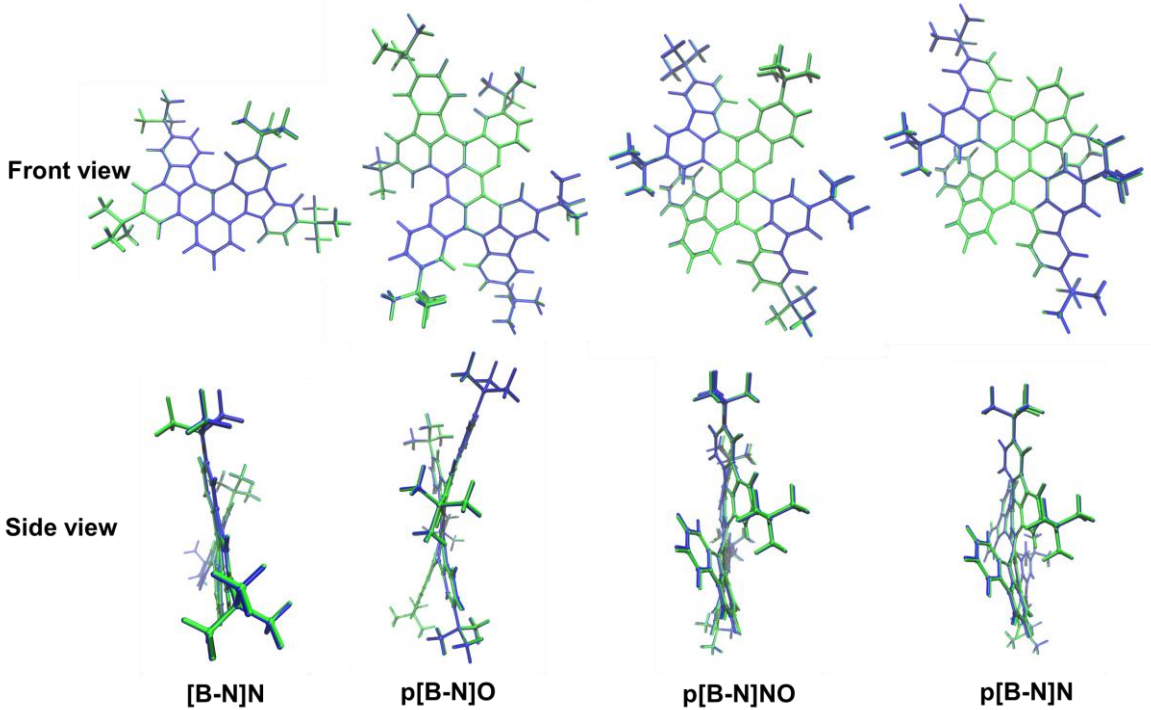


Figure S4. Comparison of the optimized structures of $[\mathbf{B-N}]N$, $p[\mathbf{B-N}]O$, $p[\mathbf{B-N}]NO$ and $p[\mathbf{B-N}]N$ in the S_0 (blue) and S_1 (green) states.

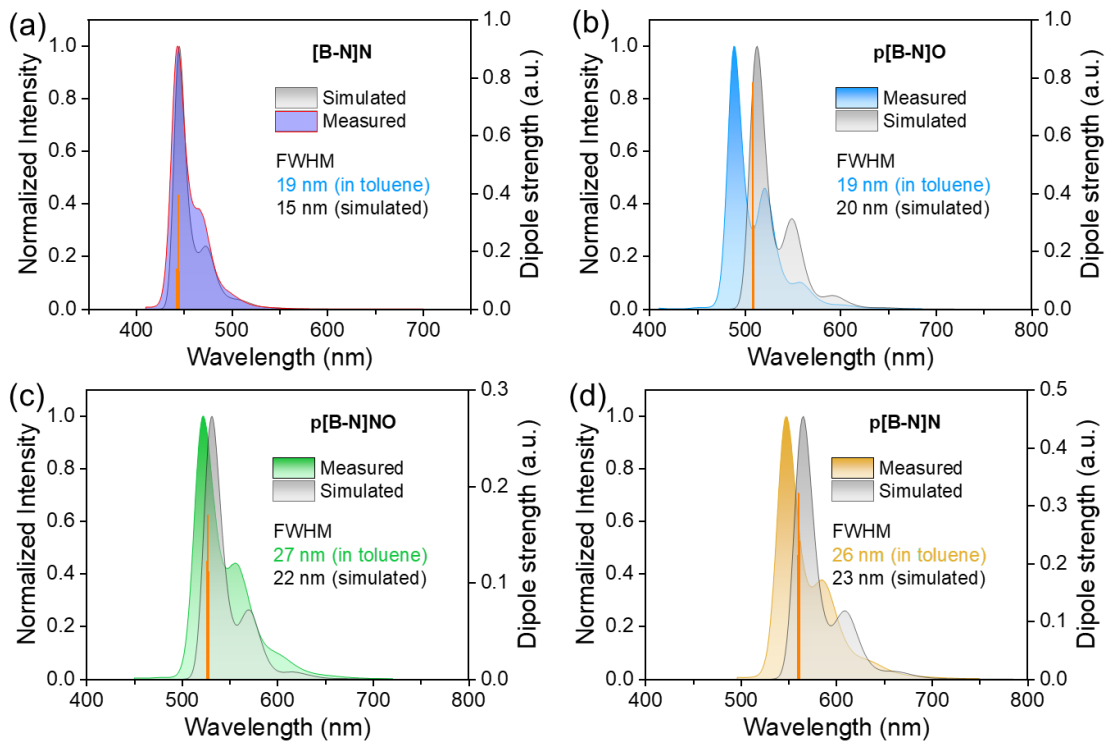


Figure S5. Contrast of emission spectra measured in toluene solution and emission spectra simulated by Franck-Condon analysis on the S_1-S_0 transition of (a) $[\mathbf{B-N}]N$, (b) $p[\mathbf{B-N}]O$, (c)

p[B-N]NO and (d) **p[B-N]N**. Band broadening simulated by mean of Gaussian functions with half-widths at half-maximum of 300 cm^{-1} .

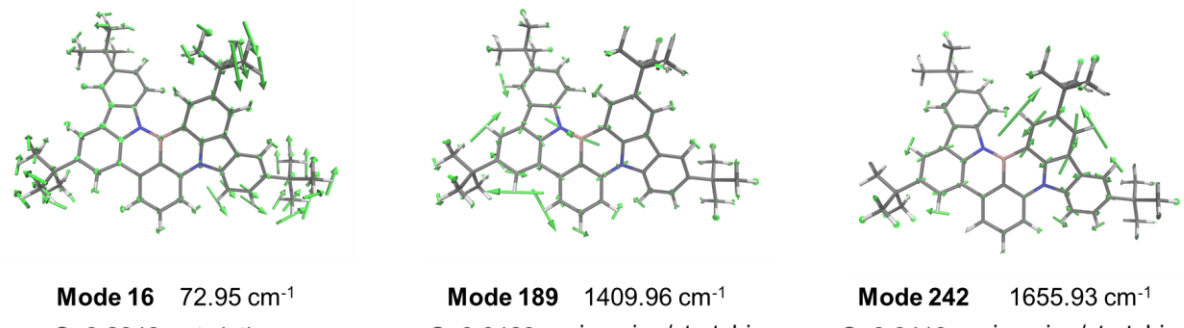


Figure S6. Normal vibrational modes in the S_0 state involved in the Franck-Condon spectral progression of **[B-N]N**.

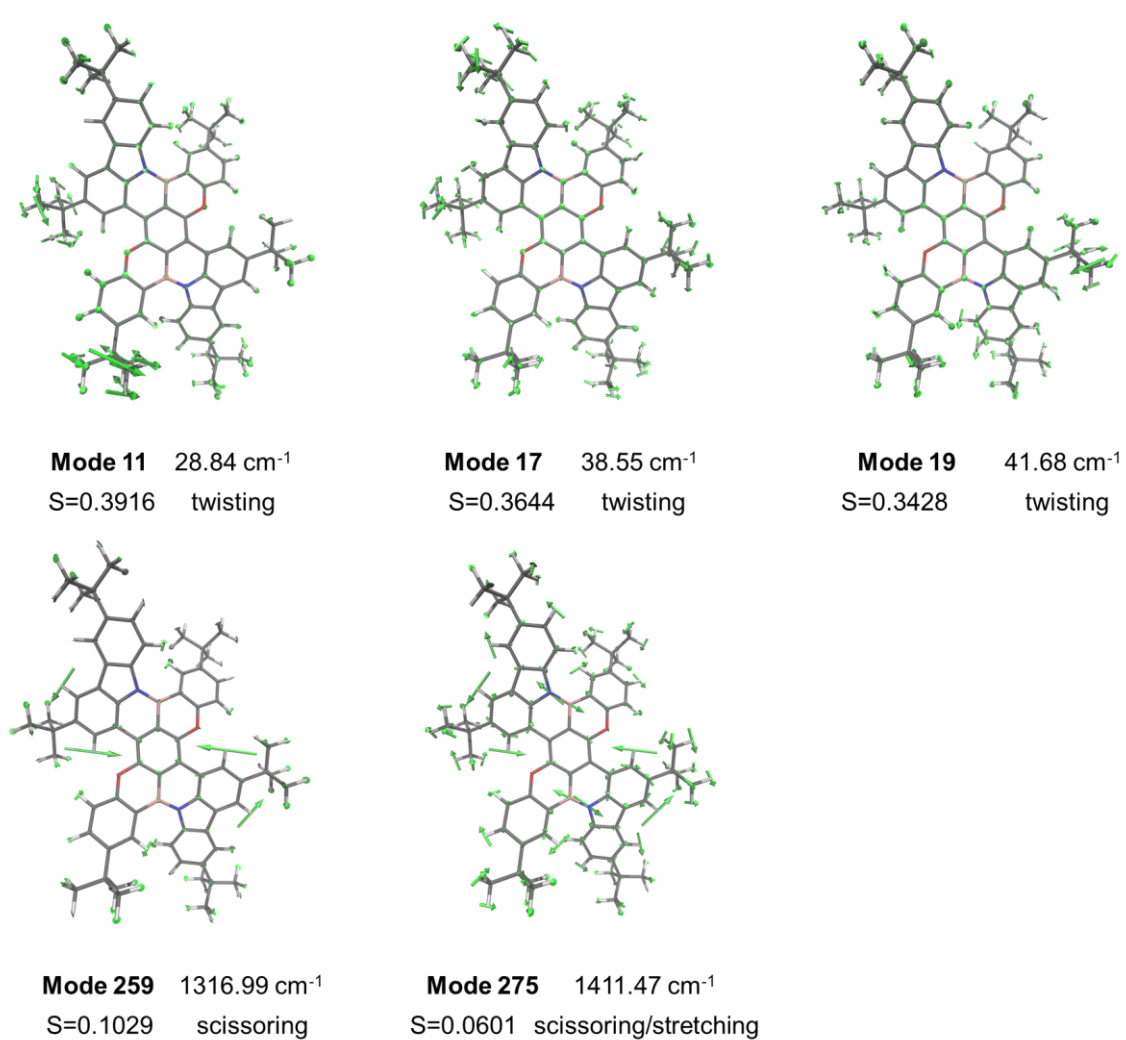


Figure S7. Normal vibrational modes in the S_0 state involved in the Franck-Condon spectral progression of **p[B-N]O**.

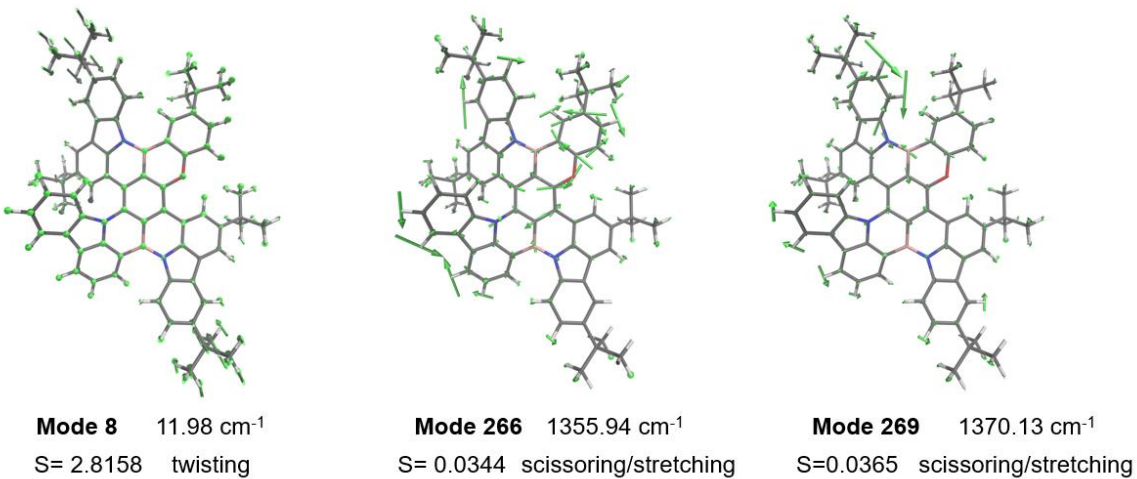


Figure S8. Normal vibrational modes in the S_0 state involved in the Franck-Condon spectral progression of **p[B-N]NO**.

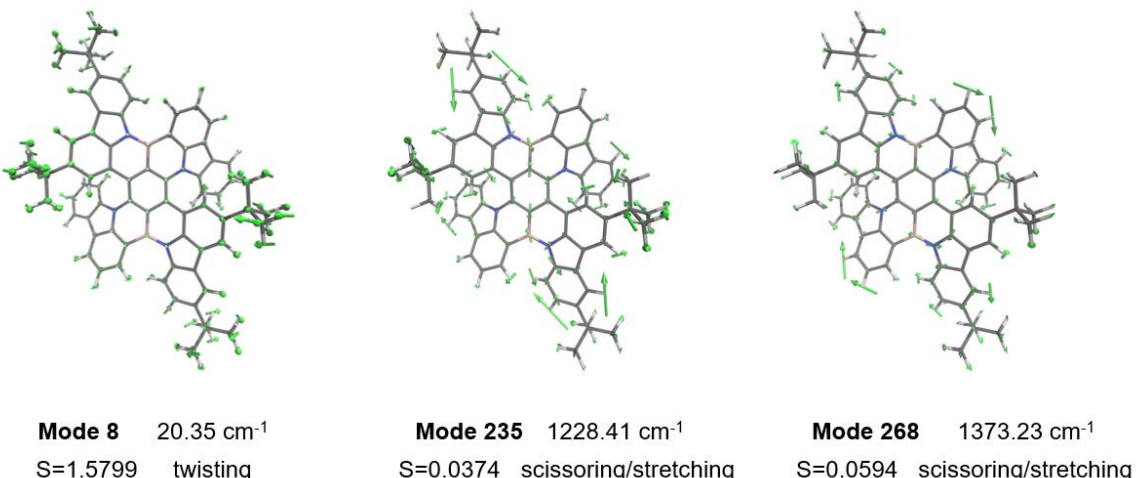


Figure S9. Normal vibrational modes in the S_0 state involved in the Franck-Condon spectral progression of **p[B-N]N**.

Table S1. Summary of TD-DFT calculation for **[B-N]N**, **p[B-N]O**, **p[B-N]NO** and **p[B-N]N** at the S_0 structures based on B3LYP/6-31G(d, p) level.

Compound	Optimized Structure	Transition	Wavelength (nm)	Energy (eV)	Oscillator Strength
[B-N]N	S_0	$S_0 \rightarrow S_1$	408.13	3.0378	0.3667
		$S_0 \rightarrow T_1$	482.08	2.5718	0
p[B-N]O	S_0	$S_0 \rightarrow S_1$	463.22	2.6766	0.5573
		$S_0 \rightarrow T_1$	590.82	2.0985	0
p[B-N]NO	S_0	$S_0 \rightarrow S_1$	489.46	2.5331	0.4101
		$S_0 \rightarrow T_1$	610.26	2.0317	0

p[B-N]N	S_0	$S_0 \rightarrow S_1$	511.32	2.4248	0.3496
		$S_0 \rightarrow T_1$	630.72	1.9658	0

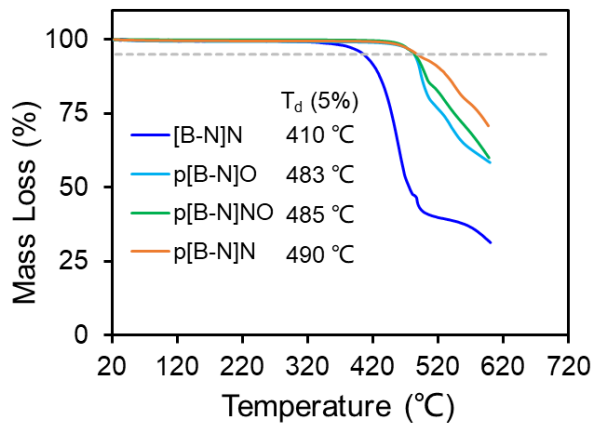
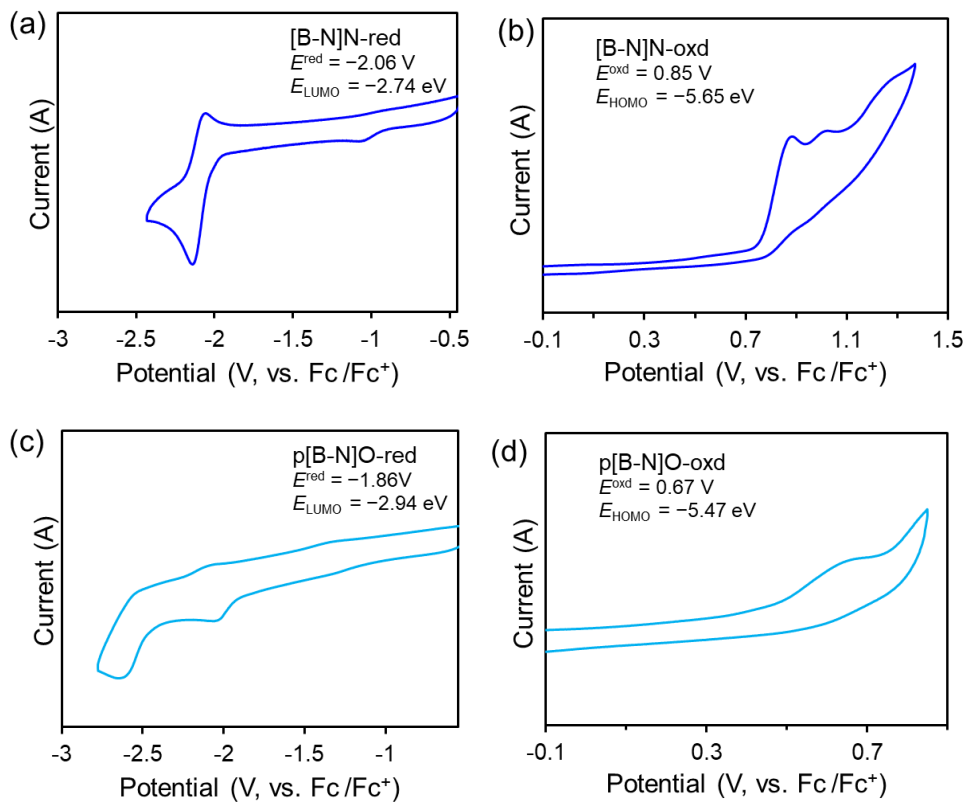


Figure S10. Decomposition temperature (T_d) with 5% weight loss for **[B-N]N**, **p[B-N]O**, **p[B-N]NO** and **p[B-N]N**.



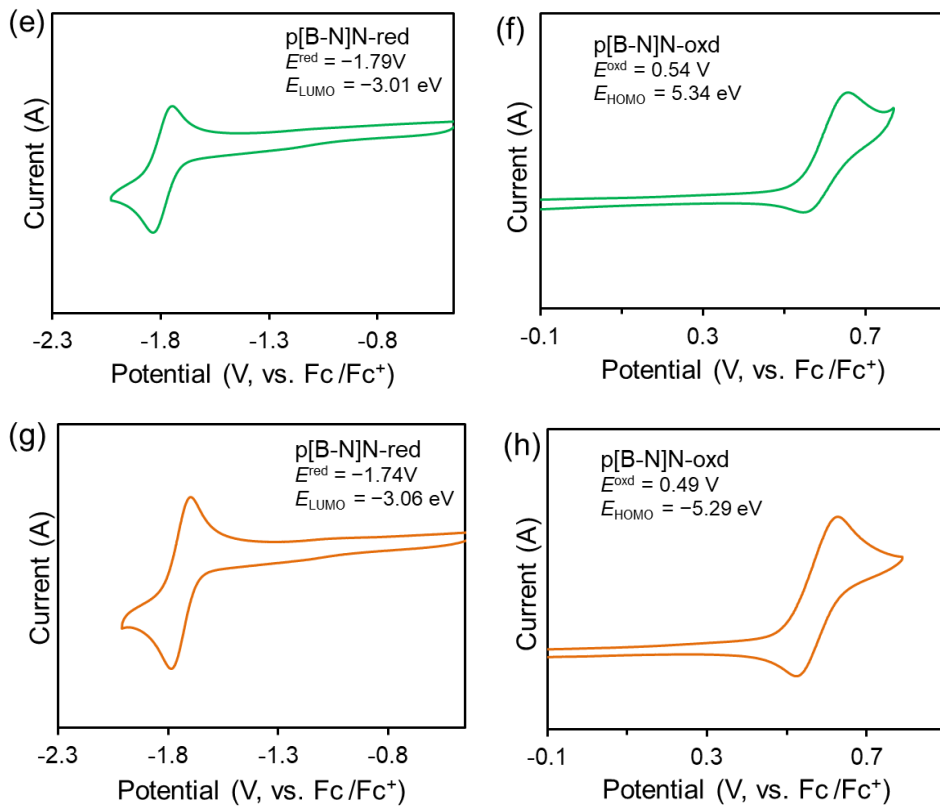


Figure S11. Cyclic voltammograms (CV) for $[\text{B}\text{-}\text{N}]\text{N}$, $p[\text{B}\text{-}\text{N}]\text{O}$, $p[\text{B}\text{-}\text{N}]\text{NO}$ and $p[\text{B}\text{-}\text{N}]\text{N}$. The CV curves were measured at room temperature with 0.1 M solution of $n\text{-Bu}_4\text{NPF}_6$ in dichloromethane for the reduction (a, c, e, g) and oxidation (b, d, f, h) scan (vs Fc/Fc^+); HOMO and LUMO energies obtained from electrochemical data.

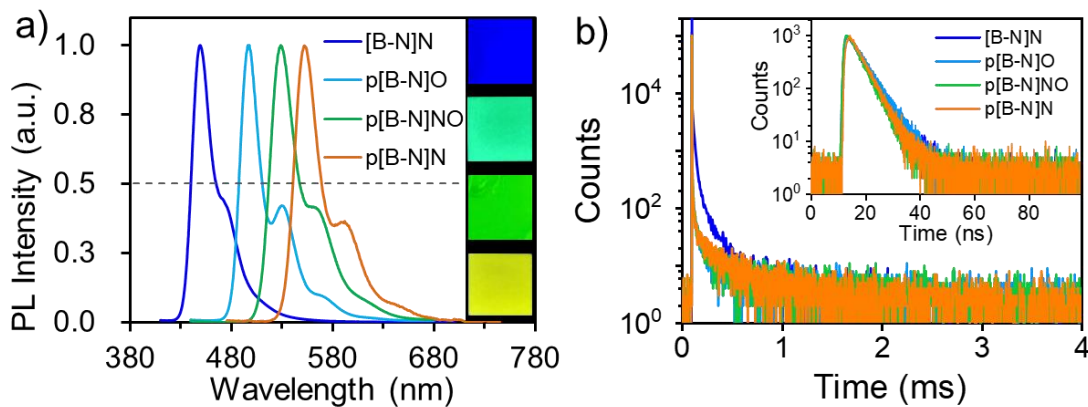


Figure S12. (a) The PL spectra and (b) transient PL curves of $[\text{B}\text{-}\text{N}]\text{N}$, $p[\text{B}\text{-}\text{N}]\text{O}$, $p[\text{B}\text{-}\text{N}]\text{NO}$ and $p[\text{B}\text{-}\text{N}]\text{N}$ doped mCPBC films.

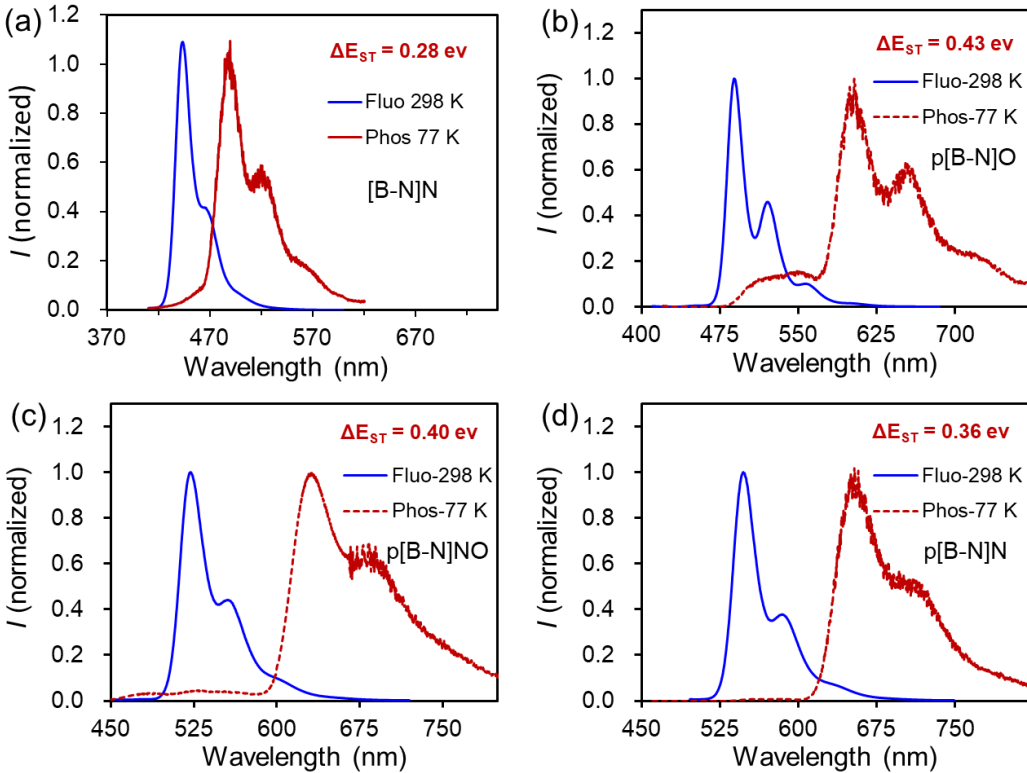


Figure S13. The fluorescence and phosphorescence spectra of **[B-N]N**, **p[B-N]O**, **p[B-N]NO** and **p[B-N]N** in toluene solution. The singlet-triplet energy gaps were estimated from the maximum peak position of fluorescence (298 K) or phosphorescence (77 K). $\Delta E_{ST}=E_S-E_T$.

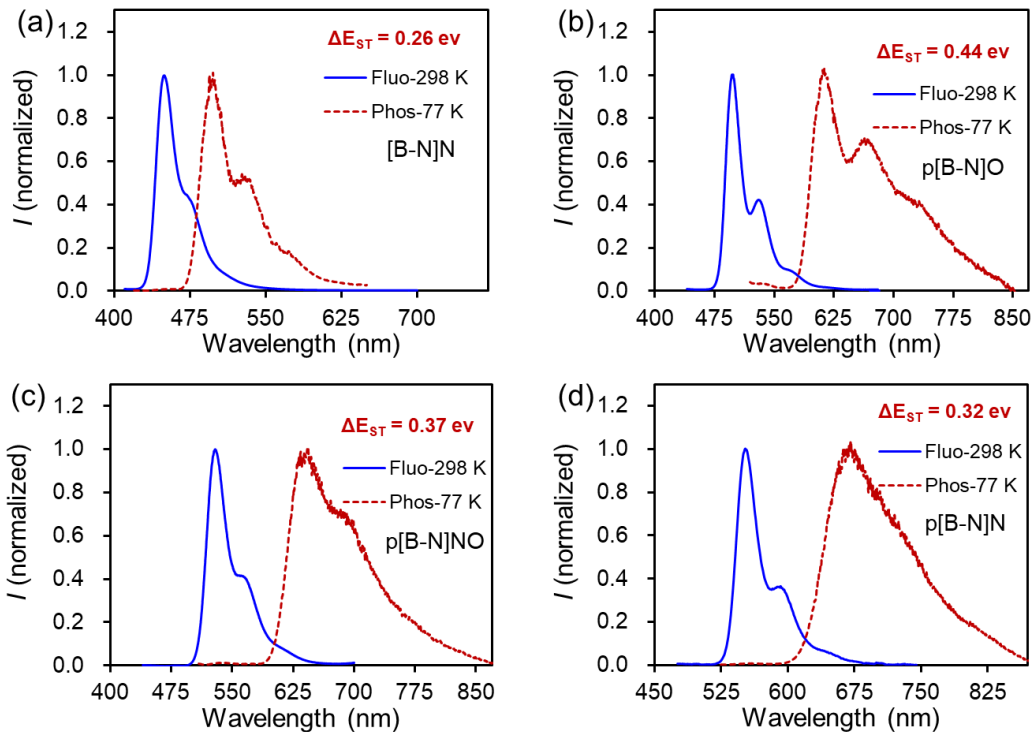


Figure S14. The fluorescence and phosphorescence spectra of 1.0 wt% doping concentration of **[B-N]N**, **p[B-N]O**, **p[B-N]NO** and **p[B-N]N** in mCPBC doped films.

singlet-triplet energy gaps were estimated from the onsets of fluorescence (298 K) or phosphorescence (77 K). $\Delta E_{\text{ST}} = E_{\text{S}} - E_{\text{T}}$.

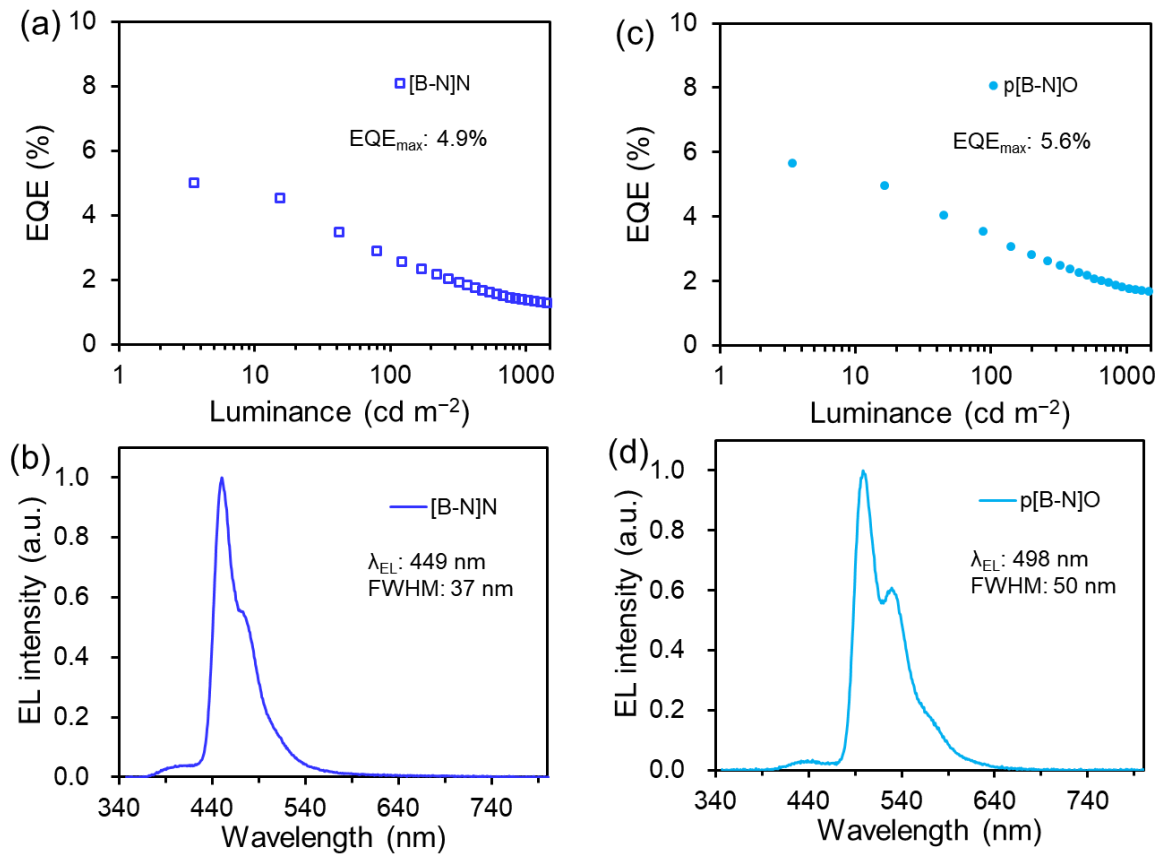


Figure S15. (a, c) The EQE versus brightness and (b, d) EL spectra for **[B-N]N** and **p[B-N]O** based devices. Based on a device structure of ITO/ NPB (30 nm)/ TCTA (5 nm)/ mCP (5 nm)/ mCPBC: 2 wt% **[B-N]N/p[B-N]O** (30 nm)/ CzPhPy (15 nm)/ DPPyA (30 nm)/ LiF (0.5 nm)/ Al (150 nm).

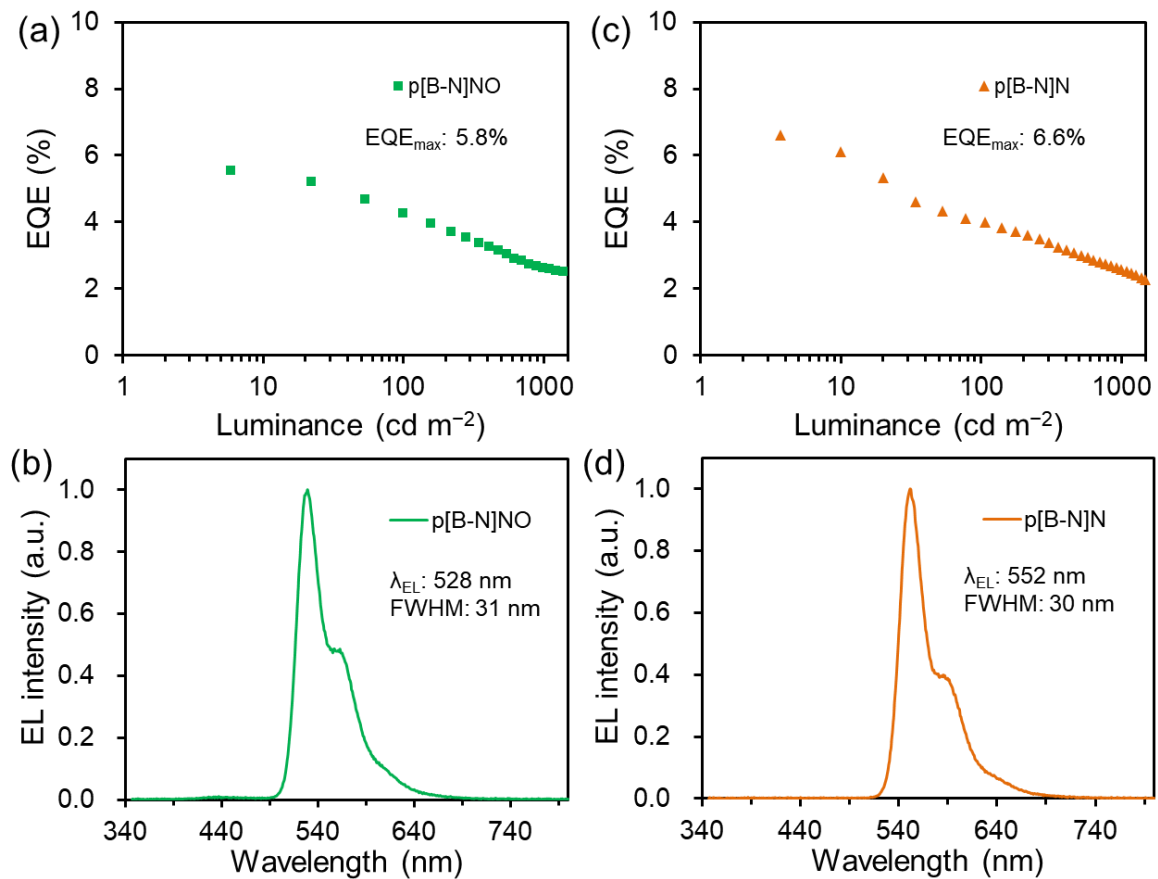


Figure S16. (a, c) The EQE versus brightness and (b, d) EL spectra for **p[B-N]NO** and **p[B-N]N** based devices. Based on a device structure of ITO/ NPB (30 nm)/ TCTA (5 nm)/ mCP (5 nm)/ mCPBC: 2 wt% **p[B-N]NO/p[B-N]N** (30 nm)/ CzPhPy (15 nm)/ DPPyA (30 nm)/ LiF (0.5 nm)/ Al (150 nm).

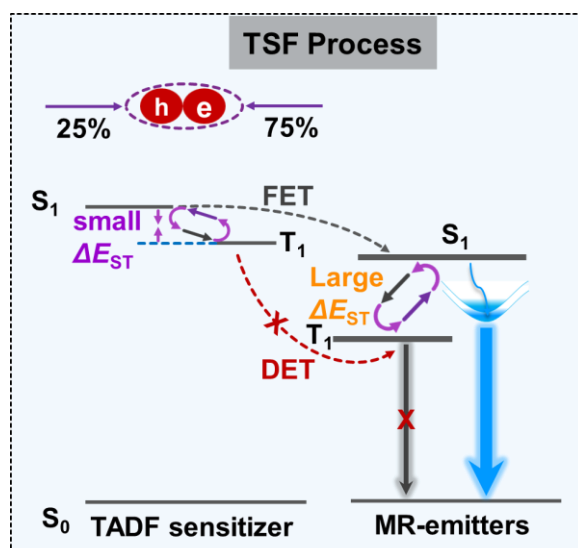


Figure S17. The energy transfer process in the TSF devices.

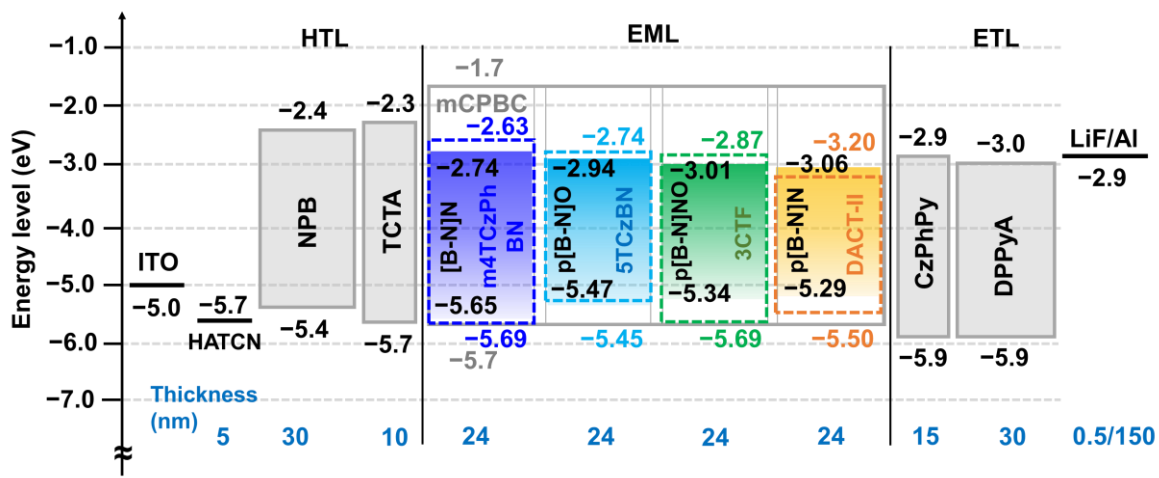


Figure S18. The device structure with energy-level diagram based on the derivatives of [B-N]N system.

Table S2. The basic material and chemical structures used in the devices.

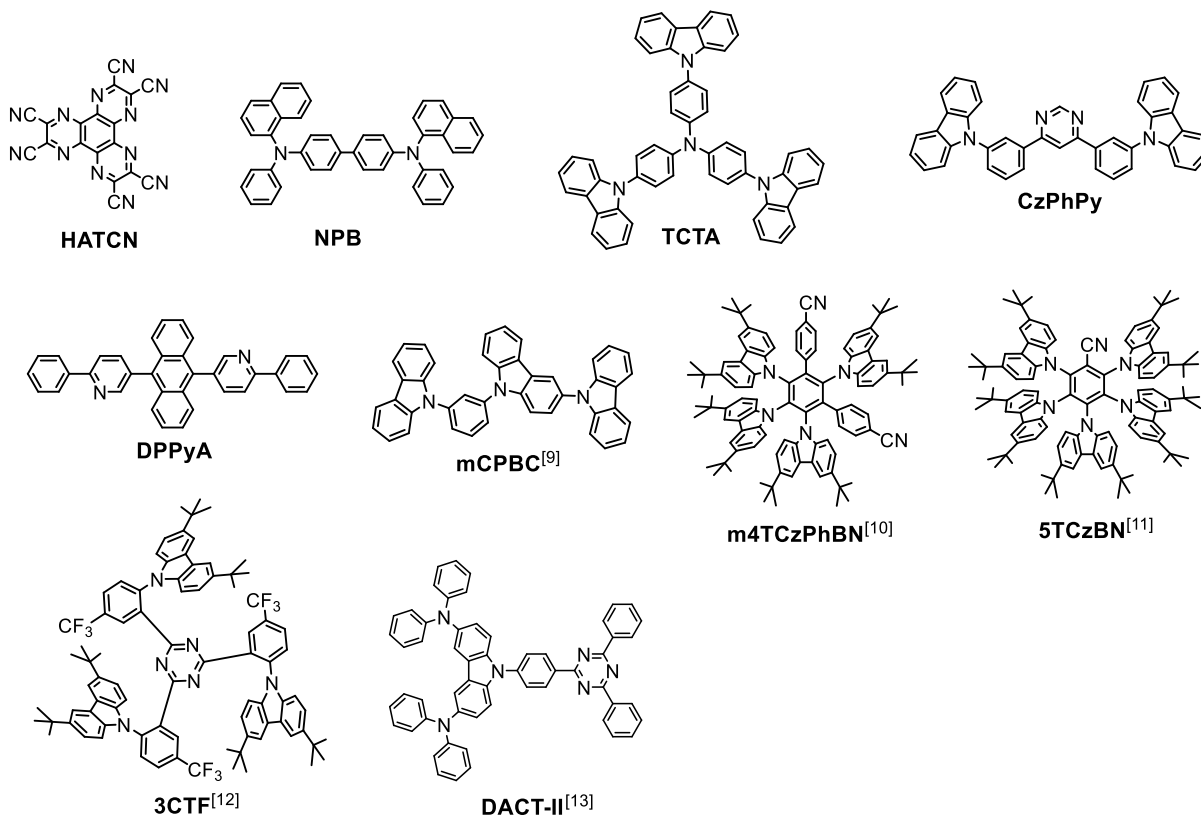


Table S3. Photophysical properties of 30 wt% sensitizer and 30 wt% sensitizer: 1 wt% MR emitter doped in mCPBC.

Compound	Doped film	λ_{PL} [nm]	FWHM [nm]	Φ_{PL} [%]	τ_{PF} [ns]	τ_{DF} [μ s]
m4TCzPhBN	30 wt%	442	52	80	5.0	1.70
[B-N]N	30 wt%:1 wt%	451	26	84	4.8	0.74
5TCzBN	30 wt%	492	82	91	11.6	6.27
p[B-N]O	30 wt%:1 wt%	497	25	95	6.9	2.94
3CTF	30 wt%	513	87	89	41.2	1.81
p[B-N]NO	30 wt%:1 wt%	528	31	92	6.7	0.81
DACT-II	30 wt%	543	96	90	8.7	0.76
p[B-N]N	30 wt%:1 wt%	551	29	91	5.7	0.42

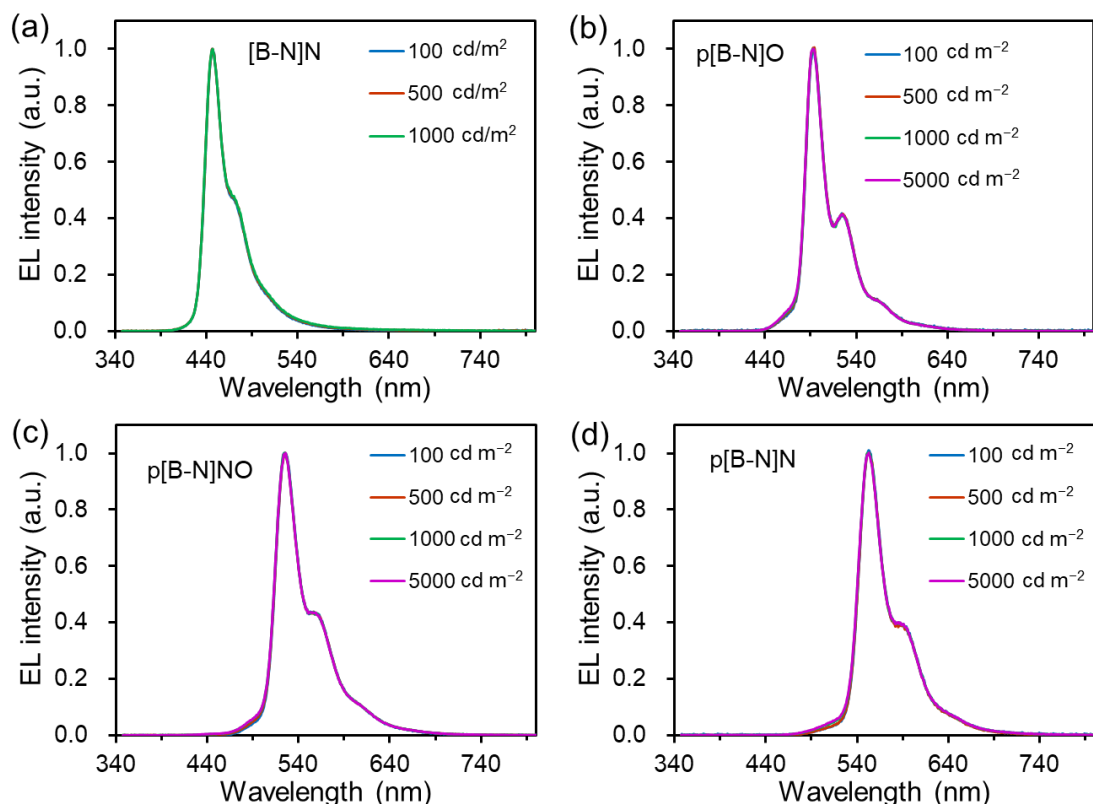


Figure S19. The EL spectra of 1.0 wt% doped devices based (a) [B-N]N, (b) p[B-N]O, (c) p[B-N]NO and (d) p[B-N]N under different brightness.

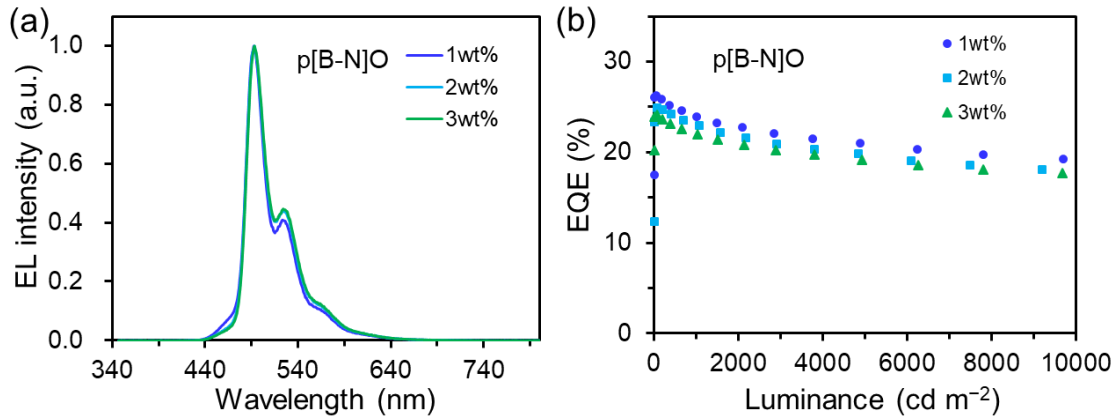


Figure S20. (a) The EL spectra and (b) EQE versus brightness characters for devices based on **p[B-N]O**. The devices based on a structure of ITO/ HATCN (5 nm)/ NPB (30 nm)/ TCTA (5 nm)/ mCPBC: 30.0% 5TCzBN: 1.0-3.0 wt% **p[B-N]O** (24 nm)/ CzPhPy (10 nm)/ DPPyA(30 nm)/ LiF (0.5 nm)/ Al (150 nm).

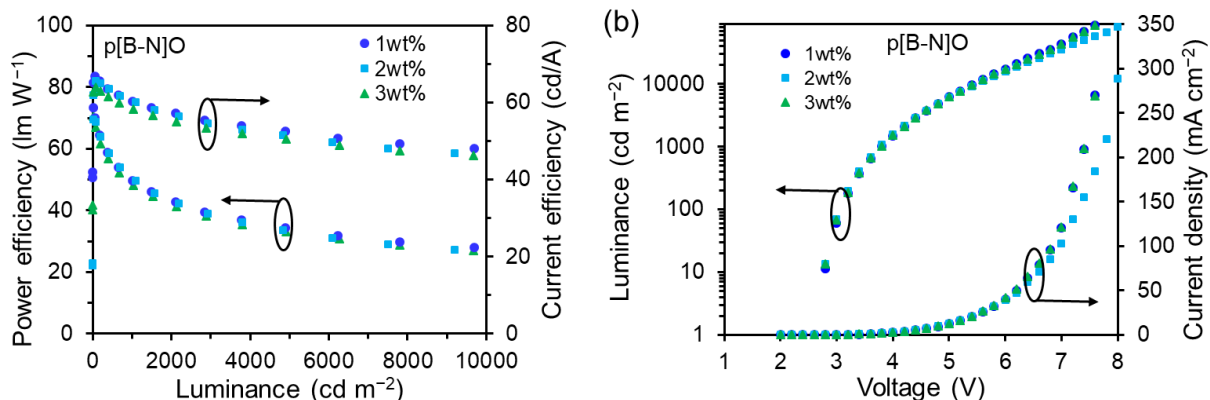


Figure S21. (a) The power efficiency and current efficiency versus brightness characters and (b) luminance-voltage-current density characters for devices based on **p[B-N]O**.

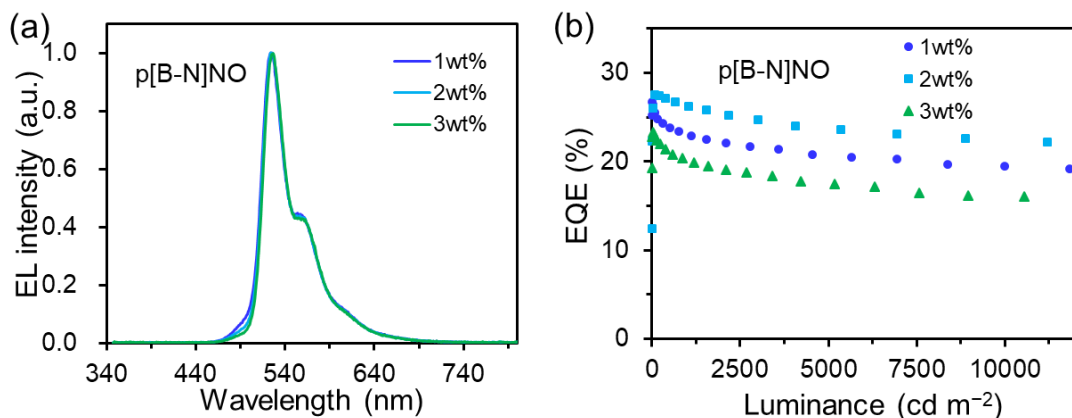


Figure S22. (a, c) The EL spectra and (b, d) EQE versus brightness characters for devices based on **p[B-N]NO**. The devices based on a structure of ITO/ HATCN (5 nm)/ NPB (30 nm)/ TCTA (5 nm)/ mCPBC: 30.0% 3CTF: 1.0-3.0 wt% **p[B-N]NO** (24 nm)/ CzPhPy (10 nm)/ DPPyA(30 nm)/ LiF (0.5 nm)/ Al (150 nm).

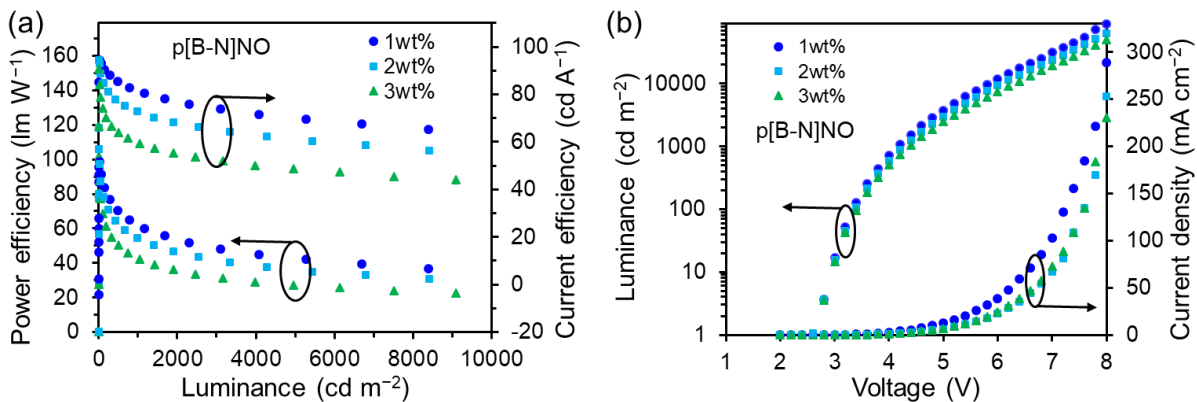


Figure S23. (a) The power efficiency and current efficiency versus brightness characters and (b) luminance-voltage-current density characters for devices based on **p[B-N]NO**.

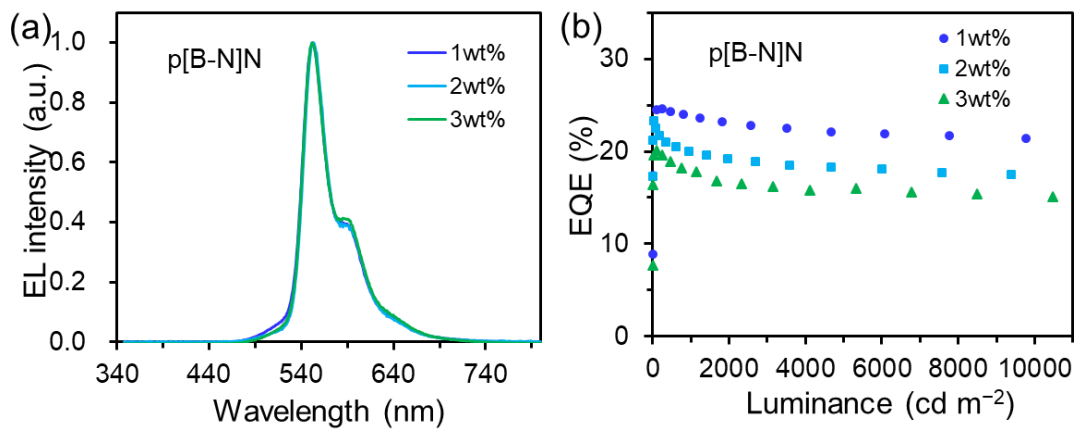


Figure S24. (a) The EL spectra and (b) EQE versus brightness characters for devices based on **p[B-N]N**. The devices based on a structure of ITO/ HATCN (5 nm)/ NPB (30 nm)/ TCTA (5 nm)/ mCPBC: 30.0% DACT-II: 1.0-3.0 wt% **p[B-N]N** (24 nm)/ CzPhPy (10 nm)/ DPPyA(30 nm)/ LiF (0.5 nm)/ Al (150 nm).

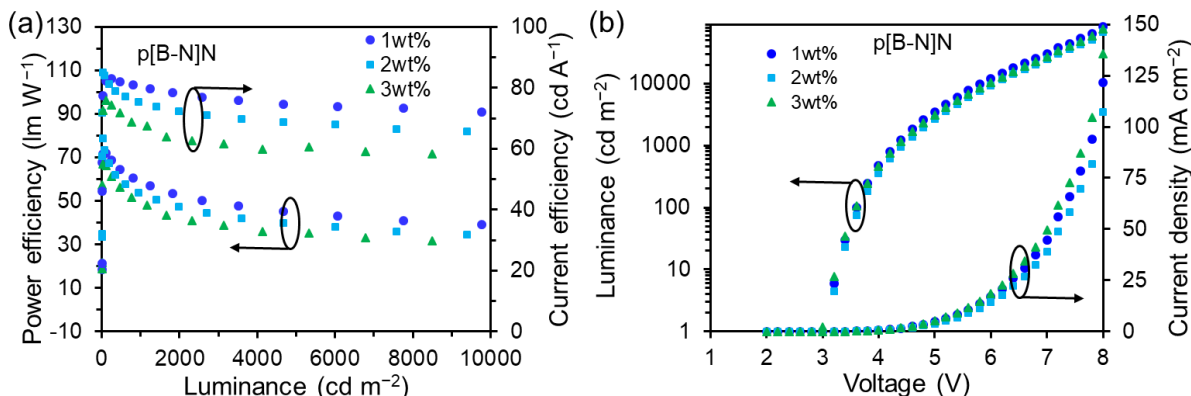


Figure S25. (a) The power efficiency and current efficiency versus brightness characters and (b) luminance-voltage-current density characters for devices based on **p[B-N]N**.

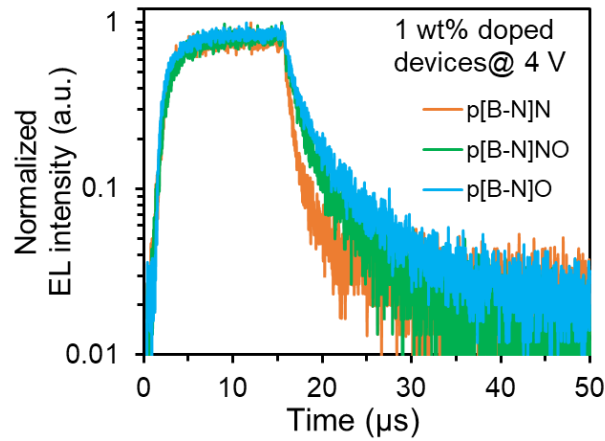


Figure S26. EL transient spectra of devices based on **p[B-N]O**, **p[B-N]NO** and **p[B-N]N** under the voltage of 4 V.

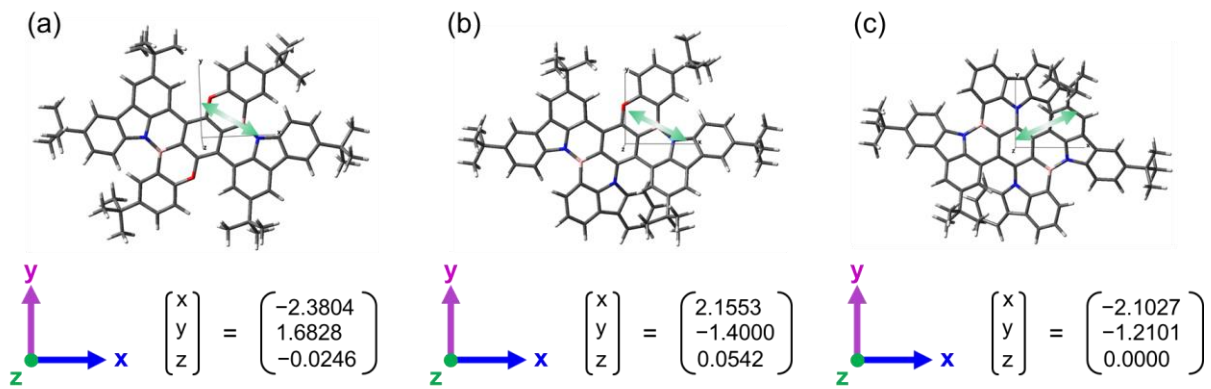


Figure S27. The optimized S_0 state geometry of (a) **p[B-N]O**, (b) **p[B-N]NO** and (c) **p[B-N]N**, and the direction of their transition dipole moments.

Table S4. Summary of the device performances of the OLEDs based on **p[B-N]O**, **p[B-N]NO** and **p[B-N]N**.

Compounds	x wt%	λ_{EL} a) [nm]	FWHM b) [nm]	V_{on} c) [V]	$L_{max}^d)$ [cd m^{-2}]	CE ^{e)} [cd A ⁻¹]	PE ^{f)} [lm W ⁻¹]	EQE ^{g)} [%]	CIE (x,y) ^{a)}
p[B-N]O	1.0	493	24.6	2.6	112000	66.8/60.2/52.6	73.2/49.8/34.4	26.3/24.0/21.0	(0.163, 0.514)
	2.0	493	24.8	2.6	108000	65.7/60.1/51.4	69.5/49.7/33.7	24.9/22.9/19.8	(0.172, 0.537)
	3.0	493	25.2	2.6	116000	64.1/58.2/50.5	70.5/48.1/33.0	24.1/22.0/19.2	(0.174, 0.544)
p[B-N]NO	1.0	524	31.6	2.6	91000	99.9/87.8/79.2	110.7/65.7/47.9	26.7/22.9/20.7	(0.303, 0.645)
	2.0	525	31.2	2.6	106000	102.0/96.6/85.8	101.0/75.9/53.9	27.6/26.3/23.6	(0.306, 0.648)
	3.0	526	30.8	2.6	111000	90.2/77.5/67.7	97.1/55.3/38.0	23.3/19.9/17.5	(0.309, 0.651)
p[B-N]N	1.0	552	31.3	3.1	127000	83.0/79.6/74.7	71.9/56.9/45.1	24.6/23.6/22.1	(0.414, 0.571)
	2.0	553	31.2	3.1	104000	85.2/73.9/68.8	78.7/50.4/40.0	23.3/19.6/18.3	(0.422, 0.567)
	3.0	553	31.1	3.0	116000	76.0/67.4/60.7	67.1/48.2/35.3	20.1/17.8/16.0	(0.423, 0.567)

[a] Value recorded at a luminance around $1,000\text{ cd cm}^{-2}$; [b] Full width at half maximum of EL given in

wavelength; [c] Turn-on voltage at the luminance of 1 cd m⁻²; [d] Maximum luminescence (L); [e] Maximum CE, value at 1,000 and 5,000 cd cm⁻²; [f] Maximum PE, value at 1,000 and 5,000 cd cm⁻²; [g] Maximum EQE, value at 1,000 and 5,000 cd cm⁻².

Table S5. All vibration modes in the S₀ state involved in the Franck-Condon spectral progression of p[B-N]O, p[B-N]NO and p[B-N]N at the (TD)B3LYP/6-31G(d,p) level.

Compound	p[B-N]O			p[B-N]NO			
vibration mode	ω (cm ⁻¹)	S	λ (cm ⁻¹)	vibration mode	ω (cm ⁻¹)	S	λ (cm ⁻¹)
1	0	0	0	1	0	0	0
2	0	0	0	2	0	0	0
3	0	0	0	3	0	0	0
4	0	0	0	4	0	0	0
5	0	0	0	5	0	0	0
6	0	0	0	6	0	0	0
7	6.52	0.00489	0.03	7	11.75	0.08741	1.03
8	11.61	0.00192	0.02	8	11.98	2.81582	33.73
9	19.66	0.03567	0.7	9	23.27	0.3321	7.73
10	25.38	0.00187	0.05	10	25.03	0.08631	2.16
11	28.84	0.39156	11.29	11	27.66	0.00002	0
12	29.76	0.10842	3.23	12	30.91	0.0399	1.23
13	30.55	0	0	13	33.06	0.00242	0.08
14	31.28	0.00648	0.2	14	36.41	0.12541	4.57
15	34.94	0.00038	0.01	15	39.93	0.00207	0.08
16	35.16	0.08805	3.1	16	41.95	0.01412	0.59
17	38.55	0.36441	14.05	17	42.35	0.00576	0.24
18	39.32	0.0763	3	18	45.58	0.1091	4.97
19	41.68	0.34281	14.29	19	57.27	0.09486	5.43
20	51.59	0.01014	0.52	20	64.1	0.01053	0.67
21	61.49	0.1885	11.59	21	69.06	0.00299	0.21
22	65.95	0.00177	0.12	22	74.44	0.00011	0.01
23	76.58	0.00762	0.58	23	77.91	0.04657	3.63
24	79.55	0.0243	1.93	24	87.78	0.13164	11.56
25	83.02	0.03857	3.2	25	90.78	0.01113	1.01
26	87.51	0.01444	1.26	26	93.28	0.00802	0.75
27	93.78	0	0	27	106.37	0	0
28	100.95	0.07831	7.91	28	112.28	0.00647	0.73
29	112.61	0.06421	7.23	29	120.89	0.01125	1.36
30	124.73	0.04051	5.05	30	124.52	0.02898	3.61
31	129.15	0.0022	0.28	31	142	0.01284	1.82
32	139.85	0.0009	0.13	32	143.2	0.00545	0.78

33	148.05	0.00703	1.04	33	148.44	0.00796	1.18
34	151.25	0.07209	10.9	34	153.31	0.00325	0.5
35	154.25	0.00161	0.25	35	159.47	0.00325	0.52
36	161.16	0.00012	0.02	36	162.63	0.00457	0.74
37	164.42	0.00054	0.09	37	168.15	0.01209	2.03
38	174.65	0.0057	1	38	190.86	0.00075	0.14
39	184.49	0.00069	0.13	39	195.54	0.01152	2.25
40	192.93	0.00039	0.08	40	198.87	0.00088	0.18
41	199.77	0.00014	0.03	41	211.48	0.00109	0.23
42	206.96	0.01993	4.12	42	220.12	0.00961	2.12
43	212.12	0.00054	0.12	43	224.14	0.01399	3.14
44	217.1	0.00001	0	44	225.72	0.01183	2.67
45	228.25	0.00307	0.7	45	232.98	0.0066	1.54
46	232.5	0.00255	0.59	46	235.35	0.00156	0.37
47	234.2	0.00013	0.03	47	236.67	0.0009	0.21
48	235.78	0.00053	0.13	48	237.65	0.00063	0.15
49	237.01	0.00004	0.01	49	238.57	0.00062	0.15
50	238.02	0.00082	0.2	50	245.45	0.02078	5.1
51	241.92	0.00521	1.26	51	250.02	0.00697	1.74
52	250.82	0.0106	2.66	52	258.27	0.00051	0.13
53	253.39	0.00033	0.08	53	264.08	0.00036	0.09
54	260.38	0.00125	0.33	54	270.67	0	0
55	263.6	0.00997	2.63	55	274.6	0	0
56	268.45	0	0	56	276.53	0.00405	1.12
57	272.31	0.01032	2.81	57	279.83	0.00352	0.98
58	273.42	0.00313	0.86	58	280.63	0.03226	9.05
59	275.69	0.00007	0.02	59	284.38	0.00939	2.67
60	278.1	0.00005	0.01	60	288.36	0.00204	0.59
61	281.36	0.00086	0.24	61	289.68	0.0434	12.57
62	284.64	0.01295	3.69	62	301.81	0.00359	1.08
63	287.51	0.00879	2.53	63	304.57	0.02202	6.71
64	290.84	0.01089	3.17	64	307.35	0.01479	4.55
65	298.25	0.00048	0.14	65	311.93	0.01234	3.85
66	300.47	0.0003	0.09	66	317.47	0.00162	0.52
67	308.79	0.00001	0	67	318.21	0.0121	3.85
68	312.4	0.01774	5.54	68	321.11	0.00046	0.15
69	315.4	0.01669	5.26	69	326.87	0.02114	6.91
70	324.54	0.03774	12.25	70	329.32	0.00718	2.36
71	325.71	0.00081	0.26	71	332.6	0.00012	0.04
72	328.21	0.01494	4.9	72	333.82	0.00028	0.09
73	330.66	0.00479	1.58	73	334.3	0.00036	0.12
74	331.95	0.00008	0.03	74	334.89	0.00011	0.04
75	332.81	0.00045	0.15	75	339.33	0.01439	4.88

76	335.02	0.0005	0.17	76	342.04	0.0097	3.32
77	335.37	0.00297	0.99	77	349.49	0.00001	0
78	336.34	0.00074	0.25	78	354.08	0.00012	0.04
79	340.92	0.00789	2.69	79	358.28	0.00024	0.08
80	347.07	0.02313	8.03	80	361.64	0.00071	0.26
81	355.07	0.01494	5.3	81	365.71	0.00011	0.04
82	355.69	0.003	1.07	82	368.52	0.00075	0.28
83	363.43	0.00016	0.06	83	371.73	0.02556	9.5
84	365.51	0.00097	0.35	84	377.33	0.0004	0.15
85	366.53	0.00001	0.01	85	380.14	0.00523	1.99
86	369.83	0.0391	14.46	86	383.21	0.00765	2.93
87	373.12	0.00083	0.31	87	389.08	0.00005	0.02
88	376.38	0.0062	2.33	88	422.5	0.00885	3.74
89	381.43	0.00004	0.01	89	428.64	0.00661	2.83
90	382.92	0.01057	4.05	90	430.49	0.00634	2.73
91	383.25	0.00155	0.59	91	435.08	0.00626	2.72
92	391.43	0.01129	4.42	92	443.28	0.00001	0
93	424.01	0.00038	0.16	93	445.61	0.00311	1.39
94	428.07	0.00038	0.16	94	448.86	0.00196	0.88
95	429.73	0.01249	5.37	95	452.33	0.00172	0.78
96	431.41	0.00019	0.08	96	453.15	0.02019	9.15
97	440.31	0	0	97	458.77	0.00001	0.01
98	444.57	0.00001	0	98	463.05	0.02297	10.64
99	447.66	0.00495	2.22	99	466.5	0.00081	0.38
100	451.96	0.00035	0.16	100	470.6	0.00023	0.11
101	452.38	0.00003	0.01	101	474.96	0.00026	0.12
102	453.04	0.00173	0.78	102	478.04	0.00009	0.04
103	460.16	0.00692	3.18	103	478.91	0.00191	0.91
104	465.94	0.00016	0.08	104	489.78	0.0142	6.95
105	472.15	0.00412	1.95	105	498.87	0.00065	0.32
106	472.91	0.00003	0.01	106	503.16	0.00048	0.24
107	478.57	0.00048	0.23	107	507.23	0.00109	0.55
108	479.09	0.00004	0.02	108	515.52	0.00773	3.98
109	485.02	0.00036	0.18	109	516.99	0.00029	0.15
110	493.09	0.00002	0.01	110	526.67	0.00025	0.13
111	501.32	0.00012	0.06	111	539.2	0.00894	4.82
112	507.37	0.0001	0.05	112	548.17	0.00111	0.61
113	509.75	0.00001	0	113	555.96	0.00134	0.74
114	517.02	0.00002	0.01	114	568.33	0.00191	1.09
115	517.94	0.00226	1.17	115	575.28	0.00046	0.26
116	531.52	0.00286	1.52	116	579.8	0.00091	0.53
117	540.99	0.00001	0	117	585.6	0.00237	1.39
118	562.47	0.00023	0.13	118	589.72	0.00036	0.21

119	565.64	0.01596	9.03	119	600.53	0.00227	1.36
120	572.66	0	0	120	601.21	0.00583	3.5
121	578.93	0	0	121	615.1	0.00248	1.52
122	585.03	0.00235	1.38	122	626.33	0.00005	0.03
123	599.52	0	0	123	631.54	0.0032	2.02
124	604.29	0.00602	3.64	124	642.95	0.00018	0.11
125	617.82	0	0	125	645.02	0.00048	0.31
126	626.8	0.01294	8.11	126	649.27	0.00227	1.47
127	631.95	0.00015	0.09	127	656.29	0.0048	3.15
128	633.49	0.01323	8.38	128	661.5	0.003	1.98
129	645.29	0	0	129	667.13	0.00001	0.01
130	658.34	0.00129	0.85	130	669.19	0.00001	0.01
131	663.57	0.00031	0.21	131	670.96	0	0
132	666.74	0	0	132	671.47	0.00044	0.3
133	669.65	0.00003	0.02	133	676.46	0.00007	0.05
134	672.94	0.00112	0.76	134	682	0.00014	0.1
135	673.27	0.00668	4.5	135	684.14	0.00442	3.03
136	675.3	0.00001	0.01	136	711.51	0.00466	3.32
137	682.53	0	0	137	713.63	0.00025	0.18
138	684.11	0.00003	0.02	138	716.41	0.00207	1.49
139	696.64	0	0	139	718.3	0.00043	0.31
140	713.74	0	0	140	737.53	0.00078	0.57
141	714.77	0.0018	1.28	141	750.78	0.00145	1.09
142	714.94	0.00375	2.68	142	757.67	0.00076	0.57
143	721.87	0	0	143	761.91	0.00237	1.8
144	754.92	0.00008	0.06	144	764.38	0.00011	0.08
145	756.61	0.00134	1.01	145	767.91	0	0
146	763.42	0.00098	0.75	146	772.92	0.00021	0.16
147	770.23	0	0	147	777.03	0.00005	0.04
148	777.03	0.00001	0.01	148	780.44	0.00857	6.69
149	779.08	0.00168	1.31	149	782.64	0.00353	2.77
150	793.25	0.00014	0.11	150	786.09	0.0016	1.26
151	795.97	0.00252	2.01	151	795.87	0.00362	2.88
152	796.43	0.00069	0.55	152	802.88	0.00229	1.84
153	798.2	0.00004	0.04	153	809.14	0.0057	4.61
154	807.07	0	0	154	810.21	0.00147	1.19
155	809.73	0.0147	11.9	155	820.3	0.00005	0.04
156	826.68	0.00001	0	156	827.38	0.00053	0.44
157	838.86	0.00003	0.02	157	840.99	0.00067	0.56
158	839.58	0.00001	0.01	158	842.08	0.00008	0.07
159	840.9	0.00003	0.02	159	842.57	0.0005	0.42
160	841.88	0.00024	0.2	160	844.68	0.00002	0.02
161	843.45	0.00004	0.03	161	846.1	0.00005	0.04

162	845.01	0.00044	0.37	162	849.62	0	0
163	847.53	0.00231	1.96	163	867.81	0.00003	0.03
164	849.9	0.00001	0	164	871.62	0.00007	0.06
165	865.8	0.01082	9.37	165	887.5	0.00137	1.22
166	894.18	0	0	166	892.55	0.00018	0.16
167	896.8	0.00032	0.29	167	894.3	0.00001	0.01
168	897.08	0	0	168	894.55	0.00005	0.04
169	902.06	0	0	169	902.97	0.00001	0.01
170	904.17	0	0	170	904.74	0.00001	0.01
171	910.9	0.00417	3.8	171	913.01	0.00011	0.1
172	914.91	0.00027	0.25	172	917.12	0.00059	0.54
173	915.97	0.0004	0.37	173	920.56	0.00052	0.48
174	926.34	0.00004	0.04	174	929.56	0.00014	0.13
175	931	0.00054	0.5	175	931.26	0.00017	0.16
176	932.51	0.00013	0.12	176	932.62	0.00011	0.1
177	933.66	0.00015	0.14	177	933.77	0	0
178	936.31	0	0	178	934.24	0	0
179	936.45	0	0	179	936.52	0	0
180	936.63	0.00002	0.02	180	936.71	0.00001	0.01
181	936.78	0.00003	0.03	181	937.26	0	0
182	938.37	0.00001	0.01	182	938.44	0.00001	0.01
183	944.07	0	0	183	944.59	0.00005	0.05
184	947.12	0	0	184	946.1	0	0
185	947.76	0.00002	0.02	185	946.62	0.00001	0.01
186	948.23	0	0	186	948.15	0.00009	0.09
187	948.34	0	0	187	948.62	0	0
188	948.81	0.00015	0.15	188	950.03	0	0
189	949.67	0	0	189	951.52	0.00001	0.01
190	950.56	0.00001	0.01	190	957.94	0.00003	0.03
191	960.19	0	0	191	961.52	0.00047	0.46
192	963.25	0.00002	0.02	192	965.04	0.00004	0.03
193	964.45	0.00003	0.03	193	972.05	0	0
194	968	0.00124	1.2	194	972.89	0	0
195	972.09	0.00001	0.01	195	973.1	0	0
196	972.95	0	0	196	973.15	0	0
197	973.02	0	0	197	973.37	0.00001	0.01
198	973.06	0	0	198	975.06	0	0
199	973.79	0	0	199	981.65	0.00215	2.11
200	973.97	0.00001	0.01	200	985.59	0.00091	0.9
201	977.78	0	0	201	991.58	0.00028	0.28
202	982.58	0	0	202	1025.71	0.00137	1.41
203	1024.7	0.0048	4.92	203	1028.07	0.00239	2.46
204	1031.82	0.00001	0.01	204	1053.02	0.00001	0.01

205	1054.77	0.00018	0.19	205	1055.6	0	0
206	1055.18	0.0005	0.53	206	1055.97	0	0
207	1056.02	0.00035	0.37	207	1056.72	0.00008	0.09
208	1056.71	0.00004	0.04	208	1057.11	0.00065	0.69
209	1056.99	0.00007	0.07	209	1058.51	0.00017	0.19
210	1057.55	0.00021	0.22	210	1061.84	0.00001	0.01
211	1061.48	0	0	211	1062.03	0	0
212	1061.94	0	0	212	1062.06	0	0
213	1062.12	0	0	213	1062.9	0.00001	0.01
214	1062.18	0	0	214	1063.12	0.00001	0.01
215	1062.21	0	0	215	1071.39	0.00014	0.15
216	1062.9	0	0	216	1073.23	0.00067	0.72
217	1074.28	0.00001	0.01	217	1091.28	0.00271	2.96
218	1075.83	0	0	218	1102.84	0.00254	2.8
219	1113.41	0.0077	8.57	219	1111.15	0.01466	16.29
220	1123.31	0.00002	0.02	220	1130.35	0.00087	0.98
221	1132.92	0.00015	0.17	221	1133.11	0.00001	0.01
222	1133.65	0.00161	1.83	222	1136.78	0.00098	1.12
223	1143.82	0.00005	0.05	223	1146.33	0.00015	0.18
224	1147.23	0.00075	0.86	224	1148.19	0.00735	8.44
225	1152.43	0.006	6.91	225	1151.41	0.004	4.6
226	1155.66	0.00026	0.3	226	1167.24	0.00126	1.47
227	1171.8	0.00012	0.15	227	1172.93	0.00001	0.01
228	1172.76	0.0001	0.12	228	1176.16	0.00114	1.34
229	1183.51	0.00015	0.18	229	1192.47	0.00025	0.3
230	1199.63	0.00002	0.02	230	1198.23	0.00021	0.25
231	1201.45	0.00052	0.62	231	1202.12	0.00003	0.03
232	1221.5	0.00006	0.07	232	1217.69	0.00059	0.71
233	1237.44	0.0033	4.08	233	1222.73	0.00112	1.37
234	1237.68	0.00917	11.35	234	1232.04	0.03169	39.04
235	1238.17	0.00023	0.28	235	1237.53	0.00074	0.91
236	1238.34	0.00095	1.17	236	1238.54	0.00004	0.04
237	1238.48	0.00021	0.26	237	1238.59	0.00009	0.11
238	1238.56	0.00001	0.02	238	1238.65	0.00002	0.03
239	1238.63	0.00004	0.05	239	1239.3	0.00006	0.07
240	1239.08	0.00006	0.08	240	1239.37	0.00025	0.31
241	1239.46	0.00001	0.01	241	1240.88	0.00048	0.6
242	1240.37	0.00146	1.81	242	1241.07	0.00026	0.32
243	1240.78	0.0003	0.37	243	1242.35	0.00047	0.58
244	1242.8	0.00024	0.29	244	1245.84	0.00664	8.28
245	1249.2	0.0006	0.75	245	1250.17	0.00007	0.09
246	1252.84	0.011	13.78	246	1257.81	0.00019	0.24
247	1257.54	0.00501	6.3	247	1264.86	0.00018	0.22

248	1266.64	0.00031	0.4	248	1269.06	0.0007	0.88
249	1271.18	0.00019	0.25	249	1275.57	0.00171	2.18
250	1274.87	0.00489	6.23	250	1278.47	0.00654	8.36
251	1278.41	0	0	251	1284.75	0.01279	16.43
252	1281.94	0.00491	6.3	252	1286.76	0	0
253	1290.26	0.00014	0.18	253	1290.07	0.00647	8.35
254	1294.56	0.00756	9.79	254	1292.13	0.00086	1.12
255	1295.89	0.01899	24.61	255	1298.3	0.00085	1.1
256	1298.83	0.00117	1.52	256	1299.53	0.0009	1.17
257	1301.76	0.00404	5.25	257	1306.96	0.01247	16.29
258	1303.47	0.00064	0.83	258	1313.88	0.00575	7.55
259	1316.99	0.10286	135.47	259	1318.13	0.00015	0.2
260	1323.89	0.0004	0.53	260	1324.26	0.00308	4.07
261	1324.59	0.04627	61.29	261	1329.11	0.02879	38.27
262	1337.64	0.00007	0.09	262	1338.97	0.00633	8.48
263	1338.04	0.00048	0.65	263	1341.49	0	0.01
264	1343.36	0.01907	25.62	264	1346.73	0.02459	33.11
265	1349.19	0.04246	57.28	265	1348.07	0	0
266	1353.03	0.00132	1.78	266	1355.94	0.03443	46.69
267	1360.82	0.00159	2.16	267	1365.5	0.01138	15.54
268	1362.66	0.00345	4.71	268	1367.55	0.00823	11.26
269	1366.83	0.00047	0.64	269	1370.13	0.03657	50.1
270	1370.2	0.00402	5.51	270	1373.83	0.01681	23.1
271	1379.12	0.03485	48.07	271	1376.59	0.00118	1.62
272	1380.25	0.00367	5.06	272	1382.04	0.00211	2.91
273	1387.69	0.00002	0.02	273	1387.38	0	0
274	1400.98	0.00021	0.3	274	1400.19	0.00199	2.79
275	1411.47	0.06012	84.86	275	1404.37	0.00658	9.24
276	1423.37	0.00168	2.39	276	1405.88	0.01651	23.21
277	1423.56	0	0	277	1423.86	0.00001	0.02
278	1425.58	0.0008	1.15	278	1425.09	0.00055	0.78
279	1425.83	0.00001	0.02	279	1425.71	0.00014	0.21
280	1426.33	0.0007	0.99	280	1426.22	0.00002	0.03
281	1426.45	0.00017	0.24	281	1426.63	0	0
282	1426.53	0	0	282	1426.75	0	0
283	1426.6	0.00001	0.02	283	1426.91	0.00009	0.13
284	1426.61	0.00001	0.01	284	1427.08	0.00002	0.03
285	1426.8	0.00019	0.27	285	1427.35	0	0.01
286	1427.38	0.00002	0.03	286	1427.4	0.00001	0.01
287	1427.49	0.0023	3.29	287	1443.09	0.00039	0.57
288	1440.57	0.00056	0.81	288	1447.47	0.00074	1.06
289	1442.79	0.00001	0.01	289	1453.93	0.00001	0.02
290	1455.01	0.00011	0.16	290	1457.92	0.0018	2.63

291	1456	0.00428	6.24	291	1458.18	0.00265	3.86
292	1457.73	0	0	292	1458.62	0.00015	0.22
293	1458.06	0.00018	0.26	293	1458.77	0.00107	1.56
294	1458.4	0.00007	0.1	294	1459.35	0.00012	0.18
295	1458.51	0.00027	0.39	295	1459.93	0.00334	4.88
296	1459.26	0.00001	0.02	296	1470.54	0.00523	7.69
297	1460.05	0.00047	0.69	297	1481.1	0.00667	9.87
298	1471.7	0.00001	0.02	298	1490.38	0.00025	0.38
299	1480.57	0.01252	18.53	299	1493.71	0.00012	0.18
300	1491.75	0	0	300	1495.65	0.00027	0.4
301	1494.74	0	0	301	1500.54	0.00029	0.43
302	1501.97	0	0	302	1511.38	0.00001	0.01
303	1512.3	0.00001	0.01	303	1512.61	0	0
304	1512.36	0	0	304	1512.67	0	0
305	1512.6	0	0	305	1512.96	0	0.01
306	1512.64	0	0	306	1513.43	0.00001	0.01
307	1512.77	0	0	307	1515.52	0.00036	0.54
308	1513.12	0	0.01	308	1516.24	0.00068	1.03
309	1515.45	0.00022	0.33	309	1516.4	0.00001	0.02
310	1516.27	0.00001	0.01	310	1516.4	0	0.01
311	1516.37	0	0	311	1517.02	0.00004	0.06
312	1516.46	0	0.01	312	1517.47	0	0
313	1516.56	0.00002	0.04	313	1518.32	0.00001	0.01
314	1516.69	0	0	314	1520.52	0	0.01
315	1517.16	0.00017	0.26	315	1520.74	0.00018	0.28
316	1517.26	0	0.01	316	1521.46	0.00006	0.09
317	1517.65	0.00024	0.37	317	1522.24	0.00014	0.22
318	1519.64	0.00014	0.21	318	1523.1	0.00019	0.29
319	1520.79	0	0	319	1527.17	0.00031	0.47
320	1521.45	0.00004	0.06	320	1529.01	0.00012	0.19
321	1523.53	0.00042	0.63	321	1532.94	0.00008	0.12
322	1527.52	0.00034	0.52	322	1534.57	0.00096	1.47
323	1529.26	0	0.01	323	1535.15	0.00006	0.09
324	1530.78	0.00018	0.28	324	1535.24	0.00162	2.49
325	1534.3	0.00001	0.01	325	1536.29	0.00001	0.01
326	1534.65	0	0	326	1537.4	0.00001	0.01
327	1535.19	0.00009	0.15	327	1537.95	0	0
328	1536.09	0.00013	0.2	328	1538.06	0	0
329	1536.82	0	0	329	1538.77	0.00003	0.04
330	1537.16	0.00001	0.01	330	1539.04	0	0.01
331	1537.29	0	0	331	1540.02	0	0
332	1537.81	0	0	332	1548.35	0.00022	0.34
333	1538.03	0	0	333	1550.32	0	0

334	1538.48	0.00001	0.01	334	1550.46	0	0
335	1538.93	0.00001	0.01	335	1550.56	0	0
336	1539.54	0	0	336	1551.2	0	0
337	1548.35	0.00005	0.08	337	1552.1	0.00001	0.01
338	1549.2	0	0	338	1588.64	0.00084	1.33
339	1549.36	0	0	339	1617.19	0.00004	0.06
340	1550.18	0	0	340	1622.86	0.00015	0.24
341	1550.49	0	0	341	1624.92	0.00015	0.24
342	1550.8	0	0.01	342	1627.65	0.00006	0.09
343	1555.26	0.00066	1.03	343	1633.67	0.00057	0.93
344	1599.63	0.00101	1.62	344	1636.57	0.00128	2.09
345	1616.9	0	0	345	1640.66	0.00349	5.72
346	1621.69	0.00031	0.5	346	1647.39	0.00558	9.19
347	1623.56	0.00021	0.35	347	1652.88	0.00018	0.3
348	1624.2	0.00066	1.07	348	1653.98	0.00024	0.39
349	1634.18	0.00143	2.34	349	1661.85	0.00217	3.61
350	1636.12	0.00573	9.37	350	1666.54	0.00199	3.31
351	1653.81	0.00006	0.1	351	1672.98	0.0002	0.33
352	1655.17	0.00115	1.9	352	1673.3	0.00084	1.4
353	1662	0.00169	2.8	353	3041.07	0	0
354	1664.31	0.0032	5.33	354	3041.07	0	0
355	1671.77	0.0001	0.17	355	3041.38	0	0
356	1673.7	0.00034	0.57	356	3041.92	0	0.01
357	3041.33	0	0	357	3041.97	0	0
358	3041.34	0	0	358	3042.06	0	0
359	3041.49	0	0	359	3042.2	0	0
360	3041.72	0	0	360	3042.45	0	0
361	3041.84	0	0	361	3042.45	0	0.01
362	3041.87	0.00001	0.04	362	3042.98	0	0
363	3042.04	0.00001	0.02	363	3049.9	0.00003	0.1
364	3042.23	0	0	364	3049.97	0.00002	0.06
365	3042.57	0	0	365	3050.11	0.00093	2.85
366	3043.08	0	0.01	366	3050.31	0.00014	0.42
367	3043.18	0	0.01	367	3050.75	0.00009	0.27
368	3043.88	0.00002	0.06	368	3105.99	0	0
369	3049.71	0.00045	1.37	369	3106.31	0	0
370	3050.08	0	0	370	3106.39	0	0
371	3050.24	0	0	371	3106.45	0	0
372	3051.19	0.00007	0.21	372	3106.68	0	0
373	3051.35	0	0.01	373	3107.05	0	0
374	3051.44	0.00053	1.62	374	3107.07	0.00001	0.03
375	3105.89	0	0.01	375	3107.41	0.00002	0.05
376	3106.19	0	0	376	3107.91	0	0

377	3106.19	0	0	377	3108.03	0	0
378	3106.77	0	0	378	3113.12	0.00001	0.02
379	3106.93	0	0	379	3113.9	0	0
380	3107.28	0	0.01	380	3114.2	0	0
381	3107.34	0	0.01	381	3114.44	0	0
382	3107.37	0	0	382	3114.62	0	0
383	3107.6	0	0	383	3115.06	0.00001	0.03
384	3107.92	0	0.01	384	3115.46	0.00017	0.52
385	3108.02	0	0	385	3115.98	0.00001	0.04
386	3108.75	0.00001	0.03	386	3116.11	0	0
387	3113.06	0	0	387	3118.99	0	0
388	3114.2	0	0	388	3120.19	0	0
389	3114.36	0	0	389	3120.46	0	0
390	3115.26	0	0.01	390	3121.21	0	0
391	3115.4	0	0	391	3121.64	0.00001	0.02
392	3115.64	0.00001	0.02	392	3121.67	0	0
393	3115.79	0.00003	0.08	393	3122.44	0	0
394	3115.93	0.00001	0.03	394	3122.75	0	0
395	3116.21	0.00001	0.04	395	3124.24	0	0
396	3116.7	0.00009	0.29	396	3124.53	0	0.01
397	3117.92	0	0	397	3125.13	0	0.01
398	3117.95	0	0	398	3185.05	0	0
399	3119.39	0.00001	0.04	399	3186.44	0.00003	0.08
400	3120.47	0	0	400	3189.65	0.00007	0.21
401	3120.7	0	0	401	3190.44	0.00001	0.02
402	3121.12	0	0	402	3195.97	0	0
403	3121.16	0	0	403	3196.1	0.00002	0.06
404	3121.21	0	0	404	3201.51	0.00002	0.05
405	3121.93	0.00002	0.06	405	3209.44	0.00004	0.12
406	3122.38	0	0	406	3209.94	0.00001	0.03
407	3122.49	0	0	407	3217.79	0	0
408	3122.76	0	0	408	3219.67	0.00003	0.08
409	3123.15	0	0	409	3221.39	0.00002	0.06
410	3124.11	0.00003	0.09	410	3222.69	0	0
411	3189.87	0	0	411	3226.95	0.00003	0.09
412	3193.22	0.00002	0.05	412	3229.09	0	0
413	3193.65	0	0.01	413	3237.54	0.00004	0.12
414	3194.94	0.00001	0.04	414	3245.32	0	0.01
415	3195.09	0.00002	0.06	415	3248.09	0.00013	0.44
416	3212.88	0.00001	0.04	416	3255.08	0.00001	0.02
417	3217.23	0	0	417	3295.19	0	0.01
418	3218.29	0	0				
419	3218.71	0.00008	0.26				

420	3223.05	0.00019	0.61					
421	3228.18	0.00016	0.52					
422	3234.65	0	0.01					
423	3235.49	0.00002	0.07					
424	3248.61	0.00014	0.45					
425	3317.02	0.00001	0.02					
426	3317.98	0.00001	0.02					
Compound	p[B-N]N							
vibration mode	ω (cm ⁻¹)	S	λ (cm ⁻¹)	vibration mode	ω (cm ⁻¹)	S	λ (cm ⁻¹)	
1	0	0	0	205	1055.32	0.00018	0.19	
2	0	0	0	206	1055.38	0	0	
3	0	0	0	207	1057.95	0.00131	1.39	
4	0	0	0	208	1058.38	0	0	
5	0.01	0	0	209	1061.73	0	0	
6	0.01	0	0	210	1061.75	0	0	
7	12.25	0.23896	2.93	211	1062.5	0.00004	0.04	
8	20.35	1.57994	32.15	212	1062.53	0	0	
9	21.87	0	0	213	1069.44	0.00373	3.99	
10	32.04	0.16946	5.43	214	1071.31	0	0	
11	32.72	0	0	215	1090.18	0.00501	5.46	
12	35.24	0.39016	13.75	216	1093.84	0	0	
13	36.5	0	0	217	1097.49	0.01217	13.35	
14	38.09	0	0	218	1110.54	0	0	
15	40.06	0.03225	1.29	219	1113.17	0.00674	7.51	
16	44.1	0	0	220	1130.52	0	0	
17	50.25	0.09621	4.83	221	1137.9	0	0	
18	50.95	0.11026	5.62	222	1138.39	0.0023	2.62	
19	58.6	0	0	223	1147.74	0.01359	15.6	
20	71.84	0	0	224	1150.06	0	0	
21	72.8	0.00079	0.06	225	1156.85	0.00446	5.16	
22	82.04	0.24904	20.43	226	1165.81	0	0	
23	84.65	0	0	227	1177.32	0.00012	0.14	
24	94.32	0.01302	1.23	228	1191.41	0	0	
25	94.6	0	0	229	1191.58	0	0	
26	110.24	0	0	230	1198.36	0	0	
27	113.44	0.01869	2.12	231	1200.15	0.00044	0.53	
28	124.37	0.02482	3.09	232	1211.88	0	0	
29	124.38	0	0	233	1222.19	0.00053	0.65	
30	139.32	0	0	234	1222.68	0	0	
31	145.44	0.00952	1.38	235	1228.41	0.03739	45.93	

32	153.48	0.01242	1.91	236	1238.39	0	0
33	159.65	0	0	237	1238.4	0.00003	0.03
34	160.63	0.04509	7.24	238	1238.48	0	0
35	170.18	0.00468	0.8	239	1239.05	0.00025	0.32
36	171.08	0	0	240	1240.24	0	0
37	180.75	0	0	241	1240.37	0.00116	1.43
38	197.16	0.00288	0.57	242	1240.65	0	0
39	202.84	0	0	243	1245.39	0.00548	6.82
40	209.86	0	0	244	1250.8	0	0
41	218.34	0.00001	0	245	1256.62	0	0
42	225.23	0.11166	25.15	246	1263.47	0.00093	1.17
43	231.53	0.00217	0.5	247	1268.25	0.00038	0.48
44	232.14	0	0	248	1273.1	0	0
45	235.21	0	0	249	1278.55	0	0
46	236.35	0.00005	0.01	250	1283.71	0.00437	5.61
47	238	0	0	251	1290.41	0.01072	13.84
48	239.81	0.00007	0.02	252	1292.81	0.00701	9.06
49	241.02	0.01654	3.99	253	1293.9	0	0
50	245.08	0	0	254	1294.85	0	0
51	260.7	0.00157	0.41	255	1298.08	0	0
52	263.35	0	0	256	1309.59	0.01305	17.1
53	274.3	0.00048	0.13	257	1314.57	0.01403	18.45
54	274.77	0	0	258	1316.09	0	0
55	277.13	0	0	259	1320.27	0	0
56	277.33	0.00021	0.06	260	1324.86	0.02104	27.88
57	290.46	0	0	261	1333.62	0	0
58	290.79	0.00994	2.89	262	1341	0	0
59	298.91	0	0	263	1343.6	0.0056	7.53
60	300.88	0.00981	2.95	264	1345.96	0.02126	28.61
61	307.11	0.0616	18.92	265	1353.55	0	0
62	311.12	0	0	266	1362.41	0	0
63	313.07	0.02157	6.75	267	1363.15	0.02735	37.28
64	316.85	0	0	268	1373.23	0.05938	81.54
65	321.64	0.00132	0.43	269	1375.3	0	0
66	325.61	0	0	270	1381.48	0	0
67	328.84	0	0	271	1382.11	0.00544	7.52
68	330.77	0.00019	0.06	272	1387.49	0	0
69	331.85	0	0	273	1389.06	0.00248	3.45
70	338.57	0.00095	0.32	274	1399.96	0.01461	20.45
71	339.2	0	0	275	1404.68	0	0
72	339.6	0.00064	0.22	276	1406.88	0.002	2.81
73	348.78	0	0	277	1410.33	0	0
74	352.42	0.00091	0.32	278	1425.56	0.00031	0.44

75	354.85	0	0	279	1426.36	0	0
76	361.28	0.00022	0.08	280	1426.49	0	0
77	363.74	0	0	281	1426.49	0	0
78	364.86	0.00015	0.06	282	1427.03	0	0.01
79	369.97	0	0	283	1427.05	0	0
80	370.65	0.02525	9.36	284	1427.29	0.00001	0.01
81	383.65	0	0	285	1427.91	0	0
82	386.16	0.01217	4.7	286	1446.44	0.00157	2.27
83	423.24	0	0	287	1451.42	0	0
84	430.88	0	0	288	1456.71	0	0
85	431.11	0.01385	5.97	289	1458.36	0.00327	4.77
86	435.18	0.00589	2.57	290	1458.49	0.01425	20.78
87	446.62	0	0	291	1458.54	0	0
88	448.44	0	0	292	1459.52	0	0
89	450.9	0.00622	2.81	293	1459.7	0.00201	2.93
90	453.09	0.02185	9.9	294	1472.73	0	0
91	455.59	0.00145	0.66	295	1482.66	0.00449	6.66
92	457.97	0	0	296	1492.85	0.00026	0.39
93	464.06	0.0269	12.48	297	1493.03	0	0
94	466.2	0	0	298	1494.61	0	0
95	476.15	0.00085	0.41	299	1495.48	0.00012	0.18
96	477.01	0	0	300	1501.51	0	0
97	479.61	0	0	301	1512.56	0	0
98	482.24	0	0	302	1512.56	0	0
99	489.66	0.00737	3.61	303	1513.35	0.00002	0.02
100	501	0.00004	0.02	304	1513.36	0	0
101	504.09	0	0	305	1515.08	0.00005	0.08
102	509.21	0	0	306	1516.66	0	0
103	522.99	0.00453	2.37	307	1516.66	0	0
104	527.23	0.01248	6.58	308	1516.99	0.00008	0.12
105	532.56	0	0	309	1517.02	0	0
106	541.78	0.00484	2.62	310	1517.89	0.00045	0.69
107	555.68	0	0	311	1518.9	0	0
108	556.57	0.00766	4.26	312	1522.02	0	0
109	561.79	0	0	313	1522.02	0.00003	0.04
110	574.28	0.00007	0.04	314	1522.94	0	0
111	579.84	0	0	315	1526.53	0.00112	1.71
112	586.02	0.0014	0.82	316	1530.59	0	0
113	587.01	0	0	317	1531.94	0.00003	0.04
114	591.63	0.00056	0.33	318	1534.46	0	0
115	595.5	0	0	319	1534.5	0	0
116	602.78	0	0	320	1535.57	0.00324	4.97
117	615.54	0.00038	0.23	321	1535.74	0	0

118	627.64	0	0	322	1537.5	0	0
119	629.2	0.00002	0.01	323	1537.61	0.00001	0.02
120	640.82	0.0008	0.51	324	1537.88	0	0
121	642.99	0	0	325	1538.34	0.00002	0.03
122	645.47	0.0005	0.32	326	1540.03	0	0
123	652.62	0	0	327	1540.12	0.00004	0.06
124	660.32	0	0	328	1550.47	0	0
125	661.41	0.00078	0.51	329	1550.48	0.00001	0.01
126	667.08	0	0	330	1551.59	0	0
127	667.9	0.00361	2.41	331	1551.64	0	0
128	672.41	0	0	332	1572.99	0.00537	8.44
129	673.49	0.00125	0.84	333	1620.32	0	0
130	676.02	0.00001	0	334	1620.65	0.00021	0.34
131	679.65	0	0	335	1625.8	0	0
132	707.8	0.01313	9.29	336	1626.4	0.00001	0.02
133	712.08	0	0	337	1633.56	0	0
134	713.62	0.00152	1.09	338	1634.89	0.00051	0.83
135	717.6	0.00007	0.05	339	1641.14	0	0
136	723.98	0	0	340	1641.36	0.00464	7.62
137	744.86	0.00705	5.25	341	1648.61	0.00857	14.13
138	750.54	0	0	342	1648.65	0	0
139	757.18	0	0	343	1653.99	0	0
140	759.77	0.00032	0.25	344	1654.52	0.00039	0.65
141	763.2	0	0	345	1666.28	0	0
142	764.56	0.00063	0.49	346	1667.17	0.00342	5.7
143	768.96	0.00103	0.79	347	1672.08	0	0
144	770.09	0	0	348	1672.3	0.00102	1.71
145	773.06	0.00148	1.14	349	3040.67	0	0
146	774.28	0	0	350	3040.68	0.00001	0.02
147	777.09	0.00888	6.9	351	3042.05	0	0
148	782.14	0	0	352	3042.05	0	0
149	782.89	0.00002	0.01	353	3042.3	0	0
150	795.48	0.00705	5.61	354	3042.31	0	0
151	803.33	0	0	355	3042.72	0	0
152	809.28	0	0	356	3042.74	0.00001	0.02
153	809.72	0.00353	2.86	357	3050.16	0	0
154	820.36	0.00078	0.64	358	3050.18	0.00002	0.05
155	820.83	0	0	359	3050.56	0	0
156	829.7	0	0	360	3050.59	0.00016	0.49
157	844.63	0.00032	0.27	361	3105.77	0	0
158	849.86	0	0	362	3105.78	0	0
159	850.38	0.00015	0.12	363	3106.45	0	0
160	858.33	0	0	364	3106.46	0	0

161	858.36	0.0061	5.23	365	3107.08	0	0
162	872	0	0	366	3107.08	0	0
163	872.15	0.00011	0.09	367	3107.87	0	0
164	883.2	0	0	368	3107.87	0	0
165	894.23	0	0	369	3114.1	0	0
166	894.63	0.00088	0.79	370	3114.15	0	0.01
167	895.22	0	0	371	3114.16	0	0
168	896.05	0.00091	0.82	372	3114.18	0	0
169	901.78	0	0	373	3115.85	0	0
170	901.82	0.00006	0.06	374	3115.92	0	0.02
171	921.18	0.00046	0.42	375	3118.51	0	0
172	921.27	0	0	376	3118.51	0	0
173	928.82	0	0	377	3120.59	0	0
174	929.99	0.00008	0.07	378	3120.6	0	0
175	932.59	0	0	379	3121.18	0	0
176	932.63	0	0	380	3121.19	0.00001	0.04
177	934.16	0	0	381	3122.86	0	0.01
178	934.26	0.00001	0.01	382	3122.86	0	0
179	936.69	0	0	383	3123.23	0	0
180	936.71	0.00001	0.01	384	3123.27	0	0.01
181	938.01	0	0	385	3185.48	0	0
182	938.37	0.00001	0.01	386	3185.48	0	0.01
183	941.61	0	0	387	3186.85	0	0
184	943.05	0	0	388	3186.86	0.00006	0.18
185	947.87	0.00001	0.01	389	3194.65	0	0
186	947.91	0	0	390	3194.66	0	0.01
187	949.74	0.00005	0.05	391	3196.33	0	0
188	950.37	0	0	392	3196.34	0.00001	0.04
189	961.04	0.00001	0.01	393	3196.42	0	0.01
190	961.36	0	0	394	3196.42	0	0
191	973.16	0.00002	0.02	395	3202.3	0	0
192	973.21	0	0	396	3202.33	0.00002	0.07
193	973.68	0	0	397	3209.95	0	0
194	973.73	0	0	398	3210	0.00005	0.15
195	975.14	0	0	399	3216.8	0	0
196	975.14	0	0	400	3216.81	0.00002	0.05
197	975.65	0.00297	2.9	401	3227.48	0	0
198	980.98	0	0	402	3227.51	0.00001	0.03
199	994.43	0	0	403	3242.56	0	0
200	994.48	0.00037	0.37	404	3242.57	0.00005	0.18
201	1027.57	0	0	405	3247.78	0	0
202	1027.9	0.00737	7.58	406	3247.78	0	0
203	1052.03	0.00034	0.35	407	3259.87	0	0

204	1052.9	0	0	408	3259.87	0.00001	0.04
-----	--------	---	---	-----	---------	---------	------

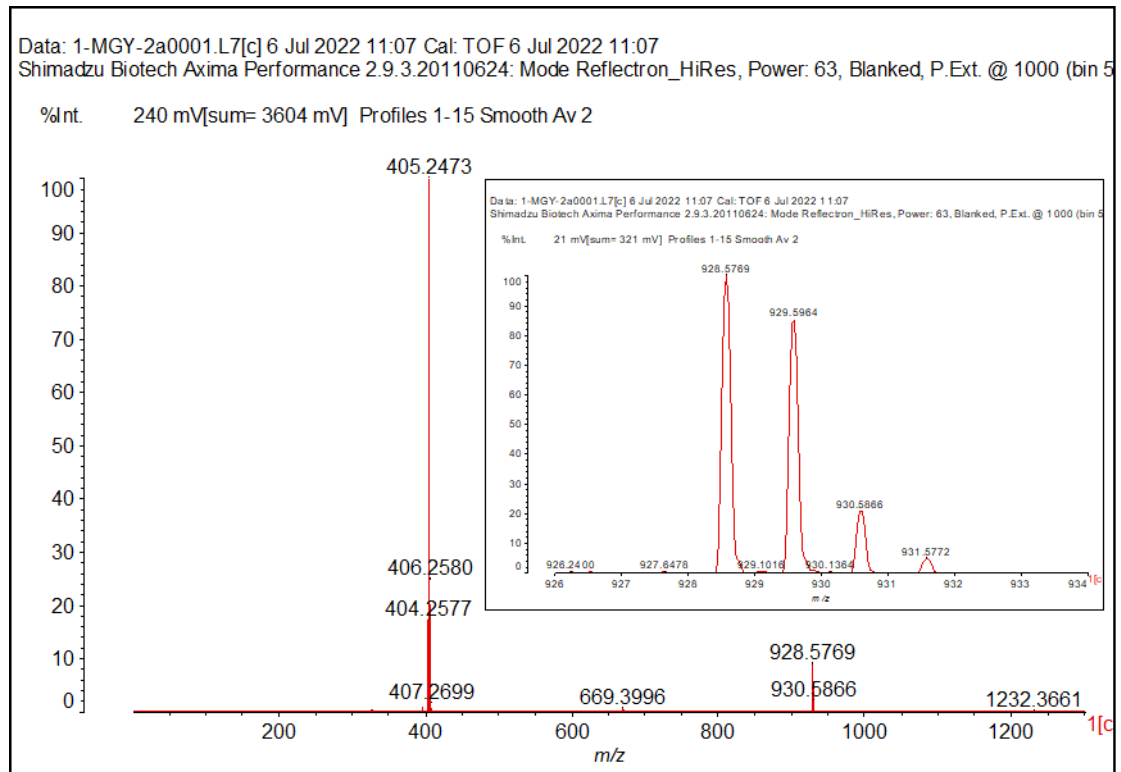


Figure S27. Mass spectrometry of **2a**.

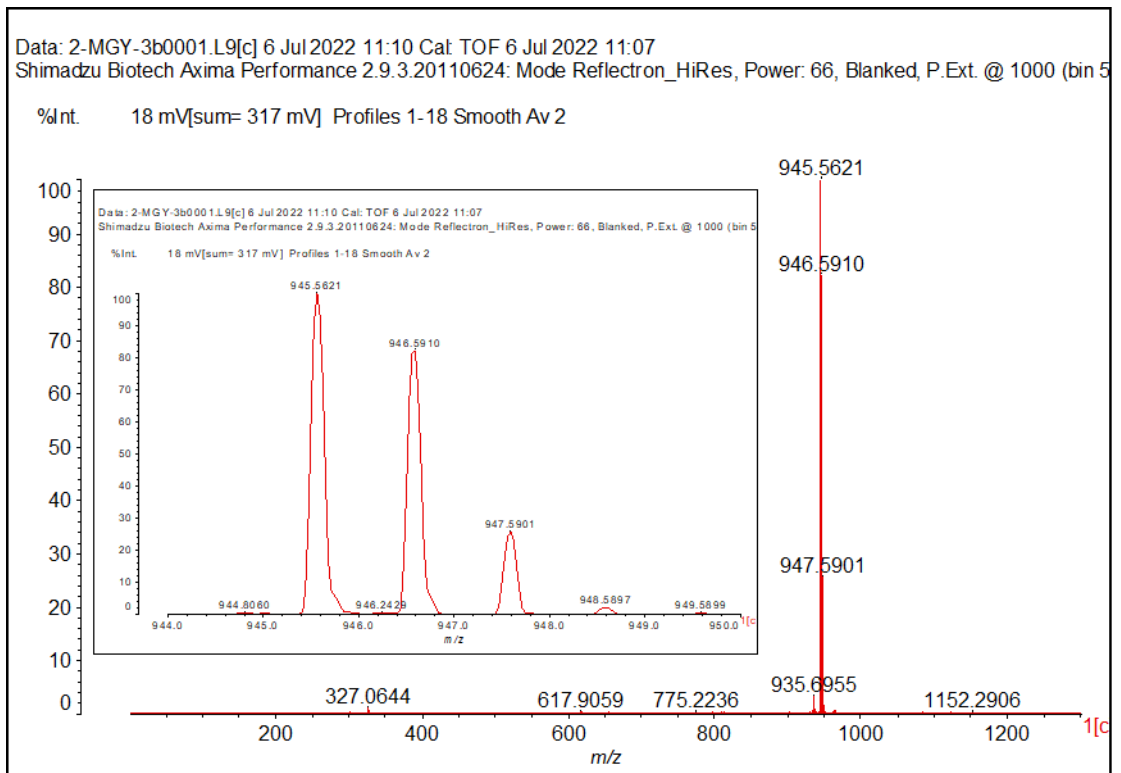


Figure S28. Mass spectrometry of **3b**.

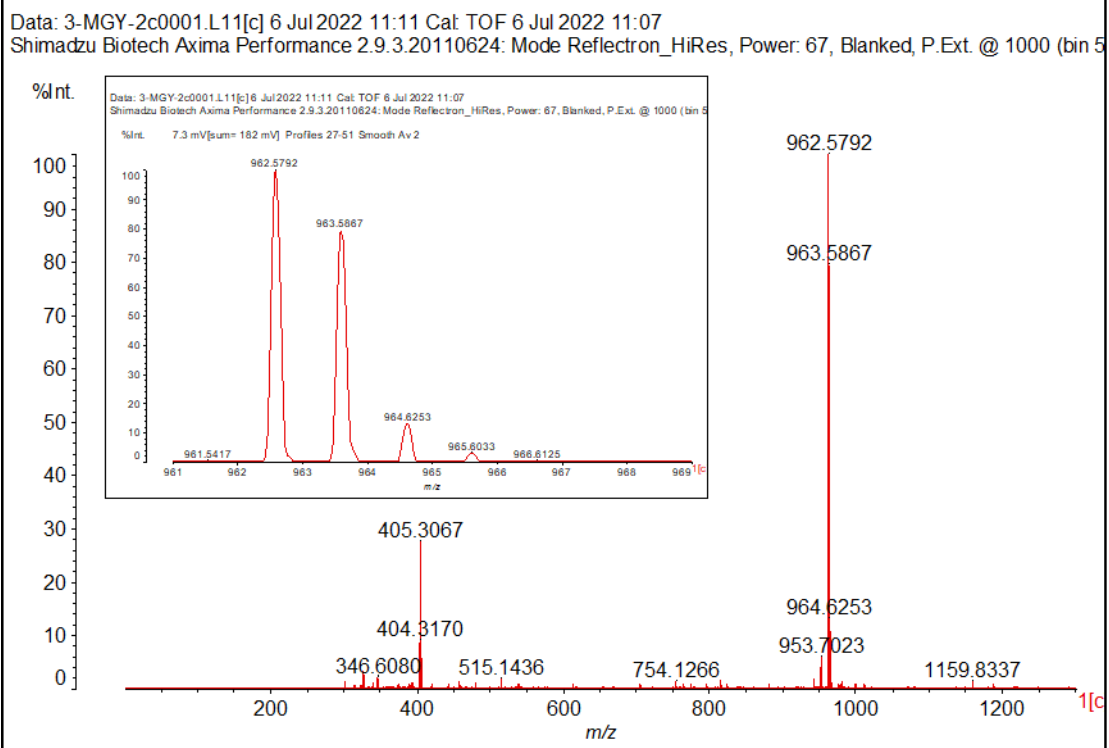


Figure S29. Mass spectrometry of **2c**.

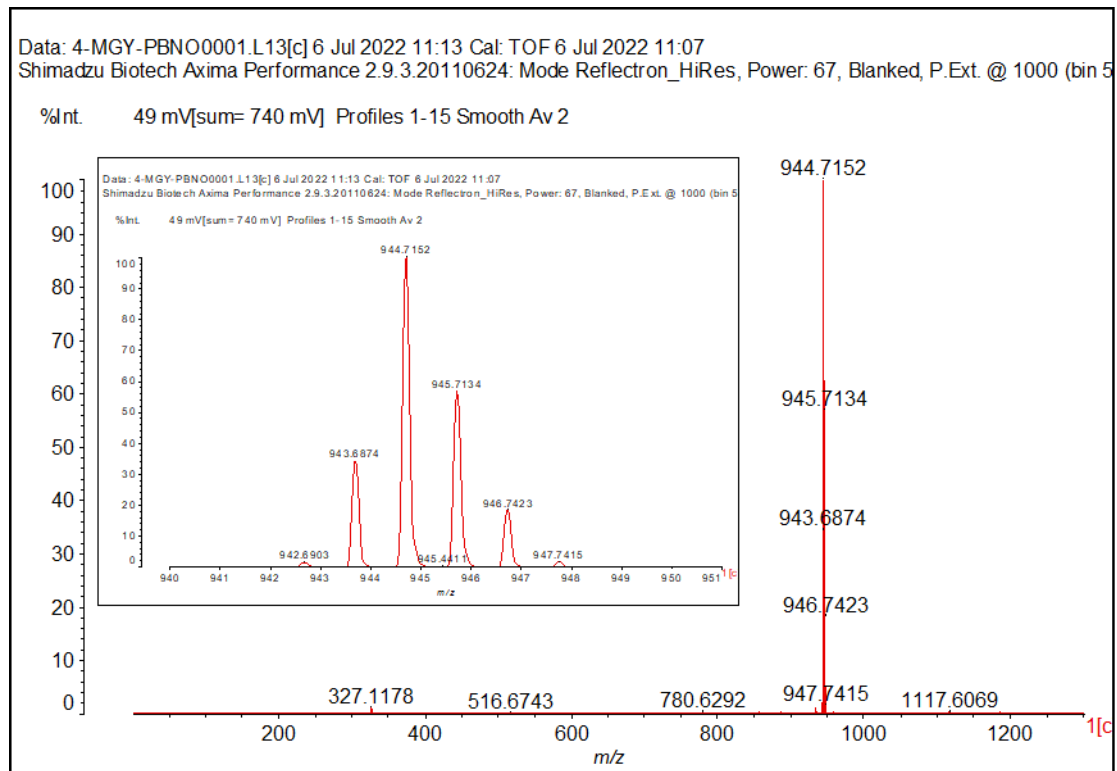


Figure S30. Mass spectrometry of **p[B-N]O**.

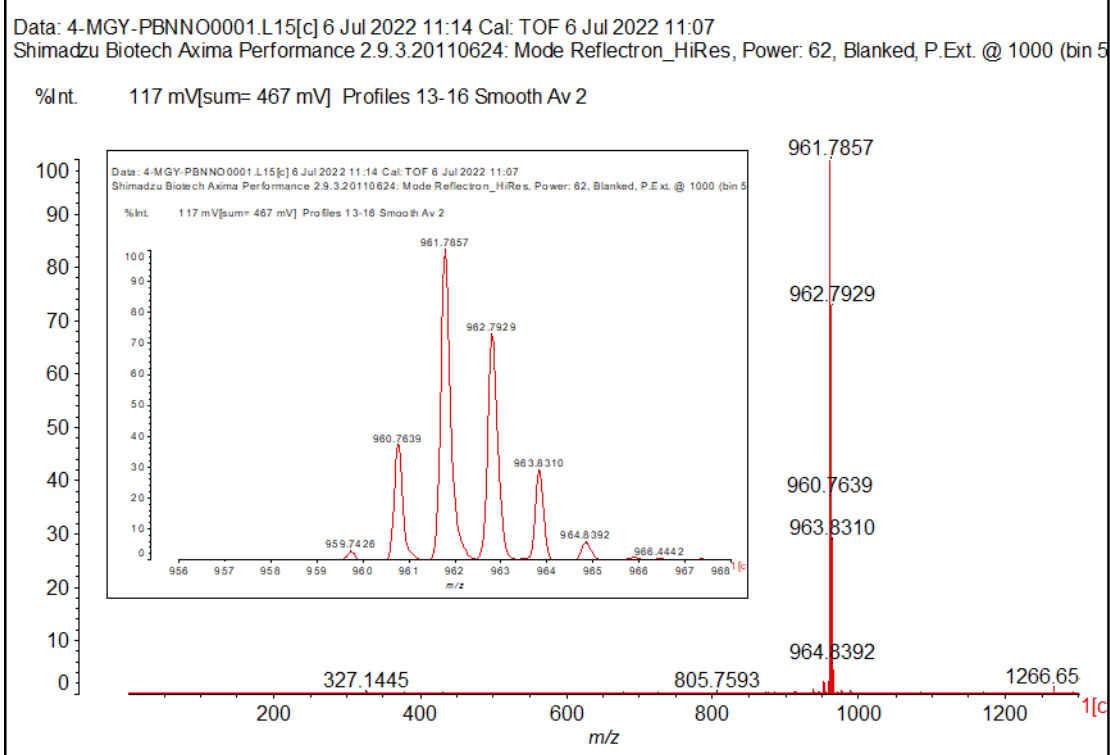


Figure S31. Mass spectrometry of p[B-N]NO.

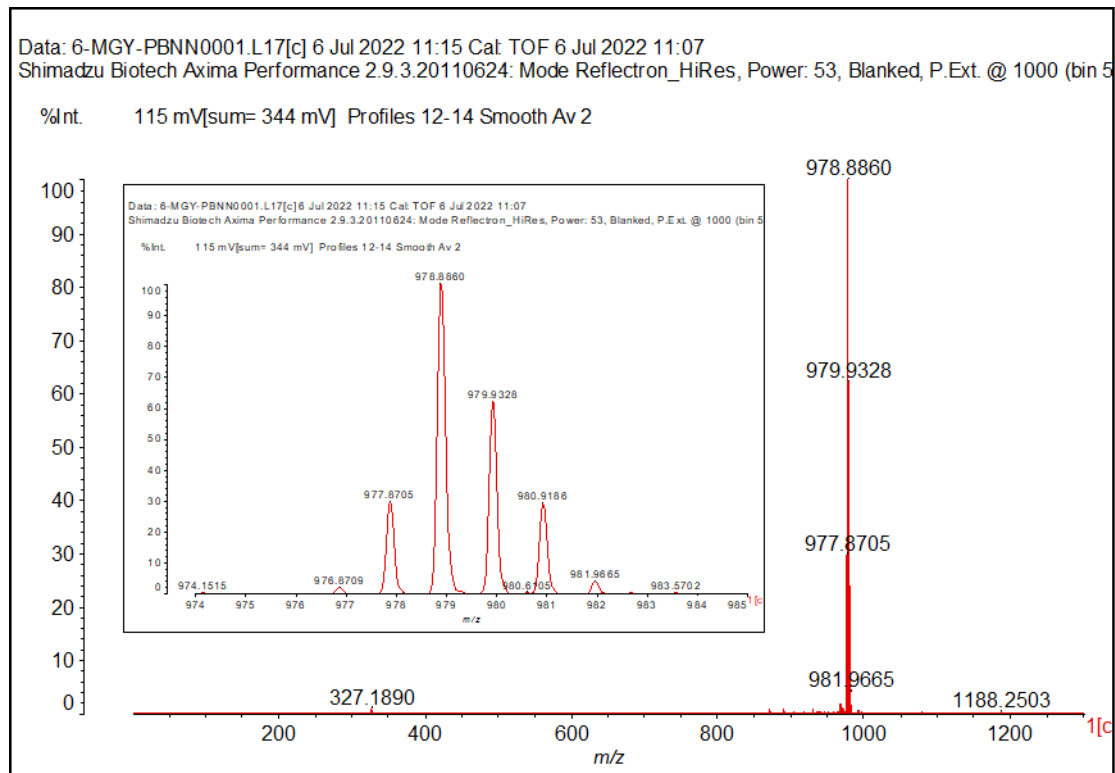


Figure S32. Mass spectrometry of p[B-N]N.

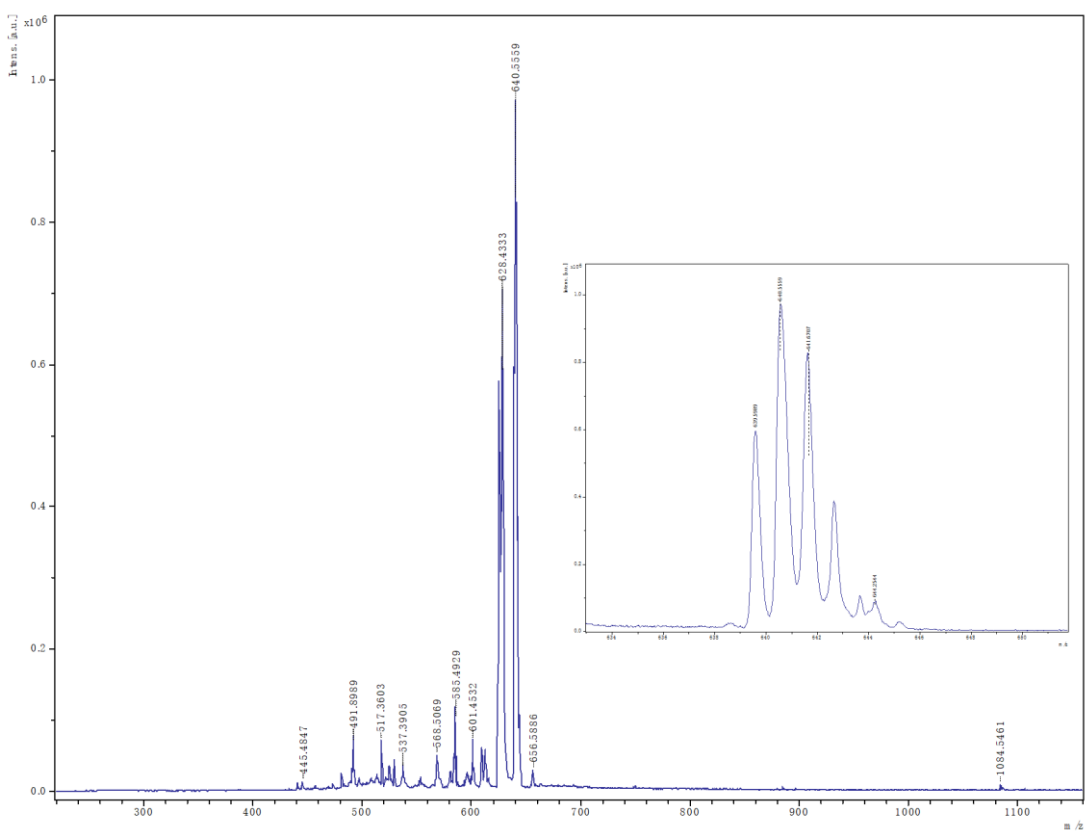


Figure S33. Mass spectrometry of [B-N]N.

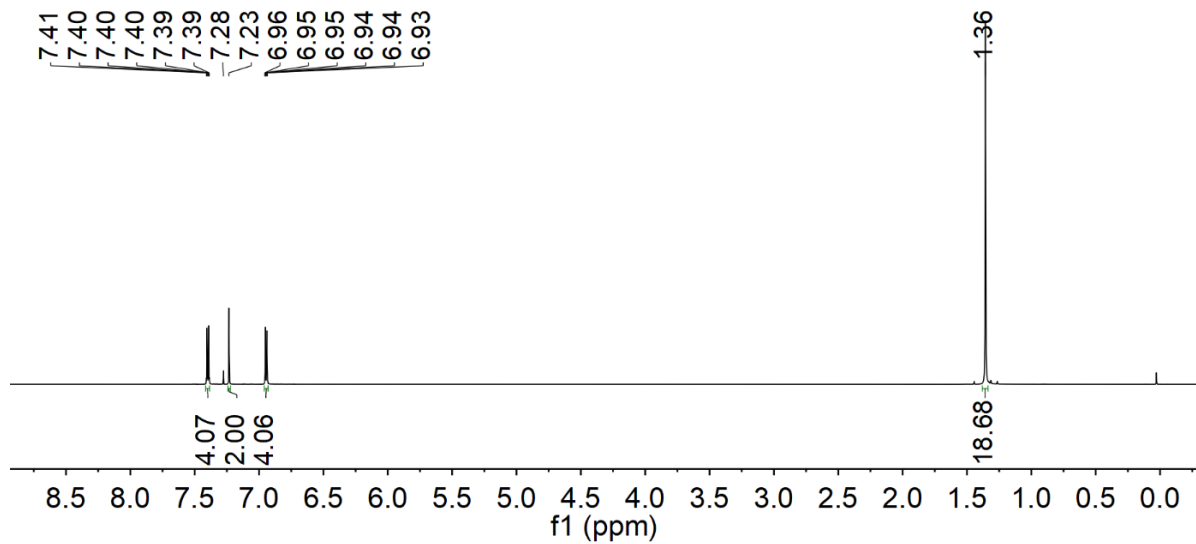


Figure S34. ^1H NMR spectrum of **1a** in CDCl_3 .

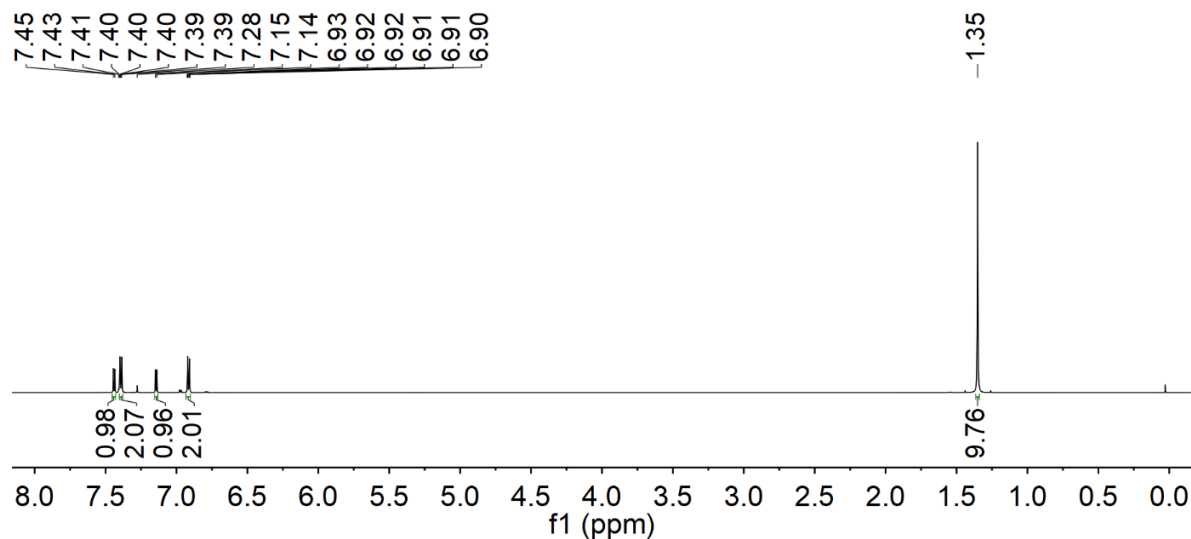


Figure S35. ^1H NMR spectrum of **1b** in CDCl_3 .

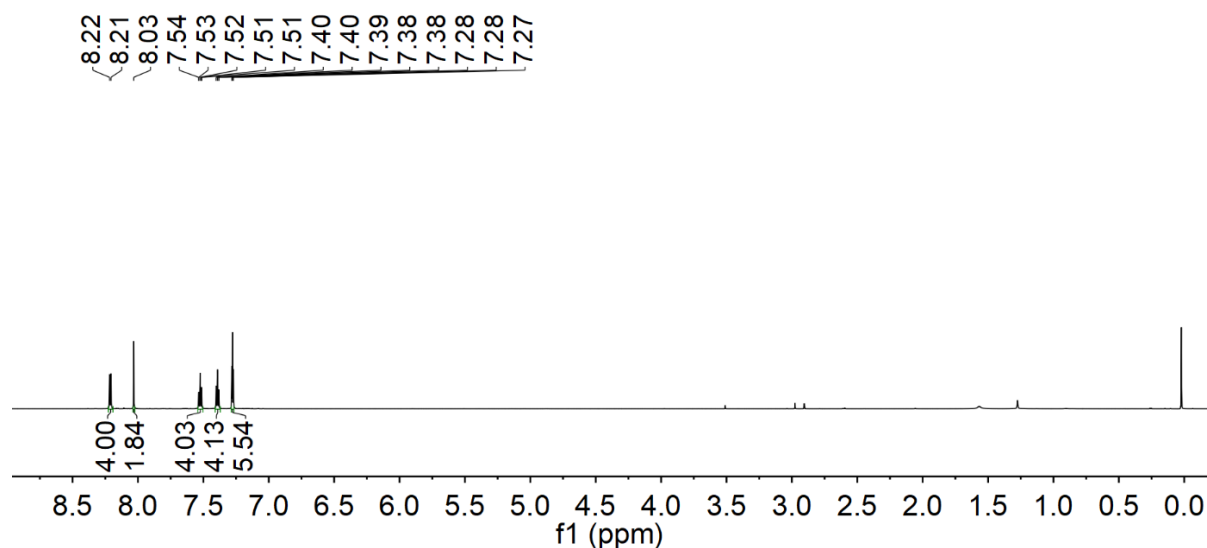


Figure S36. ^1H NMR spectrum of **1c** in CDCl_3 .

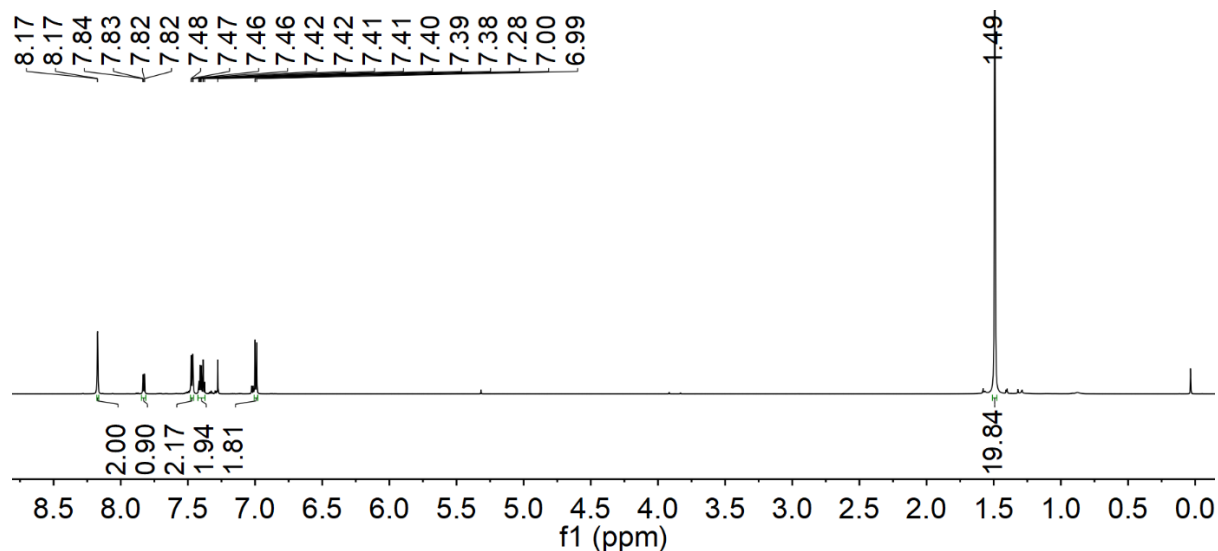


Figure S37. ^1H NMR spectrum of **1d** in CDCl_3 .

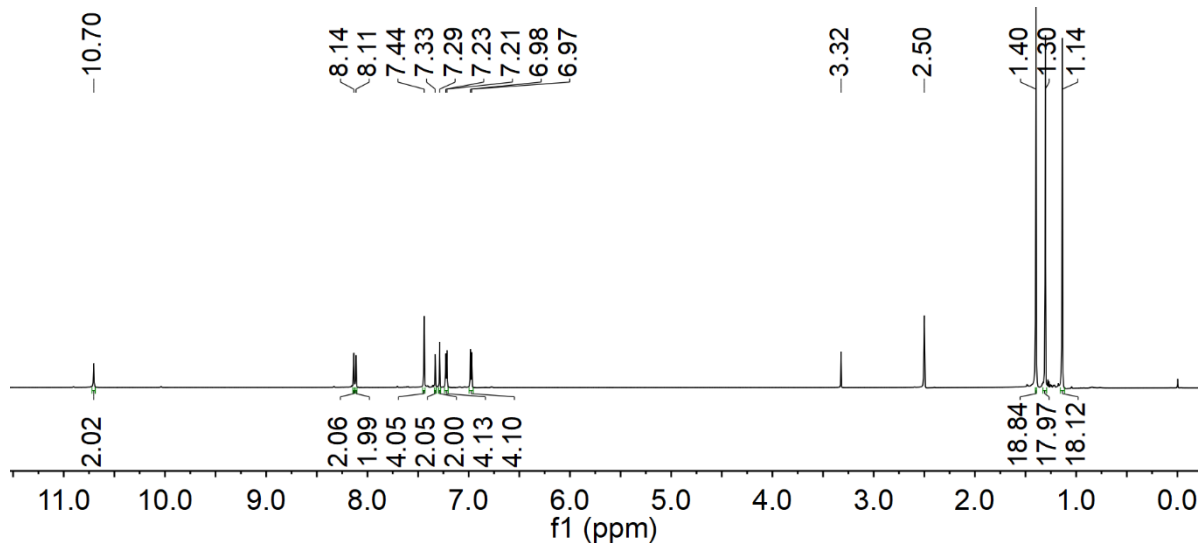


Figure S38. ^1H NMR spectrum of m **2a** in DMSO-d₆.

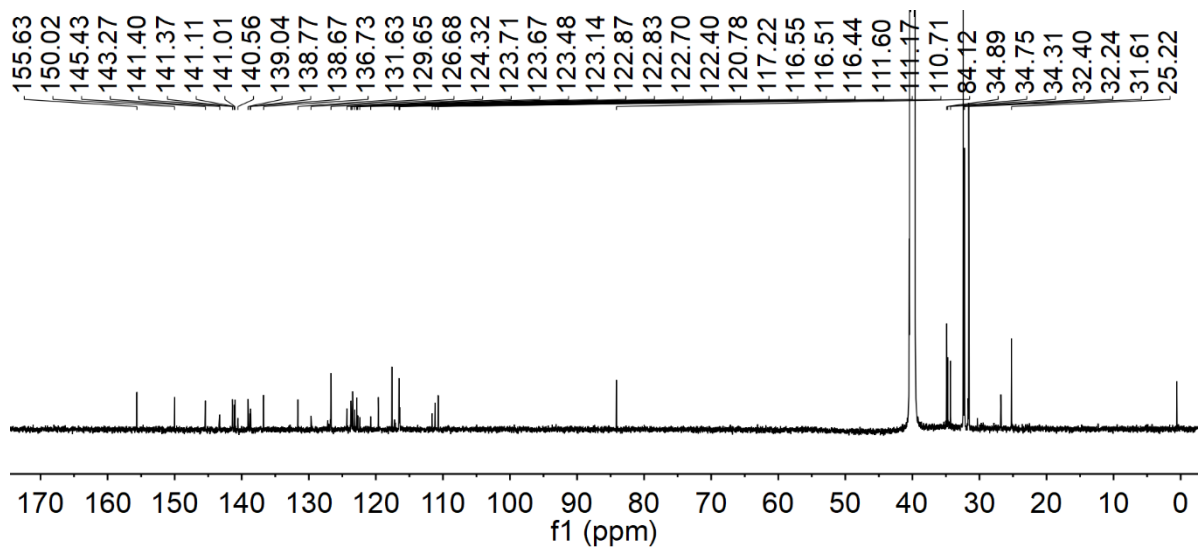


Figure S39. ^{13}C NMR spectrum of m **2a** in DMSO-d₆.

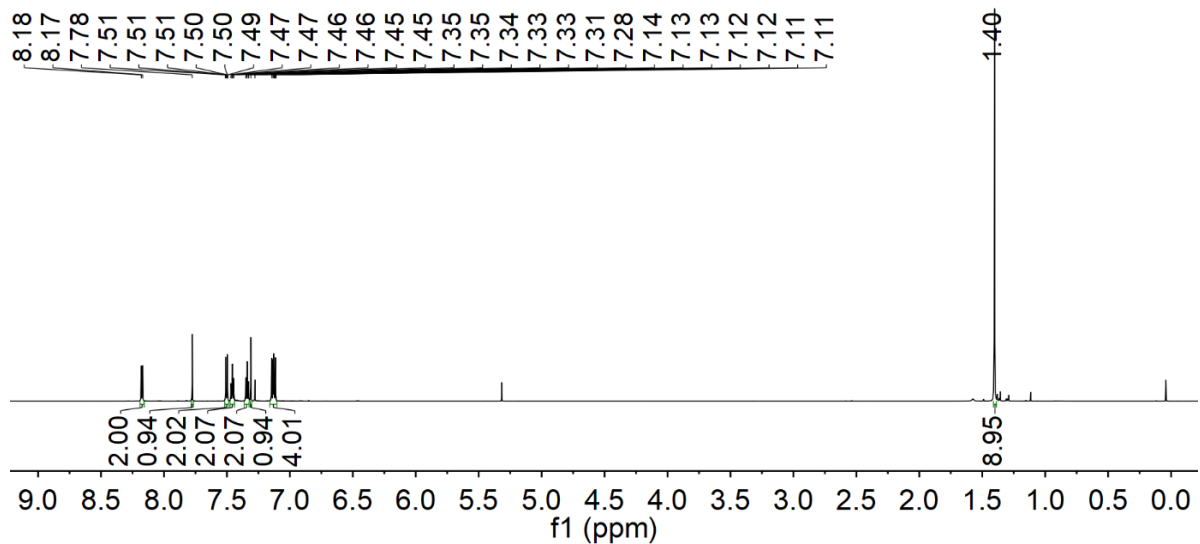


Figure S40. ^1H NMR spectrum of m **2b** in CDCl₃.

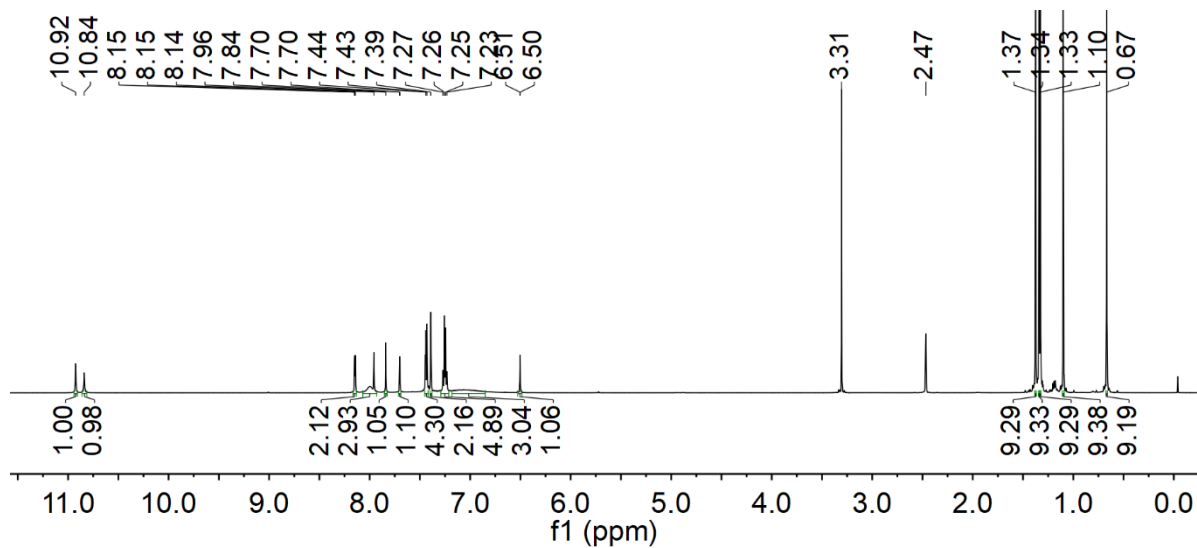


Figure S41. ^1H NMR spectrum of m **3b** in DMSO-d₆.

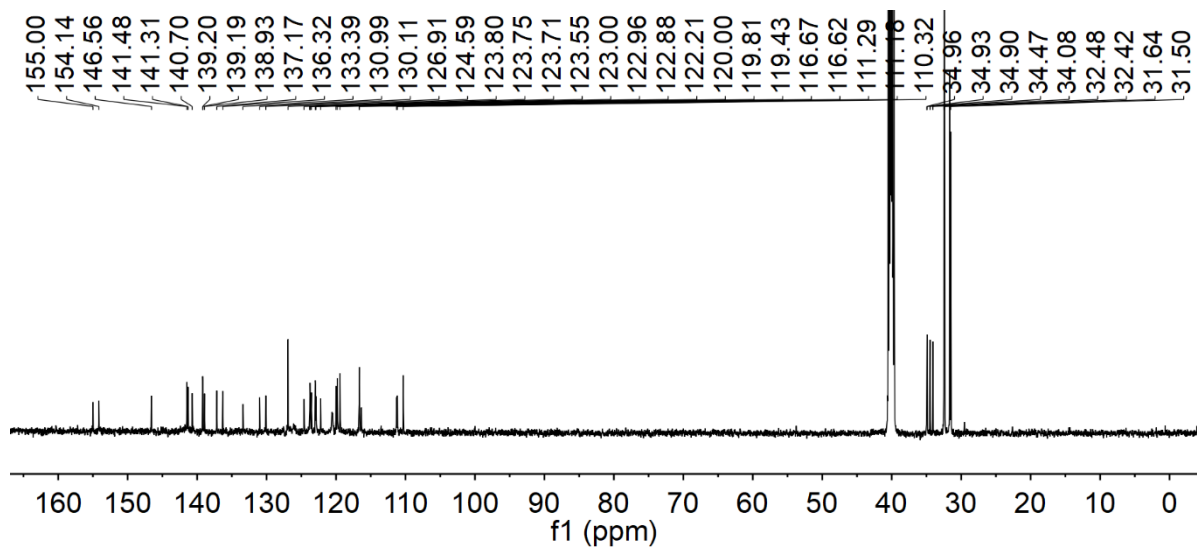


Figure S42. ^{13}C NMR spectrum of m **3b** in DMSO-d₆.

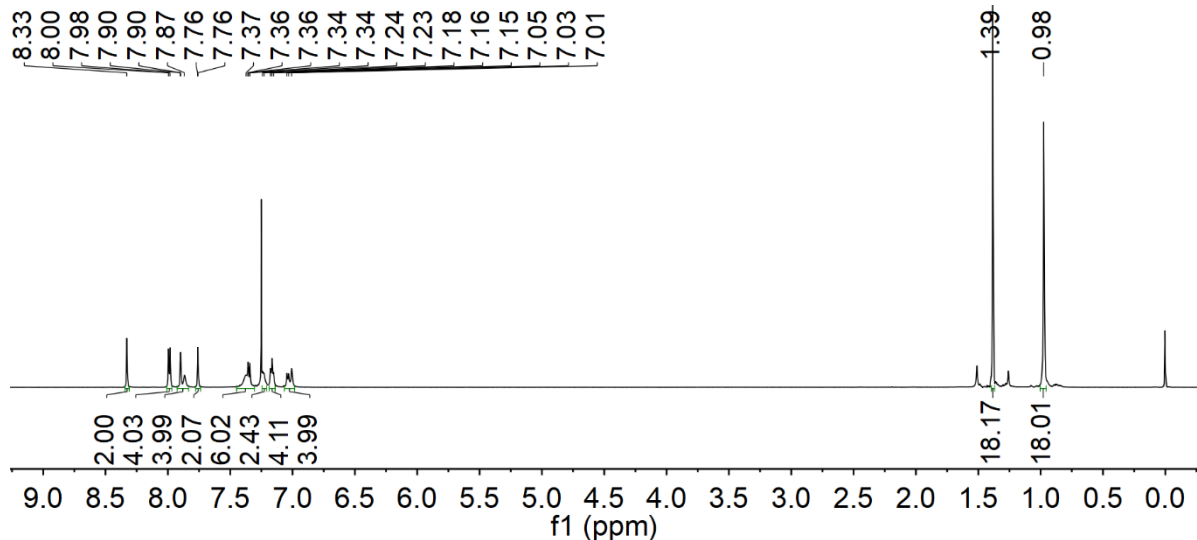


Figure S43. ^1H NMR spectrum of m **2c** in CDCl₃.

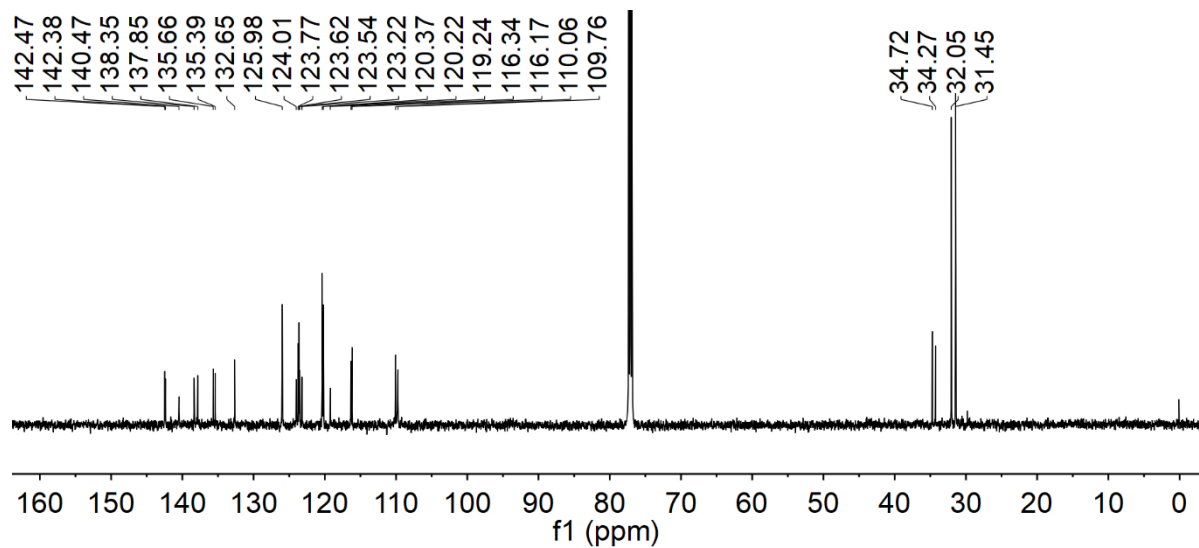


Figure S44. ¹³C NMR spectrum of m **2c** in CDCl₃.

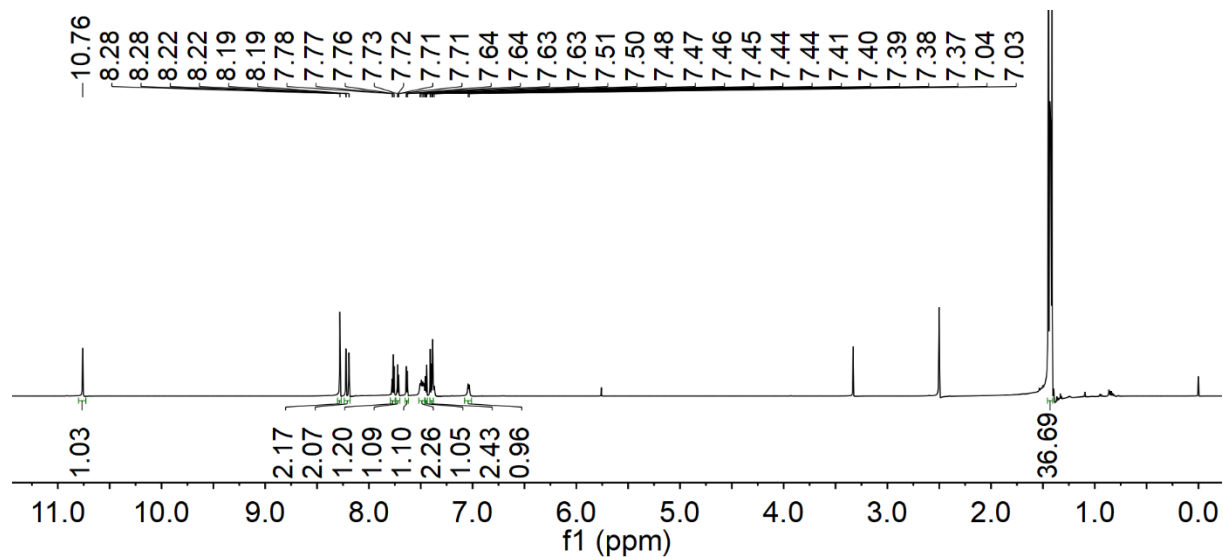


Figure S45. ¹H NMR spectrum of m **2d** in DMSO-d₆.

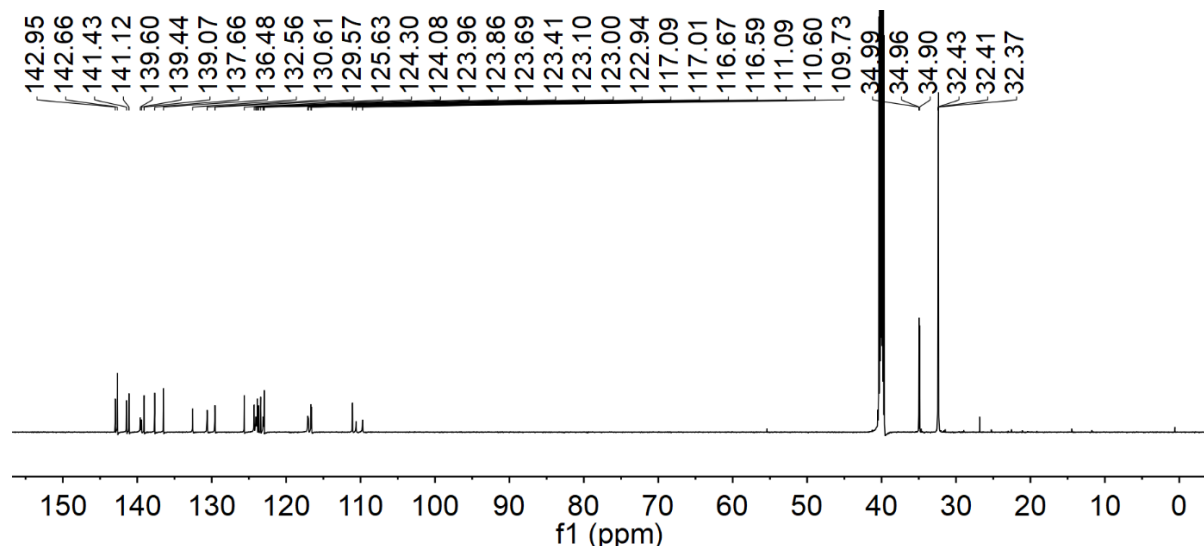


Figure S46. ¹³C NMR spectrum of m **2d** in DMSO-d₆.

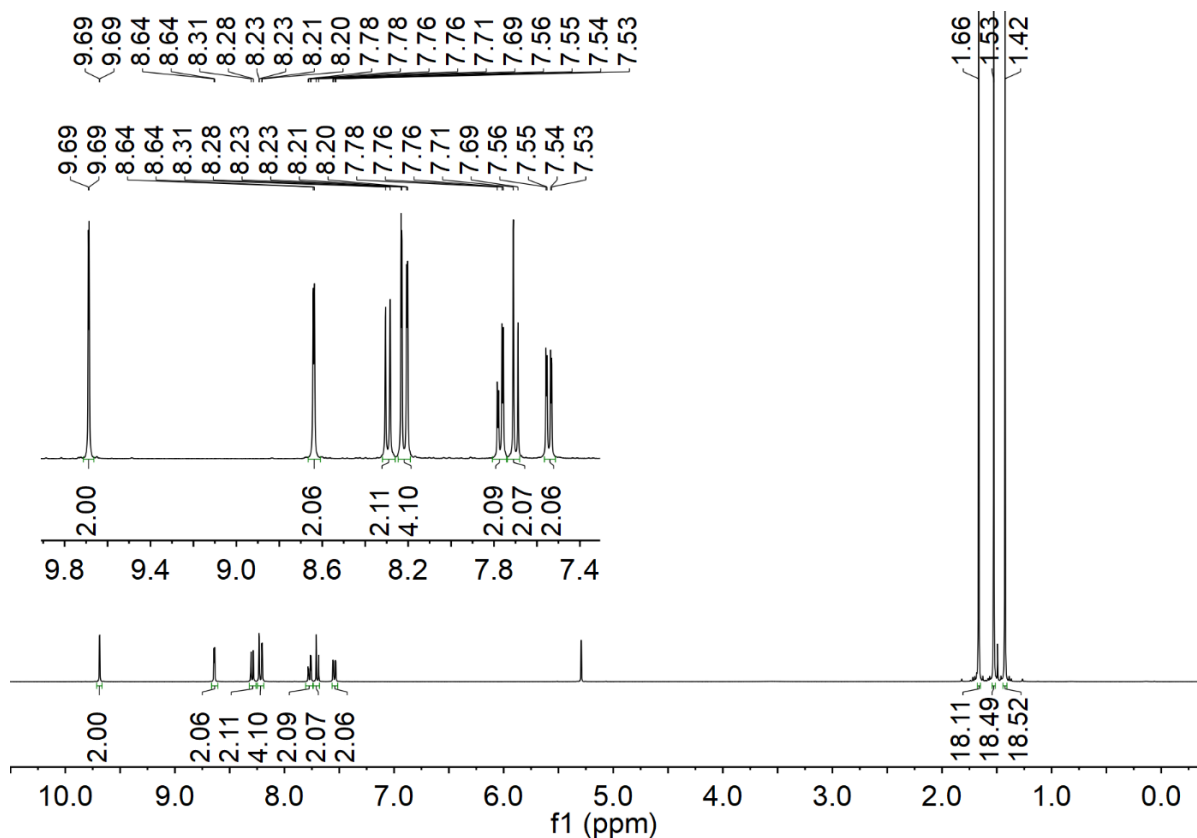


Figure S47. ^1H NMR spectrum of **p[B-N]O** in CD_2Cl_2 .

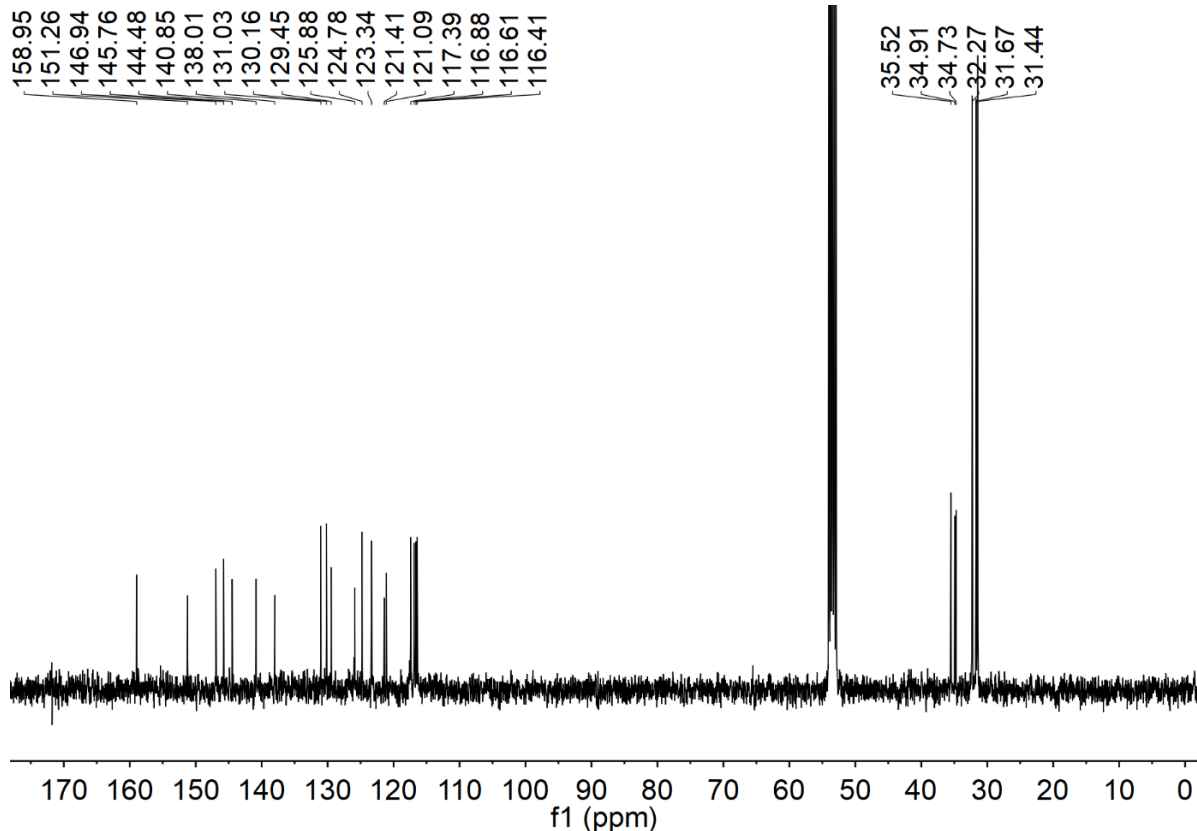


Figure S48. ^{13}C NMR spectrum of **p[B-N]O** in CD_2Cl_2 .

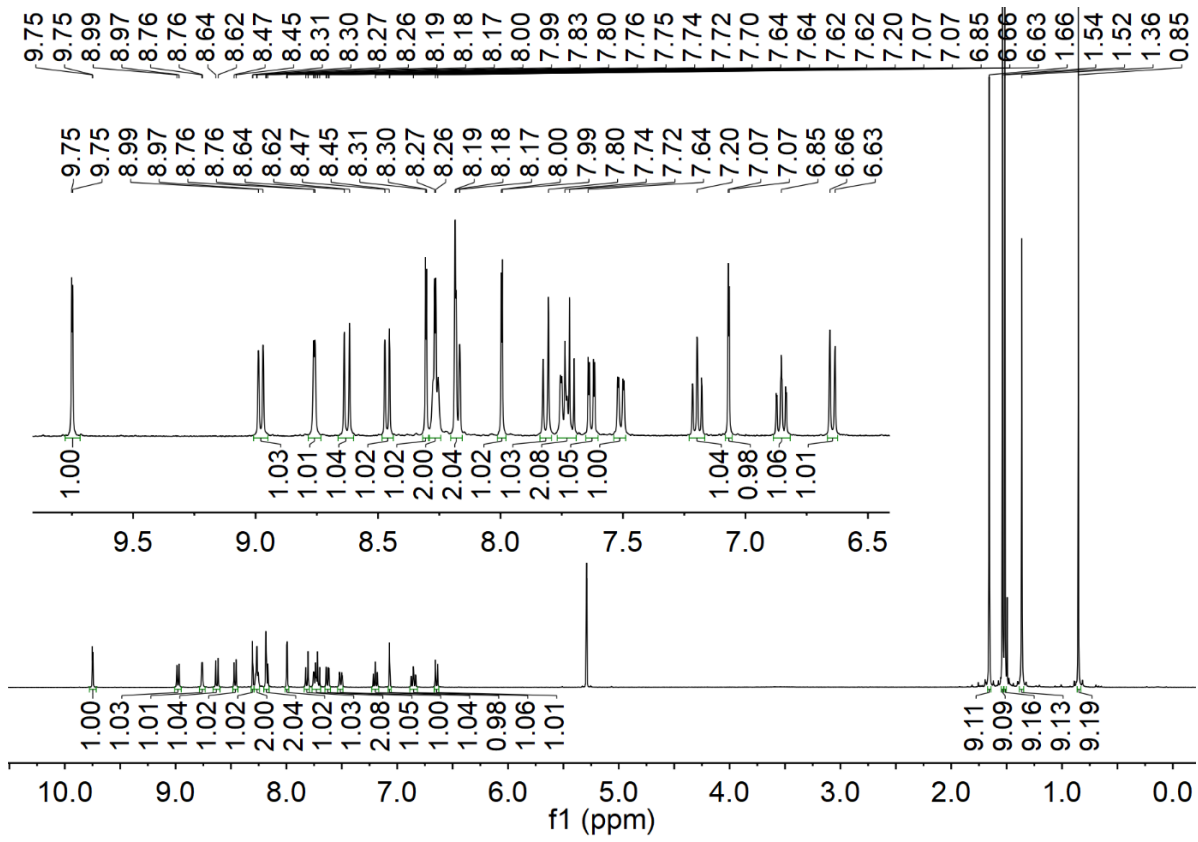


Figure S49. ^1H NMR spectrum of **p[B-N]NO** in CD_2Cl_2 .

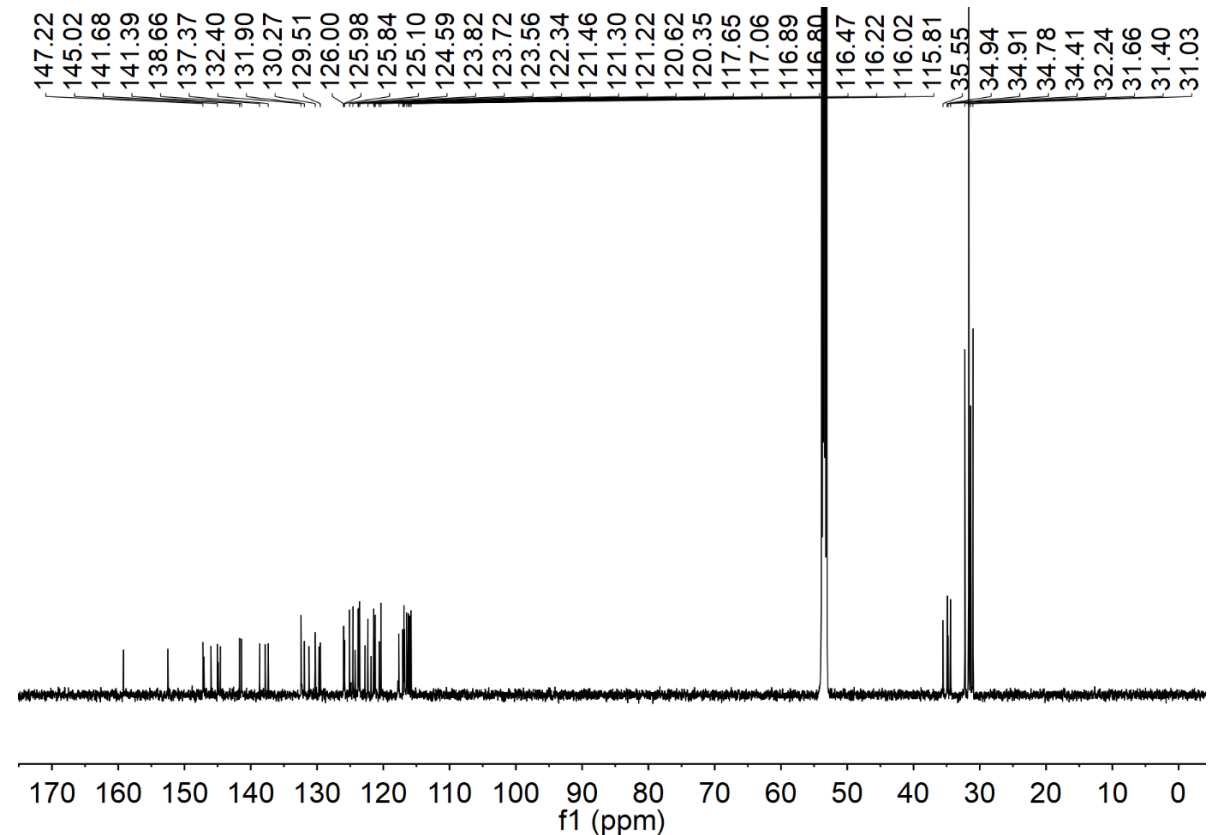


Figure S50. ^{13}C NMR spectrum of **p[B-N]NO** in CD_2Cl_2 .

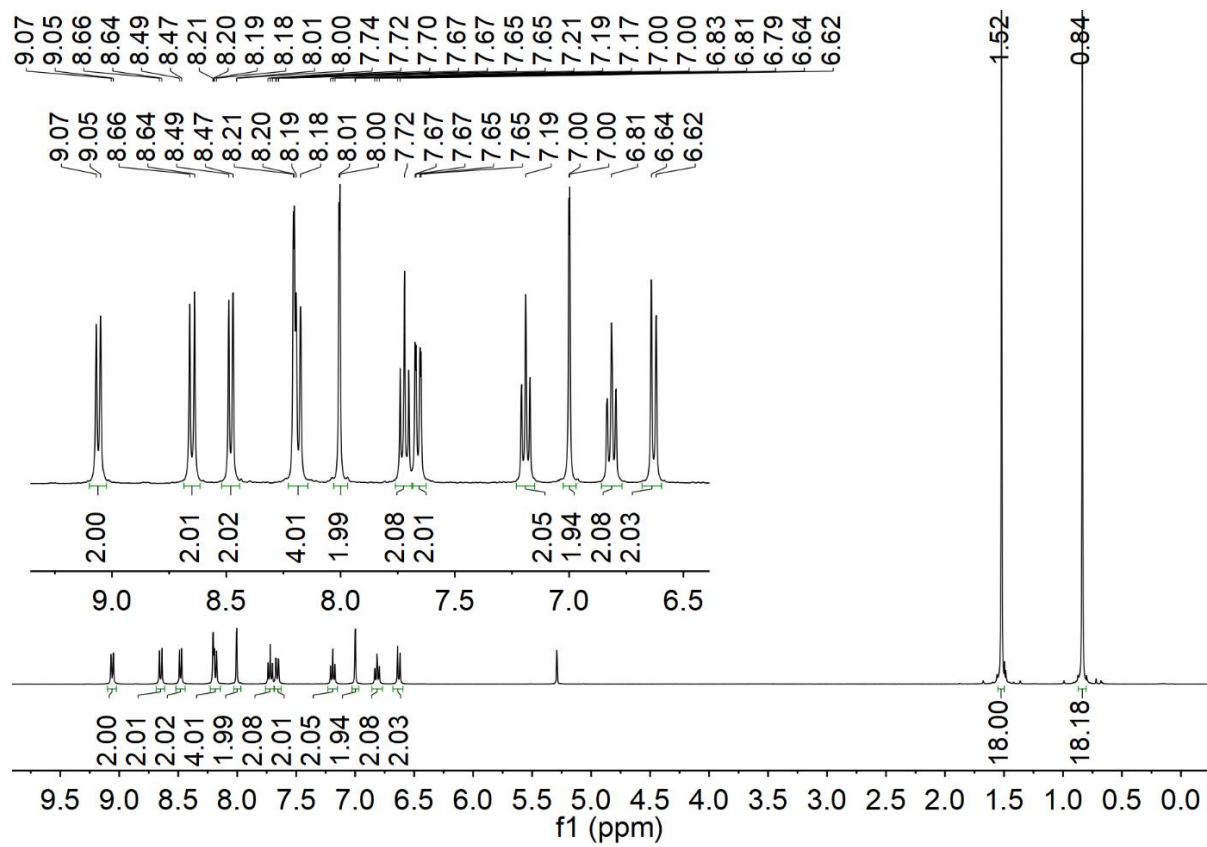


Figure S51. ^1H NMR spectrum of **p[B-N]N** in CD_2Cl_2 .

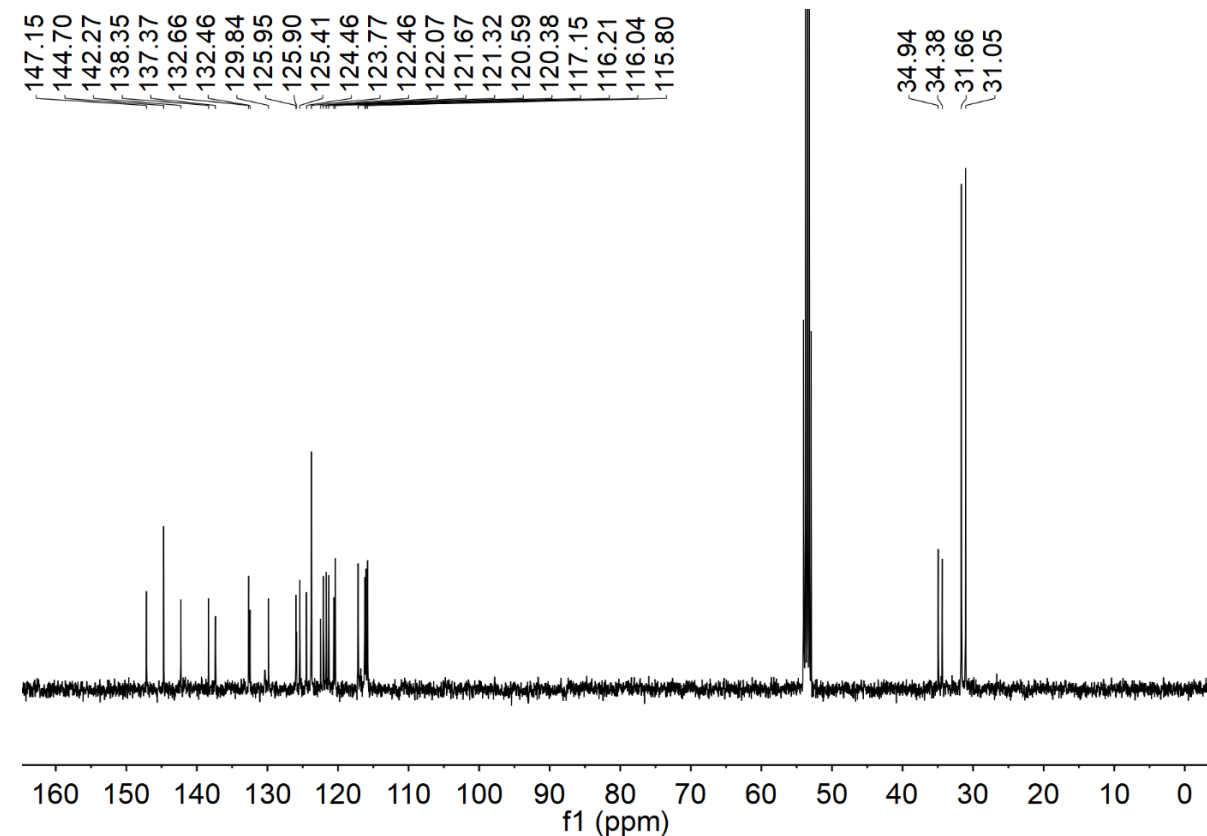


Figure S52. ^{13}C NMR spectrum of **p[B-N]N** in CD_2Cl_2 .

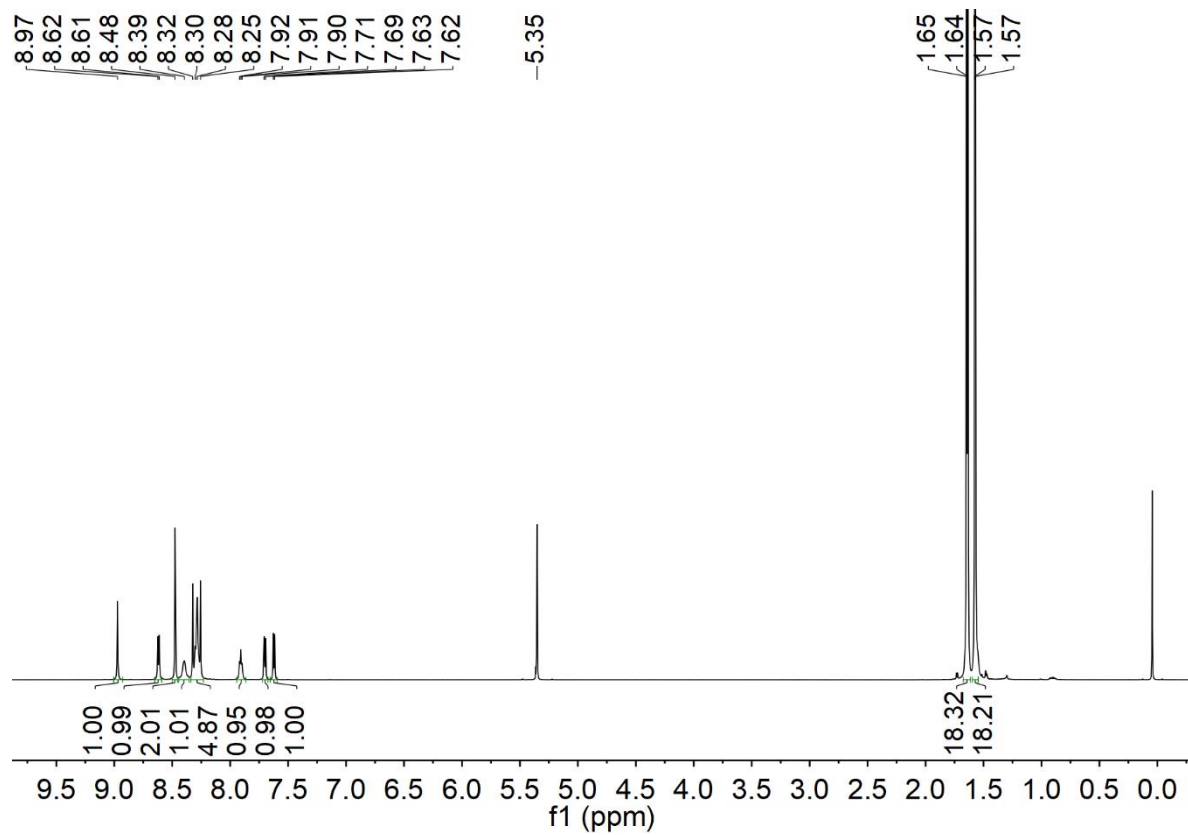


Figure S53. ^1H NMR spectrum of $[\text{B-N}] \text{N}$ in CD_2Cl_2 .

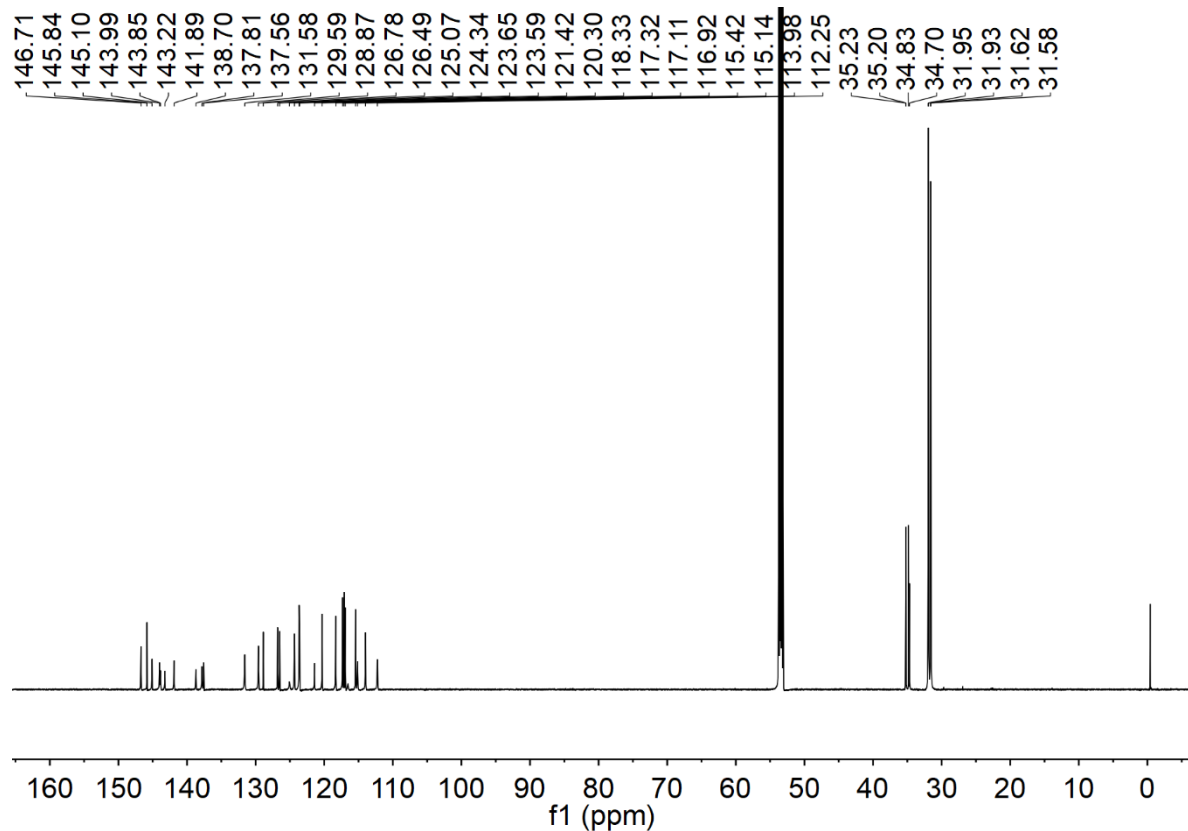


Figure S54. ^{13}C NMR spectrum of $[\text{B-N}] \text{N}$ in CD_2Cl_2 .

3. Reference

- [1] J.-D. Chai and M. H.-Gordon, *Phys. Chem. Chem. Phys.*, 2008, 10, 6615.
- [2] L. Kronik, T. Stein, S. Refaelly-Abramson, R. Baer, *J. Chem. Theory Comput.*, 2012, 8, 1515.
- [3] H. Sun, C. Zhong, J. L. Brédas, *J. Chem. Theory. Comput.*, 2015, 11, 3851.
- [4] F. Santoro, A. Lami, R. Improta, J. Bloino, and V. Barone. *J. Chem. Phys.*, 2008, 128, 224311.
- [5] Martin, R. L. Natural transition orbitals. *J. Chem. Phys.*, 2003, 118, 4775.
- [6] T. Lu, F. Chen, *J. Comput. Chem.* 2012, 33, 580.
- [7] W. Humphrey, A. Dalke, K. Schulten, *J. Mol. Graphics*, 1996, 14, 33-38.
- [8] Z. Shuai, Chin. J. Chem. 2020, 38, 1223.
- [9] P. Wei, D. Zhang, L. Duan, *Adv. Funct. Mater.* 2019, 30, 1907083.
- [10] D. Zhang, X. Song, A. J. Gillett, B. H. Drummond, S. T. E. Jones, G. Li, H. He, M. Cai, D. Credgington, L. Duan, *Adv. Mater.* 2020, 32, 1908355.
- [11] D. Zhang, M. Cai, Y. Zhang, D. Zhang, L. Duan, *Mater. Horiz.* 2016, 3, 145.
- [12] T. Huang, Q. Wang, S. Xiao, D. Zhang, Y. Zhang, C. Yin, D. Yang, D. Ma, Z. Wang, L. Duan, *Angew. Chem. Int. Ed.* 2021, 60, 23771.
- [13] H. Kaji, H. Suzuki, T. Fukushima, K. Shizu, K. Suzuki, S. Kubo, T. Komino, H. Oiwa, F. Suzuki, A. Wakamiya, Y. Murata, C. Adachi, *Nat. Commun.* 2015, 6, 8476.